

UNIVERSIDADE DE SÃO PAULO
MUSEU DE ZOOLOGIA

Ernesto Aranda Pedroso

**Systematics of Quaternary Squamata
from Cuba**

São Paulo
2019

UNIVERSIDADE DE SÃO PAULO
MUSEU DE ZOOLOGIA

Ernesto Aranda Pedroso

Systematics of Quaternary Squamata from Cuba

Sistemática dos Squamata Quaternários de Cuba

Corrected version

Dissertation presented to the
PostGraduate Program of the
Museu de Zoologia da
Universidade de São Paulo to
obtain the degree of Master of
Science (Systematics, Animal
Taxonomy and Biodiversity)

Advisor: Hussam El Dine Zaher
Co-Advisor: Luis Manuel Díaz Beltrán

São Paulo
2019

I do not authorize the reproduction and dissemination of this work in part or entirely by any electronic or conventional means

Cataloging in Publication

Serviço de Biblioteca e Documentação

Museu de Zoologia da Universidade de São Paulo

Pedroso, Ernesto Aranda
Systematics of Quaternary Squamata, from Cuba = Sistemática dos Quaternários de Cuba / Ernesto Aranda Pedroso; orientador Hussam El Dine Zaher e coorientador Luis Manuel Díaz Beltrán. São Paulo, 2018.
127p.

Dissertação (Mestrado) – Programa de Pós-Graduação em Sistemática, Taxonomia e Biodiversidade, Museu de Zoologia, Universidade de São Paulo, 2019.

Versão original

1. Squamata – Quaternário. 2. Fosséis - Squamata. 3. Sistemática - Squamata I. Zaher, Hussam El Dine, orient. II. Beltrán, Luis Manuel Díaz, coorient. III. Título.

CDU 598.112(729.1)

Pedroso, Ernesto Aranda

Systematics of Quaternary Squamata, from Cuba.

Dissertação apresentada ao Museu de Zoologia d3333 Universidade de São Paulo para obtenção do título de Mestre em Sistemática, Taxonomia Animal e Biodiversidade.

Aprovado em : / /

Banca examinadora

Prof. Dr.		Instituição	
Julgamento	<hr/>	Assinatura	<hr/>
	<hr/>		<hr/>
Prof. Dr.		Instituição	
Julgamento	<hr/>	Assinatura	<hr/>
	<hr/>		<hr/>
Prof. Dr.		Instituição	
Julgamento	<hr/>	Assinatura	<hr/>
	<hr/>		<hr/>

*A Eduardo y Edgar, pensando
en ustedes fue que pude
terminar de escribir.*

Acknowledgments

This thesis had its origin in the thought of Hussam Zaher, with the collaboration and recommendation of Luis Manuel Diaz Beltrán. To them my first thanks.

I am indebted to my parents Luis Ernesto and Rosa, for unconditionally supporting me in all my projects.

I thank my wife Jeny Larrea for understanding the importance of this step in my life and accepting the sacrifice of facing a pregnancy away from one of her main supports.

The staff of the National Museum of Natural History of Cuba deserves special attention for trust and welcoming me warmly. Thank you all, but especially Esther Perez Lorenzo, Yasmin Peraza, Surinay Betancourt!, Marcel Montano, Soraida Fiol, Alejandro Perdomo, Yamilé Lugerá, and my first tutor, Gilberto Silva Taboada.

I am very grateful to Lázaro William Viñola López, for contributing with a good part of the Thesis sample from his private collection; in addition to his valuable comments on the project. At the same time, I thank Lisbet Barban and Nayla García from the Ecology and Systematics Institute, for facilitating material loans for the Thesis.

I am grateful to Curators Addison Wynn (USNM), James Poindexter (USNM), David C. Blackburn (FLMNH), Leroy Nuñez (FLMNH), Pamela Dennis (FLMNH), and Coleman M. Sheehy (FLMNH) for sending valuable photos of their respective osteological collections.

To Miguel Ribot Guzmán (Cuban Institute of Tropical Geographic), Henrique Caldeira Costa and Fausto Barbo for the help with QGIS, shapes and maps of Cuba.

I greatly appreciate the support, sacrifice, and help of Aline Staskowian Benetti. Her heart is bigger than her chest. My time in Brazil deserves a chapter just for you.

I thank all the people who passed through the Department of Herpetology and Paleontology of the Museum of Zoologia of the USP, and they helped me in some way to obtain my results and adapt to the country. If the memory does not fail me, thanks to Alberto Carvalho, Vivian Trevine, Leo Oliveira, Bruno Zé, Paola Sánchez, Bruno Gonçalves, Bruno Navarro, Leo Malagoli, Juan Camilo Arredondo, Roberta Graboski, Ana Botallo, Felipe Grazziotin, Rose

Rodrigues, Lucas Piazzentin, Federico Alcantara, Luiz Bio, Flavio Molina. Special thanks to Daniella França, Paulo Machado, Natalia Rizzo, and Daniella Gennari, who filled the empty space left by the family.

I would like to thank in general all the Museum staff that in one way or another was part of my life. Among the students there is Rafael Dell'Erba, Priscila Carmeliet, Higor Rodriguez, Jose Vinicius, William Massaharu, Diego Cuevas, Francisco Eriberto, Vítor Abranção, Juan Pablo Botero. Among the officials there is Omair Guilherme, Marta Carreira, André Luis de Mesquita, Francisco de Assis, Altair Aparecido, Juliana Gualda, Michel Donato, Mauro Cardoso, Renato de Oliveira, Sonia Favaro, Mariana Shinohara, Vanderlei Tadeu, Eliseu dos Santos, Ileana, Cláudio Reberti. Excuse those who I do not remember the name, but rest assured that I do not forget their faces.

I remember with admiration and affection the teachers of the subjects I received. Juan Morrone, Silvio Nihei, Mario de Pinna, Diego Pol, Isabel Landim, and Gilberto Alejandro Ocampo.

For almost last and not less important to thank a group of Cubans who accompanied me and helped in these two years away from the Motherland. Hugs for Joel Lastra, kisses for Gretel Rodríguez, for Patricia González, for Mercedes Reyes, hugs for Daniel Reyes, and kisses for Fabiana Fuentes.

Finally, I would like to thank the Museum of Zoology and FAPESP in general for accepting my master's project, and financing it.

Resumo

Aranda E. (2019). Sistemática dos Squama do Quaternário de Cuba. (Dissertação de Mestrado). Museu de Zoologia, Universidade de São Paulo, São Paulo.

A paleontologia de répteis no Caribe é um tema de grande interesse para entender como a fauna atual da área foi constituída a partir da colonização e extinção dos seus grupos. O maior número de fósseis pertence a Squamata, que vai desde o Eoceno até nossos dias. O registro abrange todas as ilhas das Grandes Antilhas, a maioria das Pequenas Antilhas e as Bahamas. Cuba, a maior ilha das Antilhas, tem um registro fóssil de Squamata relativamente escasso, com 11 espécies conhecidas de 10 localidades, distribuídas no oeste e centro do país. No entanto, existem muitos outros fósseis depositados em coleções biológicas sem identificação, que poderiam esclarecer melhor a história de sua fauna de répteis. Um total de 328 fósseis de três coleções paleontológicas foi selecionado para sua análise, buscando características osteológicas diagnosticas do menor nível taxonômico possível, e comparando-os com outros fósseis e espécies recentes. No presente trabalho, o registro fóssil de Squamata foi aumentado, tanto em número de espécies quanto em número de localidades. O registro foi estendido a praticamente todo o território cubano. Restos fósseis pertencentes às espécies relatadas anteriormente são confirmados, como *Leiocephalus cubensis*, *L. carinatus*, *Tarentola americana*, *Chilabothrus angulifer* e *Cubophis cantherigerus*. Fósseis de *Amphisbaena*, *Pholidoscelis auberi* e *Leiocephalus macropus* foram descritos pela primeira vez, bem como de outros fósseis pertencentes aos gêneros *Tarentola*, *Leiocephalus* e *Chilabothrus*, mas diferentes das espécies que atualmente habitam o arquipélago. Esses resultados mostram que o registro fóssil de Squamata em Cuba é mais amplo do que era considerado anteriormente, apesar de ser composto de fósseis muito frágeis e pequenos, com pouco potencial para a fossilização. Para a paleontologia de Squamata, a descrição de novos táxons e registro de novas localidades em Cuba são os primeiros passos para estudos mais integradores sobre diversidade biológica, evolução, biogeografia, paleoambiente entre outros que contribuam ao entendimento da fauna na região do Caribe.

Palavras-chave: Cuba. Quaternário. Squamata. Fósseis.

Abstract

Aranda E. (2019). Systematic of Quaternary Squamata from Cuba. (Master dissertation). Museum of Zoology, University of São Paulo, São Paulo.

The paleontology of reptiles in the Caribbean is a topic of great interest to understand how the current fauna of the area was constituted from colonization and extinction of their groups. The largest number of fossils belongs to Squamata, ranging from the Eocene to our days. The registry covers all the islands of the Greater Antilles, most of the Lesser Antilles, and of the Bahamas. Cuba, the largest island of the Antilles, has a relatively sparse Squamata fossil record, with 11 known species from 10 locations, distributed in the West and Center of the Country. However, there are many other fossils deposited in biological collections without identification that could better clarify the history of their reptile fauna. A total of 328 fossils from three paleontological collections were selected for their analysis, searching osteological characteristics that would serve to diagnose them at the lowest possible taxonomic level, and compare them with other fossils and recent species. In the present work, the Squamata fossil record is increased, both in the number of species and in the number of localities. The registry is extended to practically all of the Cuban territory. Fossil remains belonging to previously reported species are confirmed, such as *Leiocephalus cubensis*, *L. carinatus*, *Tarentola americana*, *Chilabothrus angulifer*, and *Cubophis cantherigerus*. Fossils of *Amphisbaena*, *Pholidoscelis auberi*, and *Leiocephalus macropus* are described for the first time. Besides, other fossils belonging to the genera *Tarentola*, *Leiocephalus*, and *Chilabothrus* but different from the species that currently inhabit the archipelago, are described. These results show that the Squamata fossil record in Cuba is broader than what was previously considered, despite being composed of very fragile and small fossils with little potential for fossilization. For the paleontology of Squamata the description of new taxa and record of new localities in Cuba, are the first steps for more integrating studies on biological diversity, evolution, biogeography, paleoenvironment among others that contribute to the understanding of the fauna in the Caribbean region.

Key words: Antilles. Neogene. Lizard. Snake. Fossil.

List of figures

Figure 1. <i>Amphisbaena</i> fossil mid-body vertebra CZACC-1, in dorsal (A), ventral (B), and lateral (C) views. Scale bar = 1 mm.	32
Figure 2. <i>Tarentola</i> fossil frontal MNHNCu 73.5347-I in (A) dorsal and (B) ventral views. Scale bar = 5 mm.	43
Figure 3. <i>Tarentola</i> fossil single parietal MNHNCu 73.5343-I in dorsal (A) and ventral (B) views. Scale bar = 5 mm.	43
Figure 4. <i>Tarentola</i> fossil parietals MNHNCu 73.5343-II (right pair), -III (left pair), and -IV (left pair) in dorsal (A) and ventral (B) views. Scale bar = 5 mm.	43
Figure 5. <i>Tarentola</i> fossil occipital MNHNCu 73.5342-II in dorsal (A), lateral (B), ventral (C), and posterior (D) views. Scale bar = 5 mm.	44
Figure 6. <i>Tarentola</i> fossil left pterygoid MNHNCu 73.5351 in dorsal (A), ventral (B), and medial (C) views. Scale bar = 2 mm.	44
Figure 7. <i>Tarentola</i> fossil right maxilla MNHNCu 73.5345 (top) and right dentary CZACC 2 (bottom), in labial (A, C), and lingual (B, D) views. Scale bar = 5 mm.	44
Figure 8. <i>Tarentola</i> fossil left articular and surangular MNHNCu 73.5349-I, in dorsal (A), ventral (B), and lateral (C) views. Scale bar = 5 mm.	44
Figure 9. <i>Tarentola</i> fossil right articular and surangular MNHNCu 73.5349-II, in dorsal (A), and ventral (B) views. Scale bar = 5 mm.	44
Figure 10. Gekkota insertae sedis, fossil mid-body vertebra MNHNCu 73.5334, in anterior (A), posterior (B), lateral (C), dorsal (D), and ventral (E) views. Scale bar = 2 mm.	44
Figure 11. <i>Pholidoscelis auberi</i> fossil frontal CLV 3-I in dorsal (A), and ventral (B) views. Scale bar = 5 mm.	51
Figure 12. <i>Pholidoscelis auberi</i> fossil parietal CLV 3-II in dorsal (A), and ventral (B) views. Scale bar = 5 mm.	51
Figure 13. <i>Pholidoscelis auberi</i> fossil left maxilla CLV 3-III in labial (A), and lingual (B) views. Scale bar = 5 mm.	51
Figure 14. <i>Pholidoscelis auberi</i> fossil left anterior mandible CLV 3-IV: dentary, splenial and coronoid; in labial (A), and lingual (B) views. Scale bar = 5 mm.	51
Figure 15. <i>Pholidoscelis auberi</i> left posterior mandible, articulation of articular, angular, and surangular bones CLV 2 in dorsal (A), and ventro-medially (B) views. Scale bar = 5 mm.	51
Figure 16. <i>Pholidoscelis auberi</i> right pelvis MNHNCu 73.5312 in lateral (A), and medial (B) views. Scale bar = 5 mm.	51
Figure 17. <i>Leiocephalus macropus</i> fossil frontal CLV 1-I in dorsal (A), and ventral (B) views. Scale bar = 2 mm.	58
Figure 18. <i>Leiocephalus</i> fossil frontals of <i>L. carinatus</i> CLV 1-IV (A, B), and <i>Leiocephalus</i> sp. CLV 6-I (C, D) in dorsal (left), and ventral (right) views. Scale bar = 4 mm.	58
Figure 19. <i>Leiocephalus cubensis</i> fossil parietals CLV 1 -V (A) and CLV 4-I (B) in dorsal view. Scale bar = 5 mm.	58
Figure 20. <i>Leiocephalus</i> sp. fossil right maxilla CLV 6-V in labial (A), and lingual (B) views. Scale bar = 2 mm.	58
Figure 21. <i>Leiocephalus</i> fossil left dentary CZACC 5 in labial (A), and lingual (B) views. Scale bar = 5 mm.	58
Figure 22. <i>Leiocephalus</i> fossil right dentary CLV 1-IX in labial (A), and lingual (B) views. Scale bar = 5 mm.	58
Figure 23. Fossil left dentary CLV 1-X in labial (A), and lingual (B) views. Scale bar = 5 mm.	58

Figure 24. <i>Leiocephalus</i> sp. fossil left posterior mandible (articular, angular and surangular) CLV 5-V in dorsal (A), and ventral (B) views. Scale bar = 5 mm.	59
Figure 25. <i>Leiocephalus</i> cf. <i>carinatus</i> fossil right posterior mandibles (articular, angular and surangular) CLV 1-XI and -XII in dorsal views. Scale bar = 5 mm.	59
Figure 26. <i>Leiocephalus</i> sp. fossil left pelvis CLV 4 in medial (A), and lateral (B) views. Scale bar = 5 mm.	59
Figure 27. <i>Chilabothrus angulifer</i> fossil parietal MNHNCu 73.5311 in dorsal (A), lateral (B), and anterior (C) views. Scale bar = 5 mm.	66
Figure 28. <i>Chilabothrus angulifer</i> fossil right maxilla MNHNCu 73.5029 in dorsal (A), lingual (B), and labial (C) views. Scale bar = 5 mm.	66
Figure 29. <i>Chilabothrus</i> sp. fossil right maxilla MNHNCu 73.5322 in dorsal (A), lingual (B), and labial (C) views. Scale bar = 5 mm.	66
Figure 30. <i>Chilabothrus</i> sp. fossil left maxilla CLV 9-I in dorsal (A), lingual (B), and labial (C) views. Scale bar = 5 mm.	66
Figure 31. <i>Chilabothrus</i> cf. <i>angulifer</i> fossil right pterygoid CLV 9-II in dorsal (A), ventral (B), and lateral (C) views. Scale bar = 10 mm.	66
Figure 32. <i>Chilabothrus</i> sp. fossil right quadrate CLV 9-III in anterior (A), medial (B), and posterior (C) views. Scale bar = 3 mm.	66
Figure 33. <i>Chilabothrus</i> sp. fossil left dentary CLV 9-IV in labial (A), lingual (B), and ventral (C) views. Scale bar = 10 mm.	67
Figure 34. <i>Chilabothrus</i> fossil left compound bone CLV 9-V in lateral (A), medial (B), and dorsal (C) views. Scale bar = 10 mm.	67
Figure 35. <i>Chilabothrus</i> sp. fossil left compound bone CLV 8-I in lateral (A), medial (B), and dorsal (C) views. Scale bar = 10 mm.	67
Figure 36. <i>Chilabothrus angulifer</i> fossil right compound bone CLV 8-II in lateral (A), medial (B), and dorsal (C) views. Scale bar = 10 mm.	67
Figure 37. <i>Cubophis</i> fossil left compound bone MNHNCu 73.5376 in lateral (A), medial (B), and dorsal (C) views. Scale bar = 5 mm.	71
Figure 38. <i>Cubophis</i> fossil mid-body vertebra MNHNCu 73.5382 in dorsal (A), ventral (B), anterior (C), posterior (D), and lateral (E) views. Scale bar = 2 mm.	71
Figure 39. Zoom in posterior section of dental series of <i>Pholidoscelis auberi</i> (CLV 3-IV) in lingual view. Scale bar = 1 mm.	76
Figure 40. Zoom in Exemplar CLV 1-X. Arrows show the absence of foramina in a narrow space between teeth without crusting . Scale bar = 0.5 mm.	79
Figure 41. Distribution of the Squamata fossil record in the Antilles and The Bahamas. For detailed information see Appendix A. Text in bold are groups described in the present work. Name of the islands outside the circles. An: Anguilla, At: Antigua, Ba: Barbados, Br: Barbuda, Bs: Basse-Terre, Cr: Crooked Island, Cu: Cuba, Gt: Grande-Terre, Ga: Great Abaco, Hi: Hispaniola, Ij: Isla de la Juventud, Mo: Isla de Mona, Ja: Jamaica, De: La Désirade, Sa: Les Saintes, Mg: Marie-Galante, Np: New Providence, Pt: Petite-Terre, Pr: Puerto Rico,	

Sm Saint Martin. Name of genera within the circles: Al: *Alsophis*, Am: *Amphisbaena*, An: *Anolis*, At: *Antillotyphlops*, Ar: *Aristelliger*, Bo: *Boa*, Bi: Boidae indet., Br: *Borikenophis*, Ca: *Capitellum*, Ce: *Celestus*, Ch: *Chilabothrus*, Cl: *Clelia*, Ci: Colubridae indet., Cu: *Cubophis*, Cy: *Cyclura*, Di: *Diploglossus*, Er: *Erythrolamprus*, Ge: Gekkonidae, Gi: Gekkota indet., Ig: *Iguana*, li: Iguanidae indet, Le: *Leiocephalus*, Ma: *Mabuya*, Mg: *Magliophis*, Ne: *Nerodia*, Pa: *Pantherophis*, Ph: *Pholidoscelis*, Si: Scolecophidia indet., Sp: *Sphaerodactylus*, Ta: *Tarentola*, Th: *Thecadactylus*, Ty: *Typhlops*. * New genus record for Cuba.85

List of maps

Map 1. Distribution of <i>Amphisbaena</i> fossil in Cuba.....	85
Map 2. Distribution of fossil <i>Pholidoscelis auberi</i> in Cuba.....	86
Map 3. Distribution of fossil sample of Gekkota in Cuba.	86
Map 4. Fossil sample distribution of <i>Leiocephalus</i> , Cuba.....	87
Map 5. Fossil sample distribution of <i>Chilabothrus</i> , Cuba.	87
Map 6. Fossil sample distribution of <i>Cubophis</i> , Cuba.....	87

Institution abbreviations

AMNH: American Museum of Natural History.	MZUSP: Zoologic Museum of the São Paulo University.
CLV: Lázaro W. Viñola Collection.	OU: Sam Noble Oklahoma Museum of Natural History.
CZACC: Zoologic Collection of the Cuban Sciences Academy.	OUVC: Ohio University Vertebrate Collection.
FLMNH: Florida Museum of Natural History.	UMMZ: University of Michigan Museum of Zoology.
FMNH: Field Museum of Natural History.	USNM: United State National Museum.
MNHNCu: Cuban National Museum of Natural History.	

Osteologic abbreviations

Abd.for: Abducens foramen	Art.suf: Articular surface
Abd.fos: Abductor fossa	Art.sut: Articulation suture
Act: Acetabulum	Bas.occ: Basioccipital
Alv.tri.for: Alveolar Trigeminal nerve foramen	Bas.pt.fac: Basipterygoid facet
Ang: Angular	Bas.pt.prc: Basipterygoid process
Ang.cr: Angular crest	Ce.cl: Central column
Ang.fac: Angular facet	Ce.cr: Central crest
Ang.med.prc: Angular medial process	Ce.kee: Central keel
Ang.prc: Angular process	Cep.co: Cephalic condyle
An.lat.prc: Antero-lateral process	Tym.ne.for: Chorda tympani nerve foramen
An.cr: Anterior crest	Co: Condyle
An.gr: Anterior groove	Co.an.prj: Condyle anterior projection
An.med.not: Antero-medial notch	Cor.fac: Coronoid facet
An.med.prc: Antero-medial process	Cor.lab.prc: Coronoid labial process
An.my.for: Anterior mylohyoid foramen	Cor: Coronoid
An.op.olf: Anterior opening of olfactory canal	Cot: Cotyle
An.prc: Anterior process	Cra.cr: Cranial crest
Art: Articular	Den: Dentary
Art.co: Articular condyle	Den.cr: Dental crest
Art.dor.gr: Articular dorsal groove	Den.dor.fac: Dentary postero-dorsal facet

Den.ven.fac: Dentary postero-vental facet	Glo.are: Globular área
Den.she.fac: Dentary medial shelf facet	Hem.kee: Hemal keel
Den.prc: Dentary process	Hyp.fos: Hypophysial fossa
Den.ser: Dental series	Ili: Ilium
Des.prc: Descending process	Ili.spi: Ilium spine
Dia.phy: Diapophyses	Inf.alv.for: Inferior alveolar foramen
Dor.cr: Dorsal crest	Inf.po.prc: Inferior posterior process
Dor.prc: Dorsal process	Int.zyg.con: Interzygapophysis constriction
Dor.rid: Dorsal ridge	Int.zyg.lam: Interzygapophysis lamina
Dor.sel: Dorsum sellae	Isc: Ischium
Ect.fac: Ectopterygoid facet	Lab.rid: Labial ridge
Ect.prc: Ectopterygoid process	Lab.wll: Labial wall
Ect.lat.prc: Ectopterygoid lateral process	Lac-ju.fac: Lacrimal-Jugal facet
Ect.med.prc: Ectopterygoid medial process	Lar.for: Large foramen
Ent.fos: Entocarotid fossa	Lat.con: Lateral constriction
Ex.occ: Exoccipital	Lat.cr: Lateral crest
Fa.prc: Facial process	Lat.dep: Lateral depression
For: Foramen	Lat.kee: Lateral keel
For.mag: Foramen magnum	Lat.prc: Lateral process
For.ova: Foramen ovale	Lat.prj: Lateral projection
For.sub: Foramina subcentralia	Lat.pro: Lateral prominence
Fos.col: Fossa columellae	Ma.co: Mandibular condyle

Ma.fos: Mandibular fossa	Olf.ca: Olfactory canal
Ma.sym.fac: Mandibular symphysis facet	Pal.she: Palatal shelf
Ma.sym.tub: Mandibular symphysis tubercle	Pal.fac: Palatine facet
Mec.ca: Meckel's canal	Pal.lat.fac: Palatine lateral facet
Med.cr: Medial crest	Pal.med.fac: Palatine medial facet
Med.vn.cr: Medio-ventral crest	Pal.prc: Palatine process
Med.gr: Medial groove	Pal.ram: Palatine ramus
Med.pro: Medial prominence	Par.cot.for: Paracotylar foramen
Med.po.prc: Medial posterior process	Par.occ.prc: Paraoccipital process
Med.prc: Medial process	Par.phy: Parapophyses
Med.rid: Medial ridge	Pa.fos: Parietal fossa
Med.scr: Medial scar	Pin.for: Pineal foramen
Nas.fac: Nasal facet	Po.alv.for: Posterior alveolar foramen
Nas.prc: Nasal process	Po.dor.prc: Postero-dorsal process
Nas.pro: Nasal prominence	Po.ven.prc: Postero-ventral process
Nas.she: Nasal shelf	Po.my.for: Posterior mylohyoid foramen
Neu.arc: Neural arch	Po.op.olf: Posterior opening of olfactory canal
Neu.ca: Neural canal	Po.prc: Posterior process
Neu.spi: Neural spine	Po.she: Posterior shelf
Obt.for: Obturator foramen	Po.lat.prc: Postero-lateral process
Occ.co: Occipital condyle	Po.med.prc: Postero-medial process
Occ.rec: Occipital recess	Po.fro.fac: Postfrontal facet

Pos.zyg: Postzygapophysis	Sem.cr: Semilunar crest
Pre.art.cr: Prearticular crest	Spt.max.bas: Septomaxilla base
Pre.fro.fac: Prefrontal facet	Sma.for: Smaller foramen
Pre.an.fac: Prefrontal anterior facet	Sph: Sphenoid
Pre.po.fac: Prefrontal posterior facet	Sph.occ.tub: Sphenoccipital tubercle
Pre.max.prc: Premaxilla process	Spl: Splenial
Pre.zyg: Prezygapophysis	St.prc: Stylohyal process
Pre.zyg.prc: Prezygapophysis process	Sub.den: Subdental border
Prc.asc: Processus ascendens	Sup.alv.for: Superior alveolar foramen
Prt: Prootic	Sup.po.prc: Superior posterior process
Prt.ala.prc: Prootic alar process	Sup.occ: Supraoccipital
Prt.cr: Prootic crista	Sup.occ.cr: Supraoccipital crest
Pub: Pubis	Sup.or.prc: Supraorbital process
Pub.tub: Pubis tubercle	Sup.tem.prc: Supratemporal process
Qua.con: Quadrate constriction	Sur: Surangular
Qua.fac: Quadrate facet	Sur.an.prc: Surangular anterior process
Qua.ram: Quadrate ramus	Sur.an.for: Surangular anterior foramen
Re.prc: Retroarticular Process	Sur.cr: Surangular crest
Re.she: Retroarticular Shelf	Sur.dor.prc: Surangular dorsal process
Sa.cr: Sagittal crest	Sur.dor.cr: Surangular dorsal crest
Sca.sul: Scales sulcus	Sur.med.cr: Surangular medial crest
Sel.tur: Sella turcica	Sur.po.for: Surangular posterior foramen

Sur.ven.prc: Surangular ventral process

Ven.prc: Ventral process

Syn: Synapophysis

Ven.pro: Ventral prominence

Tra.cr: Transversal crest

Ven.gro: Ventral groove

Tym.cr: Tympanic crest

Vid.ca: Vidian canal

U.not: U-shaped notch

Ztr: Zygantra

U.op: U-shaped opening

Zph: Zygosphenon

V.not: V-shaped notch

Contents

1	INTRODUCTION	19
2	MATERIALS AND METHODS	23
2.1	SAMPLE.....	24
2.2	COMPARATIVE SPECIMENS	27
2.3	PREPARATION, AND DESCRIPTION.....	28
2.4	ILLUSTRATIONS	29
3	RESULTS.....	30
3.1	FAMILY AMPHISBAENIDAE GRAY 1825	31
3.1.1	<i>Vertebra</i>	31
3.2	FAMILY PHYLLODACTYLIDAE GAMBLE, BAUER, GREENBAUM AND JACKMAN, 2008	32
3.2.1	<i>Frontal</i>	32
3.2.2	<i>Parietal</i>	33
3.2.3	<i>Occipitals, prootics and sphenoid</i>	35
3.2.4	<i>Pterygoid</i>	37
3.2.5	<i>Maxilla</i>	38
3.2.6	<i>Dentary</i>	39
3.2.7	<i>Articular, Surangular.</i>	40
3.2.8	<i>Vertebra</i>	41
3.3	FAMILY TEIIDAE GRAY, 1827	44
3.3.1	<i>Frontal</i>	44
3.3.2	<i>Parietal</i>	45
3.3.3	<i>Maxilla</i>	45
3.3.4	<i>Dentary, Splenial, and Coronoid</i>	46
3.3.5	<i>Angular, Surangular and Articular</i>	48
3.3.6	<i>Pelvic girdle</i>	49
3.4	FAMILY LEOCEPHALIDAE FROST, ETHERIDGE, JANIES AND TITUS, 2001	51
3.4.1	<i>Frontal</i>	51
3.4.2	<i>Parietal</i>	52
3.4.3	<i>Maxilla</i>	52
3.4.4	<i>Dentary</i>	53
3.4.5	<i>Angular-Surangular-Articular complex</i>	54
3.4.6	<i>Pelvic girdle</i>	56
3.5	FAMILY BOIDAE GRAY 1825	59
3.5.1	<i>Parietal</i>	59

3.5.2	<i>Maxilla</i>	59
3.5.3	<i>Pterygoid</i>	60
3.5.4	<i>Quadrate</i>	61
3.5.5	<i>Dentary</i>	62
3.5.6	<i>Compound Bone</i>	63
3.6	FAMILY COLUBRIDAE OPEL, 1811	67
3.6.1	<i>Compound Bone</i>	67
3.6.2	<i>Vertebra</i>	68
4	DISCUSSION	71
4.1	COMPARISON AND COMMENTS	72
4.1.1	<i>cf. Amphisbaena Linnaeus 1758</i>	72
4.1.2	<i>Tarentola (Gray, 1831)</i>	72
4.1.3	<i>Pholidoscelis auberi Gray, 1827</i>	75
4.1.4	<i>Leiocephalus Gray 1827</i>	76
4.1.5	<i>Chilabothrus Duméril and Bibron, 1844</i>	79
4.1.6	<i>Cubophis cf. cantherigerus (Bibron, 1840)</i>	81
4.2	CUBAN FOSSIL RECORD.....	82
5	CONCLUSIONS	89
6	REFERENCES	91
7	APPENDICES	104
7.1	APPENDIX A. SQUAMATA FOSSILS KNOWN IN THE ANTILLES AND THE BAHAMAS. THE LOCALITIES OF CUBA ARE THE ONES REPORTED BEFORE THE PRESENT WORK.	105
7.2	APPENDIX B. LOCALITIES OF FOSSIL SAMPLE, CUBA.	116

1 Introduction

The Antilles are recognized as an exceptional biogeographic scenario (Losos & Ricklefs, 2010), by the extinction, colonization and adaptive radiations experienced by some of their zoological groups (Hedges, 1989; Pregill & Olson, 1981; Silva, Duque, & Díaz-Franco, 2007). From 40 million years ago there are permanent islands in the Antillean region (Iturralde-Vinent, 2005), and since then the evolutionary history of the lineages has begun (Silva et al., 2007). The main hypotheses for the arrival of terrestrial fauna are: (1) the formation of Gaarlandia during the Eocene-Oligocene transition, a chain of islands that functioned as a filter for the passage of species (Iturralde-Vinent, 2006); and (2) oceanic dispersion by rafting or intense meteorological phenomena (Buskirk, 1985; Hedges, 2001). However, there are some faunal examples for the Gaarlandia existence (Alonso, Crawford, & Bermingham, 2012), until now, no geologic data demonstrated the existence of a continuing land between the Birds Arc and the Lesser Antilles (Ali, 2012).

Squamata reptiles may have used either of these two routes to colonize the Antilles and irradiate. Molecular data accord with geological data, sustaining a Cenozoic arrival to the Antilles for all Squamata groups (Gamble et al., 2011; Hedges, 1996), except for the endemic Cuban genus *Cricosaura*. This last genus is a very ancient relic, possibly from the Upper Cretaceous, although controversial because so far no fossil remains were found on any of the islands (Gauthier, Kearney, Maisano, Rieppel, & Behlke, 2012; Savage, 1964). The genera *Cyclura* and *Leiocephalus* probably arrived during mid-Cenozoic, while the other genera of Squamata colonized the region more recently (Hedges, 2006).

The record of Squamata fossils has very good studies in some islands like Hispaniola, Puerto Rico, Antigua, Guadalupe Islands, and some of the Bahamas Bank (Bochaton et al., 2015; Etheridge, 1965; Pregill, 1981; Pregill, Steadman, Olson, & Grady, 1988; Pregill, Steadman, & Watters, 1994; Steadman et al., 2015). Other islands of the Antilles are still much less studied, or not studied at all, concerning their paleofauna of Squamata. Oldest fossils are from the Miocene of the Dominican Republic amber (Daza & Bauer, 2012; Queiroz, Chu, & Losos, 1998) and from a Puerto Rican lignithic clayey (MacPhee & Wyss, 1990). These fossils

give us some understanding about times and forms of colonization in the Antillean territories.

In the Antilles, Cuba is the largest island, with an approximate area of 110 km² and a maximum elevation of 1974 m.s.l (National Office of Statistic and Information, 2017). The autochthonous fauna of Cuban lizards are grouped into eight families, nine genera, and 99 species (Rodríguez-Schettino et al., 2013; Uetz, Freed, & Hošek, 2018). The two most diverse families are Dactyloidae with 64 species, all belonging to the genus *Anolis* (95.3% of endemism) and Sphaerodactylidae (22 species, 86.3% of endemism), composed of the genera *Sphaerodactylus*, and *Aristelliger*. Snakes are grouped into four families, nine genera, and 42 species. The most diverse families are Tropicophiidae (16 species, all endemic) and Typhlopidae (12 endemic species and 1 introduced). While amphisbaenians are grouped into two families, Amphisbaenidae with three species of the genus *Amphisbaena*, and Cadeidae, with two species of the genus *Cadea* (Rodríguez-Schettino et al., 2013; Uetz et al., 2018). This last family is endemic.

All known fossil records of Squamata are from the Pleistocene-Late Holocene age, mainly associated to cave deposits (Consuegra, 2014). So far, registered species from the western and central part of the country are *Anolis lucius*, *A. equestris*, *A. porcatus*, *A. luetogularis*, *A. chamaleonides*, *Tarentola americana*, *Leiocephalus cubensis*, *L. carinatus*, *Cyclura nubila*, *Chilabothrus angulifer*, e *Cubophis cantherigerus* (Arredondo, 1997; Arredondo & Villavicencio, 2004; Brattstrom, 1958; Jiménez, Condis, & García, 2005; Jiménez & Valdés, 1995; Koopman & Ruibal, 1955; Orihuela, 2012; Salgado, Calvache, Macphee, & Gould, 1992; Varona & Arredondo, 1979), which represents 7.5% of the extant Cuban Squamata autochthonous fauna (Torres, Rodríguez-Cabrera, & Romero, 2017).

So far, there is not a study dedicated to this fossil group. The papers in which fossil species of Squamata are reported, mention them as an associated fauna of fossil mammals and birds (Arredondo, 1997; Jiménez et al., 2005; Koopman & Ruibal, 1955; Orihuela, 2012; Varona & Arredondo, 1979), without a properly description, or images for illustration.

The lack of effort and specialists in this field limits the correct identification of the species, or in the worst of cases, leave the piece indeterminate (Pregill, 1992). So far, the method used in Cuban fossils is the empirical comparison with current species, without verify all the

characters that could help to identify the species. In addition, there is a poor representation of Cuban species in osteological collections, which can lead to erroneous assignment of a character to a species given that the range of variation for a character is deduced from only one, or a few individuals (Pregill, 1992). Therefore, studies of paleoenvironment (Arredondo & Villavicencio, 2004), biological diversity (Consuegra, 2014; Rodríguez-Schettino, 2003), and extinctions (Díaz-Franco, 2004; Pregill & Olson, 1981) are incomplete without a good understanding of Squamata paleofauna.

In this work, we propose to perform a detailed description of the Quaternary fossil remains of Squamata, based on defined osteological characters; and conduct a survey of the Cuban fossil record.

2 Materials and Methods

2.1 Sample

A total of 328 fossils were analyzed (Table 1), belonging to the Fossil Reptile Collection of the National Museum of Natural History of Cuba (MNHNCu), to the Zoological Collection of the Cuban Academy of Sciences (CZACC), and to the private collection of Cuban collaborator Lázaro William Viñola López (CLV). The sample is a selection of the most preserved, and most complete fossils available in each collection. Due to lack of curatorial work many exemplars are without catalog number or grouped in batches. For present work, a temporary classification was made with these specimens until they are reincorporated into their proper collections. Cases without a catalog number were numbered in crescent order with Arabic numerals (1, 2, 3...). In cases with different bones or characteristics in the same batch, they were numbered with Roman numerals in crescent order (I, II, III...).

Table 1. Classification, and quantity of Cuban fossil sample from Cuban National Museum of Natural History (MNHNCu) Cuban Zoologic Academy of Sciences Collection (CZACC), and particular collection of Lázaro William Viñola (CLV), used in present work.

Catalog number	Suborder	Classification	Bone	Number of Exemplars
CLV 1	Sauria	I, II, III, IV	Frontal	5
		V, VI	Parietal	2
		VII	Maxilla	15
		VIII, IX, X	Dentary	36
		XI, XII, XIII	Posterior mandible	3
CLV 2	Sauria		Posterior mandible	4
CLV 3	Sauria	I	Frontal	9
		II	Parietal	5

		III	Maxilla	4
		IV	Dentary	14
CLV 4	Sauria	I	Parietal	1
		II	Pelvis	12
CLV 5	Sauria	I, II	Dentary	11
		III, IV, V	Posterior mandible	3
CLV 6	Sauria	I, II, III, IV	Frontal	4
		V	Maxilla	6
CLV 7	Serpentes	I, II	Dentary	2
CLV 8	Serpentes	I, II	Compound bone	2
CLV 9	Serpentes	I	Maxilla	2
		II	Pterygoid	2
		III	Quadrate	1
		IV	Dentary	1
		V	Compound bone	2
CZACC 1	Sauria		Vértebra	1
CZACC 2	Sauria		Dentary	1
CZACC 3	Sauria	I	Frontal	7
		II	Maxilla	3
		III	Dentary	4
CZACC 4	Sauria	I	Maxilla	1

		II	Dentary	4
CZACC 5	Sauria		Dentary	1
CZACC 6	Sauria		Dentary	1
CZACC 7	Sauria		Dentary	15
CZACC 8	Sauria		Dentary	1
MNHNCu 73.5029	Sauria	I	Maxilla	1
		II	Dentary	1
MNHNCu 73.5041	Sauria		Dentary	6
MNHNCu 73.5311	Serpentes		Parietal	1
MNHNCu 73.5312	Sauria		Coxal	2
MNHNCu 73.5322	Serpentes		Maxilla	2
MNHNCu 73.5328	Serpentes		Posterior mandible	1
MNHNCu 73.5334	Sauria		Vertebra	1
MNHNCu 73.5335	Serpentes		Pterygoid	1
MNHNCu 73.5342	Sauria	I, II, III, IV, V	Occipital	5
MNHNCu 73.5343	Sauria	I, II, III, IV	Parietal	18
MNHNCu 73.5345	Sauria		Maxilla	60
MNHNCu 73.5347	Sauria	I, II	Frontal	10
MNHNCu 73.5349	Sauria	I, II, III	Posterior mandible	9
MNHNCu 73.5350	Sauria		Dentary	10
MNHNCu 73.5351	Sauria		Pterygoid	10

MNHNCu 73.5376	Serpentes	Compound bone	1
MNHNCu 73.5379	Sauria	Posterior mandible	1
MNHNCu 73.5380	Serpentes	Pterygoid	1
MNHNCu 73.5382	Serpentes I, II	Vertebra	2

(Source: Aranda, 2019)

2.2 Comparative specimens

Comparative materials are composed of museum specimens, photos, 3D images from Digimorph (digimorph.org/index.phtml), Morphosource (www.morphosource.org), and Sketchfab (sketchfab.com/feed), and specimens directly from collections in the field. In some cases reliable and clear photographs of articles were used.

Amphisbaenidae: *Amphisbaena alba* FMNH 195924. **Boidae:** *Boa constrictor* FMNH 31182; *Chilabothrus angulifer* AMNH 77596, AMNH 64611, UMMZ 176924, USNM 132741, USNM 167529, MNHNCu 63.032; *Chilabothrus chrysogaster* UMMZ 176925; *Chilabothrus exsul* AMNH 73005, FLMNH 56944, UMMZ 176925; *Chilabothrus fordii* AMNH R40116, UMMZ 173415; *Chilabothrus gracilis* AMNH R42997, FLMNH 69149, UMMZ 176908; *Chilabothrus inornatus* USNM 306209, USNM 72749, AMNH R70023, FLMNH 11753, UMMZ 176908; *Chilabothrus monensis* UMMZ 177006; *Chilabothrus striatus* AMNH 155262, AMNH 70263, FLMNH 56282, USNM 259534, USNM 225060, USNM 59918; *Chilabothrus strigilatus* AMNH R70263; *Chilabothrus subflavus* FLMNH 11990, UMMZ 181121, USNM 292500, USNM 292499; *Corallus annulatus*, OUV 9719; *Eunectes murinus* FLMNH 84822; *Eunectes notaeus* MZUSP 8503. **Dipsadidae:** *Arrhyton dolichurum* MNHNCu 63.106; *Cubophis canterigerus* MNHNCu 63.033, UMMZ 85940; *Caraiba andreae* MNHNCu 63.087; *Natrix natrix* FMNH 30522; *Natrix tessellata* UMMZ 56568. **Phyllodactylidae:** *Tarentola americana* MNHNCu 23.4967 MNHNCu 63.099; *Tarentola annularis* UMMZ 134662; *Tarentola mauritanica* UMMZ 87112; *Thecadactylus rapicuda* UMMZ 95146. **Sphaerodactylidae:** *Sphaerodactylus caicosensis* UMMZ 95971; *Sphaerodactylus dimorphicus* UMMZ 167681; *Sphaerodactylus celicara* UMMZ 167731; *Sphaerodactylus armasi* UMMZ 167687; *Teratoscincus przewalskii*

UMMZ 171013. **Leiocephalidae:** *Leiocephalus carinatus* MNHNCu 23.2037, MNHNCu 23.5095, MNHNCu 63.085, MNHNCu 63.104; *Leiocephalus cubensis* MNHNCu 63.023; *Leiocephalus macropus* MNHNCu 23.4216; *Leiocephalus raviceps* MNHNCu 23.2012; *Leiocephalus stictigaster* MNHNCu 23.1089, MNHNCu 23.1254; *Leiocephalus barahoensis* USNM 260564. **Teiidae:** *Pholidoscelis auberi* MNHNCu 23.4293, MNHNCu 63.105; *Ameiva ameiva* UMMZ 245032; *Aspidoscelis tigris* FMNH 161622; *Cnemidophorus murinus*, OU 39632; *Callopietes maculatus* FMNH 53726; *Teius teyou* FMNH 10873; *Tupinambis teguixin* FMNH 22416.

2.3 Preparation, and Description

Most of the fossils studied were already partially cleaned, requiring only the use of needles and brushes for the removal of sediment still present, not embedded. However some materials presented regions with mineralization, permineralization, recrystallization, sediment filling, and crusting. Those exemplars were cleaned using ultrasonic water waves. They were put in small glass containers full of running water and immersed in a small pool of the equipment, also filled with running water for 5 minutes. Ultrasonic washing machine was model USC 750, ultrasonic frequency of 25 KHz, ultrasonic power of 100 Watts RMS. Although effective in most of exemplars, some were affected physically by its fragility.

Taxonomy follows the latest proposal for Squamata reptiles by Zheng and Wiens (2016). Samples were observed and compared to the optical stereoscope searching for diagnostic characters as specific as possible. When was not possible found a diagnostic character, the material was associated with the most similar taxon. A geographical criterion was followed when no differences were found between fossils and the closest recent taxon. Osteologic nomenclature follow Benites (2015), Čerňanský and Smith (2018), Conrad (2008), Daza et al. (2008), Estes et al. (1988), Etheridge and Queiroz (1988), Evans (2008), Frazetta (1959), Gauthier et al. (2012), Ikeda (2007), Oelrich (1956), Pregill (1992), Russel and Bauer (2008), Scanferla et al. (2016), Smith and Scanferla (2016), Stephenson and Stephenson (1956), Torres-Carvajal (2003), and Zaher and Scanferla (2012).

Fossils were represented by multifocal and simple photographs. Multifocals were carry out with a stereomicroscope Leica M205a equipped with a digital camera DFC425 using the software Leica Application Suite (3.8). Other were simple photographs, taken with camera Canon EOS DIGITAL REBEL XT, Nikon D3400, and with stereomicroscopy Nikon SMZ 745T equipped with a digital camera EUREKAM 3.0 using the software BELView (6.2.3.0). Bones were represented in dorsal, ventral, lateral, medial, anterior and posterior views. In specific case of maxilla and dentary, they were also represented in labial and lingual views. Proportions of bones were obtained by measurements relationships. Measurements were made with a 0.02 mm error caliper, or using the rule of the software TPSdig 2.11 (Rohlf, 2001) over photographs. TPS was also used to measure angles in the photo.

Recent comparative specimens were examined on the high-resolution X-ray microCT scan. According to their sizes, the specimens were individually mounted on falcon tubes, to keep them immobile while the scanning was realized. The studied specimens were scanned using the Phoenix v|tome|x m (General Electric Company) housed at the Microtomography Laboratory of the Museum of Zoology of the University of São Paulo. To acquire the scans a microfocus tube 300 was used and different settings applied to optimize the scan quality. The best results were obtained using 75 kV and 200 μ A, with 500 ms per projection image, averaging 1 and skipping 0 images per position. To reconstruct the image it was used the Data Reconstruction software (GE Company). The rendering and analysis of the datasets were conducted using the software VG Studio Max (2.2.3.69611, 64bits). Analysis of reconstructions were performed using the software 3D Builder (Microsoft Corporation).

2.4 Illustrations

Figures were constructed using the software Adobe Photoshop CC 2017, and Adobe Illustrator 2017 CC. Deposit locations were obtained by the collection label. The coordinates of these localities were obtained by direct observation on the topographic cartography of Cuba (Instituto Cubano de Cartografía y Catastro, 1957) with Lambert conical projection system of Cartesian coordinates. The localities are in the UTM system, from the 17Q (North Cuba) and 18Q (South Cuba) zones, Northern Hemisphere. Coordinates were georeferenced in the Convert Geographic Units resource of the Yellowstone Research Coordination

Network website (www.rcn.montana.edu/Resources/Converter.aspx), using the WSG-84 datum. Maps were constructed using the QGIS Desktop 2.18 software.

3 Results

Bone Descriptions

Systematic paleontology

Order Squamata Opper, 1811

3.1 Family Amphisbaenidae Gray 1825

Genus cf. *Amphisbaena* Linnaeus 1758

3.1.1 Vertebra

An almost complete vertebra of the middle of the body, according to Bolet et al. (2014) and Zangerl (1945), show characters of *Amphisbaenia* (CZACC 1, Figure 1). The vertebra is rather small (1.91 mm of body length), dorso-ventrally compress in general aspect, constricted in dorsal view between the pre- and postzygapophyses show all margins smooth. It lacks left prezygapophyses. Right prezygapophysis is antero-dorsally directed, about 20° up with respect to the transversal axis, and 45° with respect to the longitudinal axis. Articular surfaces are drop-shaped and face upward. It presents a large, blunt prezygapophyseal process, a little less wide than the articular surface.

Synapophyses are massive and globular, ventro-laterally directed, and well-defined from the vertebral body. The interzygapophyseal constriction is deep, almost half the width of the distance between postzygapophyses. It describes a regular curve without angulation. Postzygapophyses open laterally, about 22° with respect to the horizontal axis. Articular facets are dorsally sloped, about 28° with respect to the transversal axis. Articular surfaces are drop-shaped as that of the prezygapophyses.

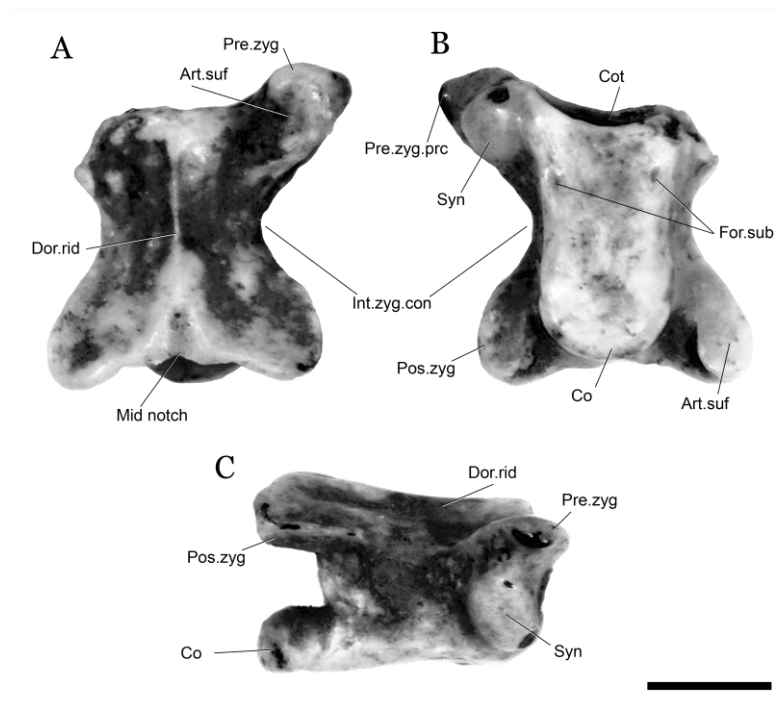
Dorsal surface is smooth. The neural spine is absent, but a sort of sagittal ridge is developed. Neural arc describes a convex curve, being more evident in anterior view than in posterior. There is no zygantra, nor zygosphene. In dorsal view, the anterior edge of the neural arch is almost straight, it lacks *pars tectiformis*, whereas posterior edge is mid notched. The median

notch is delimited both sides by a small convexity. Dorsal surface of the arch surrounding such median notch form a ridge V-shaped opening backward.

Neural canal has a semicircular shape, dorso-ventrally compressed anteriorly, and laterally compressed posteriorly. Posterior output is higher and wider than anterior. Due to sediment incrustations, it cannot be seen if paracotylar foramen is present. Ventral surface of the centrum is entirely flat and wide, without hemal keel, instead it presents a mid shallow groove. Lateral edges are almost parallel from the cotyle to the condyle. Both sides in anterior third of the body appear the outline of two foramina subcentralia.

Both the cotyle and condyle are flattened dorso-ventrally, they are twice as wide as high. In ventral view, the lower rim of the cotyle is regularly concave and posteriorly placed as compared to the dorsal rim. Condyle is moderately inclined dorsally, with articular surface slightly visible in ventral view. That is why dorsal edge of the condyle is placed more posteriorly than the ventral edge.

Figure 1. *Amphisbaena* fossil mid-body vertebra CZACC-1, in dorsal (A), ventral (B), and lateral (C) views. Scale bar = 1 mm.



(Source: Aranda, 2019)

3.2 Family Phyllodactylidae Gamble, Bauer, Greenbaum and Jackman, 2008

Genus Tarentola (Gray, 1831)

3.2.1 Frontal

Frontals of MNHNCu 73.5347 (I, II), and CZACC 3-I batches are present on the sample. They have a general cup-shape with a posterior base twice wider than anterior width, and two thirds wider than middle width (Figure 2). Dorsal surface is smooth in all samples. Total length varies between 11 and 12 mm.

Anterior region edge has a dorsal surface marked by three processes, and in a ventral level, it has a shelf between process, where articulate nasal bones. All three anterior processes are triangular, with the base of the middle seven times wider than lateral bases. This makes tiny the laterals process respect the middle. Also, its middle tip is more anterior projected than lateral tips. Anterior shelf describes a similar morphology than dorsal surface, with three processes, although with fewer width differences in bases. Anterior dorsal surface is a little concave, due to a depression of the central region. Antero-laterally emerges a convex shelf that goes from the latero-anterior process until the end of the anterior widened region. The shelf connects with a lateral scar in the first half of the lateral wall. Both the shelf and the scar function as articulation surfaces of prefrontal bones.

Frontal mid-region becomes narrow and widens in the posterior region. Posterior region develops lateral process both sides of the bone, each with a small foramen in the dorsal surface. Posterior edge is straight, sometimes slightly concave. It articulates with the parietal posteriorly and laterally develops a short shelf where articulate with postfrontals.

Ventrally frontal form a tunnel by the fusion in the midline of both cranial crests, closing the olfactory canal, an apomorphy of gekkotans (Gauthier et al., 2012). The tunnel is a little smaller than the total length, located almost in the middle of the bone. Transversal section of the tunnel is oval anteriorly, evolving backward to a triangle in the middle with round vertices, with the base upwards, and returning to an oval section in the posterior end. A low ridge runs along the midline of the tunnel roof. Three processes appear in the anterior edge of cranial crests: one central, anteriorly directed, with a pointed end, and irregular curved

lateral edges; and two laterals both sides of the central one, ventro-anteriorly directed, rounded.

A V-shaped scar open posteriorly in the ventral edge of the tunnel. Posterior edge of this scar is slightly projected ventrally, only 5347-II this posterior edge become a ventral keel, that differentiate from the straight border of the tunnel in lateral view. Posterior borders of crista cranii diverge into branches after the V-scar, opens forming another V, ending in each postero-lateral process.

3.2.2 Parietal

Parietals are flat and smooth. All samples are from the MNHNCu 73.5343 (I, II, III, IV) batch, with four variations. Only 5343-I (Figure 3) present single, strongly fused parietals, without medial articulation mark, rest are half parietals from paired parietals (Figure 4). Paired parietals present a straight medial edge that forms almost a right angle with the anterior edge, however, most of the middle corners are broken. Anterior edge is straight, with pointed processes in lateral corners, antero-laterally oriented. A small and shallow concave curve in the anterior edges precedes medially the process.

A constriction marks the middle lateral edge of parietals. It appears a little before the imaginary line that divided anterior half from posterior. In most samples, the constriction penetrates about one-fifth or one-fourth the length of anterior edge, only in 5343-I constriction achieves one-third of the anterior border. Anterior to the constriction lateral edge is straight, posteriorly is convex, ending over the second third of the supratemporal process. From lateral constriction level emerge a low, postero-medially oriented, S-shaped crest, that reach the posterior edge, and ends in the postero-medial process of the parietal. In 5343-I, who have the two parietal halves fused, both crests together seem like a curly bracket turn back. In dorsal view, appear a narrow shelf behind the crest, however this shelf could be reduced as in 5343-III.

Posterior edge present a postero-medial process, that could be rounded or pointed, but this character seems modified according to the preservation process. Length of this process vary in the sample, from a third of the base of the process to a little more than half of it. Posterolateral corners develop elongated supratemporal process, posteriorly divergent. Antero-dorsally, this processes are relatively wide, due to the curve of the lateral parietal

edge, and posteriorly, they are latero-medially compressed, developing sharp dorsal and ventral crests. Dorsal crest occupies about two-thirds of the process, it could end dorsally (most fossil sample), or could ends in the lateral wall of the process (5343-IV).

Ventral surface has a general shape similar to dorsal surface but narrower, as consequence, appear a shelf on laterals. Each lateral edges of the ventral surface present a cranial crest diverging anteriorly. Crests gradually increase its high backward, ending in a peak, except in 5343-I and -IV. A narrow groove accompanied the crest medially. Anteriorly, between cranial crests, occur two concavities each side of the midline. In 5343-I both elevations are separated by a low mid-crest. A transversal crest appear a little anterior to the posterior edge of the parietal. This transversal crest goes from one ventral crest to the other, and forms a right angle with the mid-crest.

Cranial crests and supratemporal process define a continuous and concave wall in lateral view, with the dorsal surface above of it. Two foramina are present, one in the anterior end of the wall and another about the middle. Fossil parietals 5343-I have characters that belong to the genus *Tarentola*, but they differ from *T. americana* in the aforementioned morphological structure, so they must belong to a species of new record for Cuba. In addition to being a rare record of fused parietals within Gekkonidae.

3.2.3 Occipitals, prootics and sphenoid

Sample has occipitals elements, prootics and sphenoid fused, forming a solid unit. Exemplar 73.5342-I present one complex of supraoccipital, exoccipital, basioccipital and prootics; 73.5342-II presents other two presenting the same bones before, adding the sphenoid (Figure 5); 73.5342-III presents other two, and 73.5342-V presents two loose sphenoids. All exemplars lost basipterygoid process of the sphenoid.

Supraoccipital form the postero-dorsal arc of the braincase, and the superior arc of the foramen magnum. It articulates postero-laterally with exoccipitals and antero-laterally with prootics. The supraoccipital crest raised in all the antero-posterior mid-line, from the highest point of the foramen magnum until upper point of the supraoccipital. Supraoccipital present a single, medial, *processus ascendens*, with a low trilobed dorsal edge, character observed in specimens of *Tarentola*.

Lateral face of the supraoccipital is separated from their posterior face by a postero-lateral crest, antero-laterally oriented. In 5342-I this crest is raised, and seems a circular arc, tapering the posterior half of the supraoccipital crest in lateral view; while in 5342-II, and -III is flattened, allowing to see the supraoccipital crest in lateral view. A ridge appears in the posterior surface of the bone, running ventro-laterally from the base of the *processus ascendens* until the posterior corner of the postero-lateral crest. Two grooves appear above and below the ridge, the ventral groove continues in the paraoccipital process dorsal groove of the exoccipital. Both the ridge and grooves of posterior face are absent in 5342-I and the observed *Tarentola*. Supraoccipital develops the upper part of tympanic bullae both sides of the braincase. Tympanic bullae have round edges, they penetrate into the braincase leaving a small space in the dorsal half. Ventral half of the braincase remains wide.

Each exoccipital presents a paraoccipital process laterally oriented, forming an almost 90° angle with the antero-posterior axis. Processes are widened vertically, from the medial end to the lateral, however, all lateral ends are broken off. Posteriorly, a transversal ridge emerge in the upper half of the process, from the foramen magnum to the lateral end; leaving small grooves above and below in the process. Exoccipitals connect with antero-ventral border of prootics by the *crista prootica*, a sharp crest, ventro-laterally oriented. Latero-ventrally, exoccipital form the posterior edge of the foramen ovale, prootic form the anterior edge. Foramen ovale has its longer axis antero-posterior oriented, representing a little more than half of the occipital recess total length.

Basioccipital has an octagonal general shape in ventral view, with the postero-lateral sides concave. Anterior side articulate with sphenoid bone in a slight W-shaped suture posteriorly oriented, but only 5342-II preserved this suture. Each lateral side possesses a spheno-occipital tubercle, ventrally oriented. Spheno-occipital tubercles have convex edges that converge ventrally in a pointed end. They are ventro-laterally oriented, except in 5342-III that are ventrally oriented. Tubercle lateral side is open in the occipital recess, who has a drop-water shape ventrally inclined in the longitudinal axis. Latero-ventral exoccipital edge forms the *crista interfenestralis* (anterior edge) of the occipital recess, while basioccipital form the *crista tuberalis* (posterior edge).

At the posterior end, basioccipital present the medial part of the occipital condyle. Postero-ventral end of the exoccipital form lateral parts of the condyle. Condyle is bean-shaped with the convex edge turned down. All fossil sample present the three parts fused as a unit. Basioccipital part is retired ventral and anteriorly, leaving a central space where articulates the odontoid process of the atlas-axis complex.

Sphenoid bone appears articulated in 5342-II,-III, and loose in 5342-V. Besides the articulation postero-ventrally with the basioccipital, it articulates postero-dorsally with prootics. It has a general square-shaped body, with two elongated basipterygoid processes in antero-lateral corners, about 1.2 times longer than sphenoid body length. Basipterygoid process has expanded anterior ends. Anteriorly sphenoid possess a *sella turcica*, characterized by an elevated, concave *dorsum sellae*, higher on the lateral alar processes than in the middle. A foramen for the abducens nerve open anteriorly a little above the center of each alar process.

Anterior vidian canal open between the medial wall of the basipterygoid process and a descending plate of the *dorsum sellae*, until the medial antero-ventral edge of the sphenoid. Both descending plates form the hypophysial fossa, in the center of the *sella turcica*. Only 5342-V preserves a complete anterior edge of this fossa, base of two small and cylindrical *trabeculae cranii* antero-dorsally oriented, continuing posteriorly in two low *cristae trabeculares*. A pair of internal carotid foramina opens both lateral sides of the fossa.

Laterally, sphenoid has the entocarotid fossa (Daza et al., 2008), delimited dorsally by the lateral edge of the alar process and ventrally by the ventral edge of the basipterygoid process. Behind this fossa occur the lateral opening of the vidian canal. Ventral surface has a depressed central area, with two small foramina inside.

Prootics are a pair of bones that articulates dorso-posteriorly with supraoccipital, posteriorly with exoccipital, postero-ventrally with basioccipital, and ventro-anteriorly with sphenoid. It is free anteriorly and dorso-anteriorly. They present a great alar process, antero-dorsally oriented. This process, latero-medially compressed, is triangular, with the base postero-ventrally oriented. Medially, a deep groove accompanied alar process base from about the middle until the postero-dorsal end, reaching the supraoccipital.

Laterally, crista prootica is divided into three sections, an antero-lateral shelf, postero-dorsal oriented; a short, postero-ventral crest, a ventral continuation of the anterior edge of the alar process; and a slight concave curve from the alar process base to the postero-medial region in articulation with exoccipital. Anterior shelf articulates medially with alar process of the sphenoid and is characterized by the foramen for the trigeminal nerve in their dorso-medial corner.

3.2.4 Pterygoid

Twenty-one pterygoids appear in the MNHNCu 73.5351 sample. All S-shaped, with palatine ramus, widened and quadrate ramus slender and elongated (Figure 6). Palatine ramus lateral edge is convex, ending anteriorly in a slender and pointed ectopterygoid process anteriorly oriented. Medial edge is concave, ending anteriorly in a thin triangular palatine process medially oriented. Between both edges, there is a thin plate, slightly depressed dorsally where lies the ocular globe. Anterior edge is transversely convex. A notch appears on the antero-lateral margin of the plate. This notch defines the ectopterygoid process in lateral edge. An articulation facet with palatine appears on the palatine process base.

Lateral edge of the palatine process has a coronoid facet, drop-shaped, whose edges emerges dorsal- and ventrally to form a low crests on each plane. Ventrally, a row of foramina could be seen around the plate margins.

Posteriorly, pterygoid possess the quadrate ramus. In the transition region from palatine to quadrate ramus appear some foramina of variable position and diameter. Quadrate ramus is slender, elongated, laterally concave, a little longer than half pterygoid. Anterior region of quadrate ramus is marked by a deep, semispherical fossa columellae (Evans, 2008), where ventral end of epipterygoid is inserted. Next to the fossa, on the medial edge, there is a drop-shaped basipterygoid facet, where articulates basipterygoid process of the sphenoid. Dorsal border of the facet rises over the fossa columellae level, developing a short, round crest.

Posterior to the fossa columellae, appear a deep groove, almost half the width of the ramus. It closing posteriorly towards the medial side, at the same time, that opens the quadrate articular facet on the lateral side. However, sometimes the groove could be dorsally connected with quadrate facet, being the latter a continuation of the former.

3.2.5 Maxilla

Samples of CZACC 3-II and MNHNCu 73.5345 (Figure 7 A, B) have phyllodactylid maxillas. Dental series define a straight line, except anteriorly that slightly curves inwards. Teeth are small, homodonts, pleurodonts, cylindrical and acute. Central ones of both the maxilla and dentary are about 1.3 times larger than the anterior and 1.8 times than posterior ones. Teeth crowns are unicuspid, pointed, nearly straight, and curved lingually. A labial wall protects dental series, covering two-thirds of the teeth. Labial surface is smooth, pierced by two longitudinal rows of foramina, one above teeth, and another in the base of the ascendant facial process, a little higher than the first.

Anteriorly, maxilla presents a nasal shelf, triangular in dorsal view. Labial edge of this shelf form the ventral margin of the naris, also is anteriorly pointed. Lingual corner of the shelf develops the premaxillary process, round, antero-ventrally oriented, and longer than lateral point.

All samples have a dorsal region of ascending process broken off. The base of the process is about half the total length of maxilla, it rise with antero-posterior convex margins, and slightly tilt inward. A relatively big foramen occur in the antero-ventral face of the ascending process, corresponding to the superior opening of the alveolar canal. Above this foramen, the ascending process develops a nasal prominence with a central notch, seen in some samples.

A long shelf projects medially, above the dental series. It goes, in a horizontal plane, from behind the nasal shelf, until the posterior end of the bone. A round constriction divides nasal shelf from medial, at the same transversal level of the alveolar canal opening. Medial shelf widens under the ascending process region and narrows after it. A shallow longitudinal groove appears over the shelf within limits of the ascending process. The groove ends posteriorly in the posterior alveolar foramen. Maxilla ends posteriorly in a narrow, pointed process. Medially, this process develops a longitudinal cavity where articulates the jugal bar.

3.2.6 Dentary

Four localities present dentaries, corresponding to MNHNCu-73.5350, CZACC 2 (Figure 7 C, D), CZACC 3-III, and -7. Dentaries are thin, straight structures, except for its anterior end that slightly curve inward and downward. Teeth have the same structure than that of the maxilla,

small, homodonts, pleurodonts, cylindrical, unicusps, pointed, and tips curved lingually. Central teeth exceed anterior and posterior teeth. A Labial wall protects dental series, covering two-thirds of the teeth. Labial surface is smooth, pierced by a longitudinal row of foramina. A low crest occurs below the foramina.

Teeth are over a subdental shelf called *crista dentalis* (Oelrich, 1956). *Crista dentalis* is thin anteriorly and gradually increases in size backward, achieving half of the total height in the central region, and reaching the dorsal edge at the postero-dorsal point. Meckel's canal is closed lingually. It opens antero-ventrally in a foramen located in the mandibular symphysis facet. This facet is drop-shaped, located antero-laterally in the frontal face of the dentary. Ventrally in the symphysis surface appears a flat tubercle, postero-ventrally oriented.

A V-shaped scar appears in the posterior surface of the *crista dentalis*, that penetrates until the twelfth tooth counting from back to front in the dental series. Inside the V-scar, occurs a U-shaped notch, opening in the same direction of the scar, and smaller than this.

Posterior edge of dentary is marked by three pointed processes. Only CZACC 2 preserve all, the rest of exemplars have them broken off. Superior process emerges from the postero-dorsal edge and is the smallest of the three. Middle process, is a little longer than superior, both are closer one to each other, on the upper half of the lateral view. Between both processes, inserts lateral ramus of coronoid in a short, deep scar that penetrates until the penultimate tooth level. Inferior process of the dentary is the longest, about four times superior process, and twice the middle process. It emerges from the ventral posterior edge. Between them and the middle process creates a rounded notch where articulates the surangular.

3.2.7 Articular, Surangular.

Pieces of MNHNCu 73.5349-I (Figure 8), -II (Figure 9), and -III correspond to fusiform complex of the surangular and articular are present for one locality with three variations.

Surangular is a fusiform bone that forms the lateral wall of the mandibular fossa. Lateral surface differentiates in an external surface which is inserted between medial and ventral posterior processes of dentary, and an internal surface that enters in dental cavities. Surangular possess two foramina, one antero-dorsal, and another postero-dorsal. Latero-

dorsal area is flattened, separated from dorsal and latero-ventral areas by well-defined longitudinal keels, starting on the antero-dorsal foramen and ending on the condyle lateral edge. Both keels are longitudinal, ventral one is almost straight in lateral view, dorsal one is S-shaped, with the convex part anteriorly, and concave part posteriorly. Only 73.5349-III do not present an antero-dorsal foramen, and the latero-dorsal area is more rounded, with a slightly indication of ventral keel.

Mandibular fossa opens dorso-medially, is drop-shaped, with the widened part backward, and is about one-third of external surangular surface. Surangular wall is taller than articular one. Dorsally, surangular wall of 73.5349-II presents a flat surface near the condyle, not present in the rest of fossils or recent specimens. By the other side, articular wall present a groove dorsally, some did not preserve it, those whose did present a small crest on the medial edge of the groove. Anteriorly, mandibular fossa presents the posterior opening of the Meckel's canal. In those whose lacks anterior part of articular, it could be seen the way of this canal through the medial wall of the surangular.

Articular develop the mandibular condyle posterior to the mandibular fossa, about one fifth the length of the external surangular surface. The articular surface is almost circular, with a central, longitudinal crest that divided the surface into two concave halves. From the posterior of the medial half of the mandibular condyle emerge a large retroarticular process, as long, or slightly longer than mandibular condyle. Dorsal surface is concave, as a continuation of the concave surface on mandibular condyle. Lateral edges rise both sides the concave surface, developing two crests, tympanic crest (lateral) and medial crest (Oelrich, 1956). Both crests curve to lateral side and go widening backward. None of fossil exemplars preserve the posterior edge of this process. A *chorda tympani* foramen is present on the antero-medial corner, almost in the boundary with the mandibular condyle.

Gekkota insertae sedis

3.2.8 Vertebra

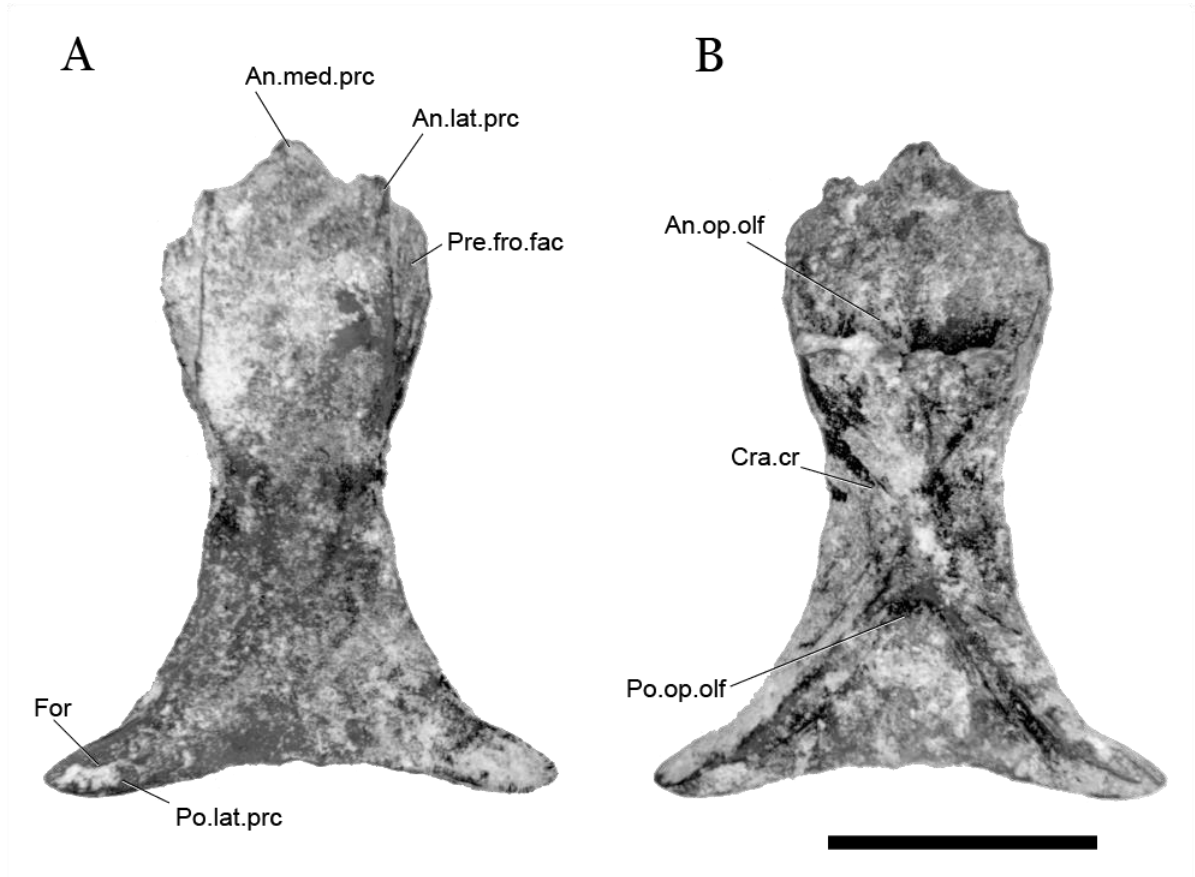
A vertebra of the middle of the body MNHNCu 73.5334 (Figure 10), appear too eroded by the taphonomic process. Its amphycelic condition is is a diagnostic character for the

Gekkota, within reptiles. The cotyle presents a roughness indication of insertions of cartilages, typical of young individuals. The posterior cavity is so eroded that it has an open hollow, possibly due to the low development of the tissue in juvenile ages.

The neural spine is low, slightly raised from the neural arch, with the same height all along, although the posterior part is eroded. The neural arch is low, and the neural canal has a semicircle transversal format. The canal presents a medial crest that divided the floor into two grooves. The pre- and postzygapophyses are reduced, slightly external and dorsally oriented. Vertebra does not conserve articular surfaces of the zygapophyses. The diapophyses were also lost. It presents the interzygapophysis constriction in the lateral walls of the vertebra. The hemal keel is low and short, the hypapophysis is absent. Both sides of the keel are shallow oval depressions, with presence of the foramina subcentralia, not aligned transversally.

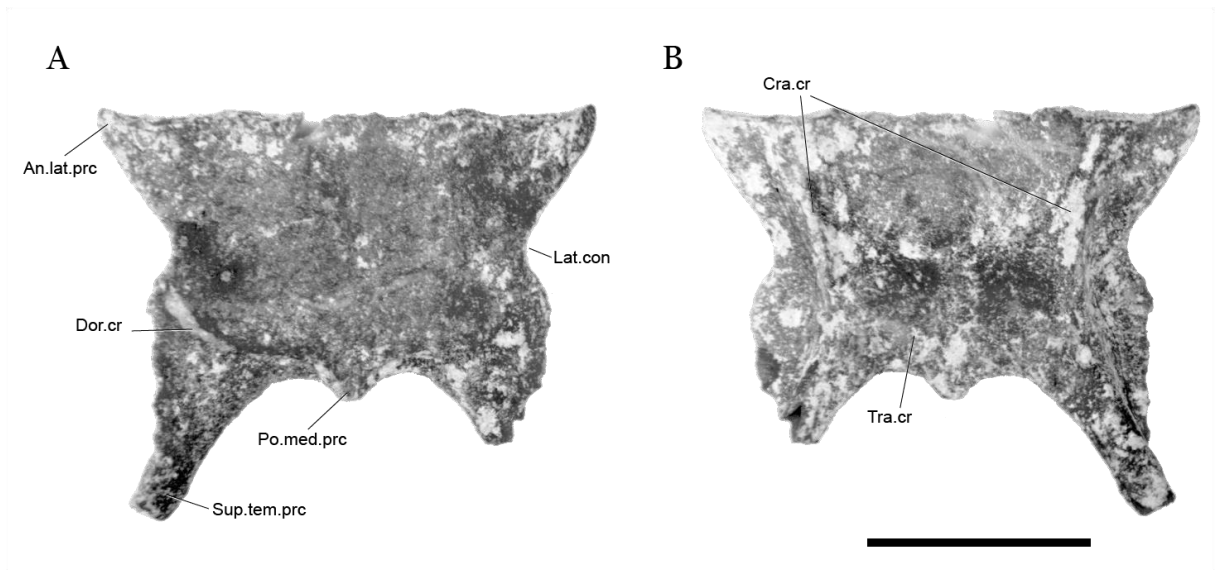
Zygantra and zygosphene, are above the plane of the pre- and postzygapophyses. The articular surfaces of the zygosphene are not conserved. In dorsal view, its anterior edge is plane, with round lateral ends. Posterior edge of the zygantra is lobed, convex in dorsal view, with a notch in the middle, where the neural spine ends. The articular facets of the zygantra are oblique and dorso-medially oriented. Before their articular surfaces, there are cavities, opened in their latero-dorsal walls.

Figure 2. *Tarentola* fossil frontal MNHNCu 73.5347-I in (A) dorsal and (B) ventral views. Scale bar = 5 mm.



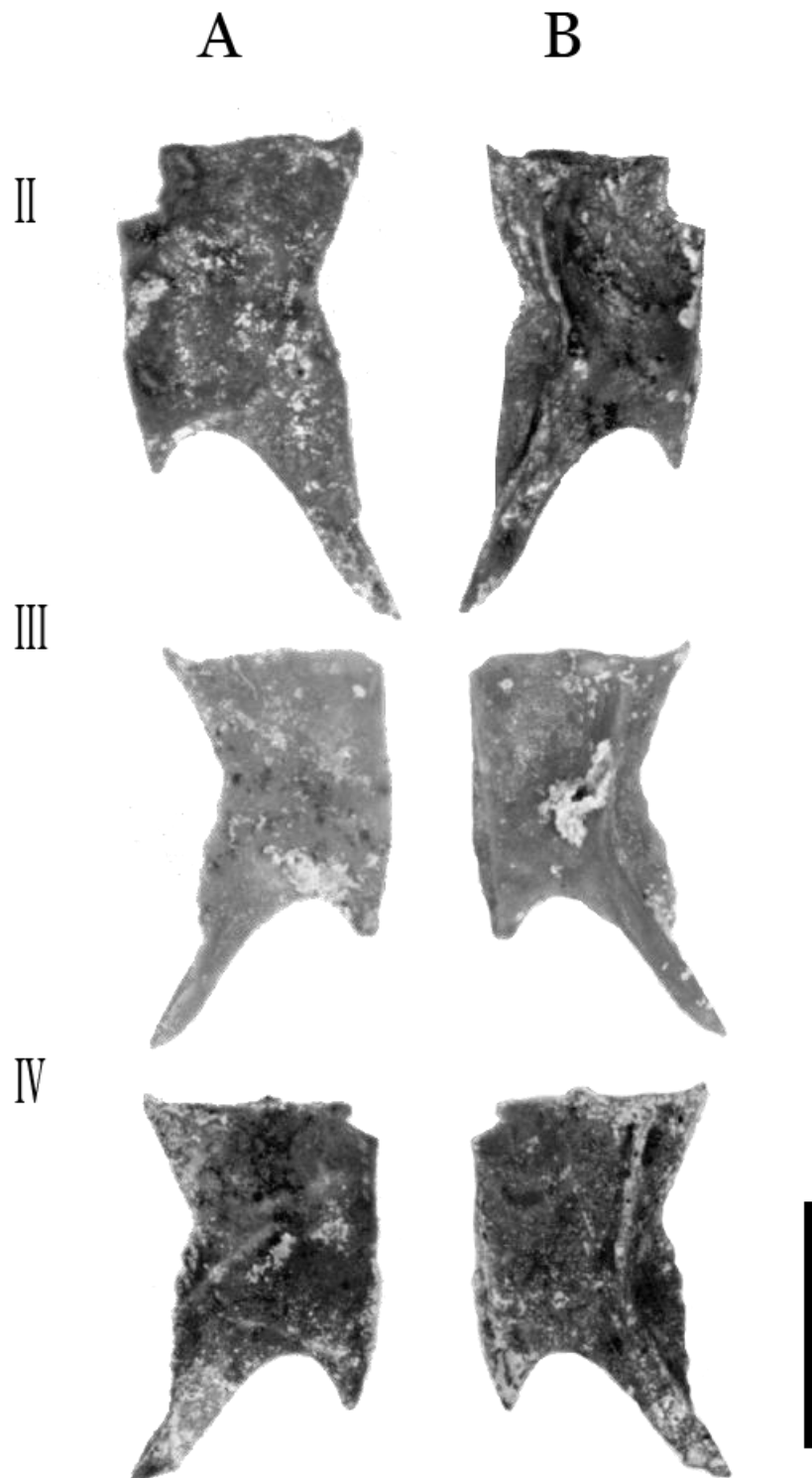
(Source: Aranda, 2019)

Figure 3. *Tarentola* fossil single parietal MNHNCu 73.5343-I in dorsal (A) and ventral (B) views. Scale bar = 5 mm.



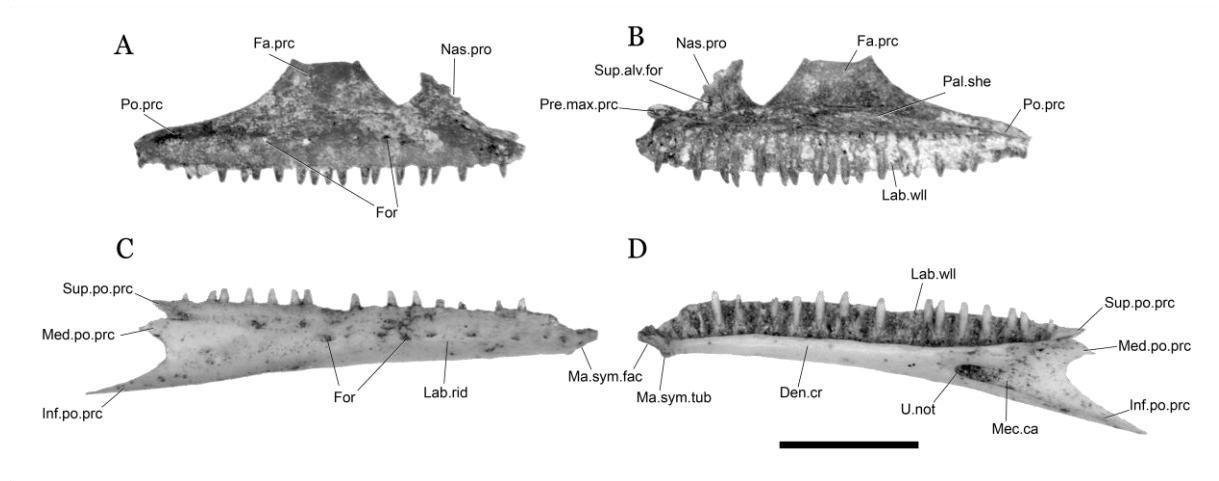
(Source: Aranda, 2019)

Figure 4. *Tarentola* fossil parietals MNHNCu 73.5343-II (right pair), -III (left pair), and -IV (left pair) in dorsal (A) and ventral (B) views. Scale bar = 5 mm.



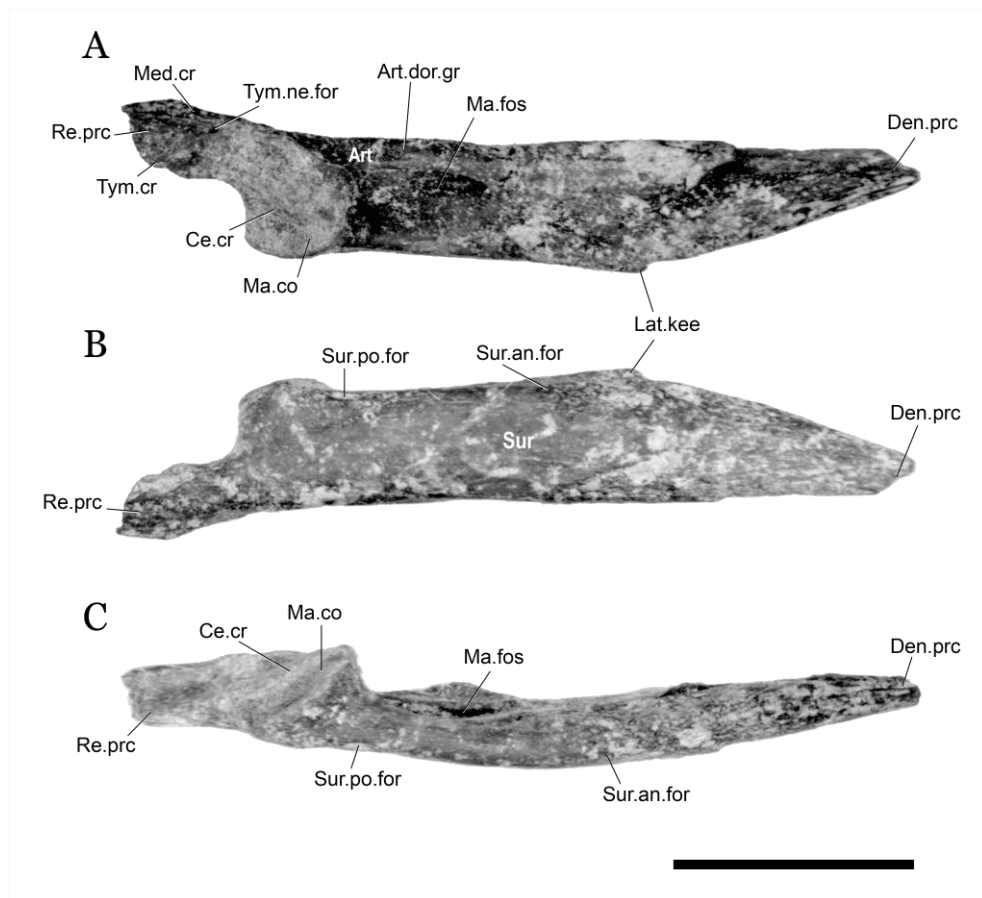
(Source: Aranda, 2019)

Figure 7. *Tarentola* fossil right maxilla MNHNCu 73.5345 (top) and right dentary CZACC 2 (bottom), in labial (A, C), and lingual (B, D) views. Scale bar = 5 mm.



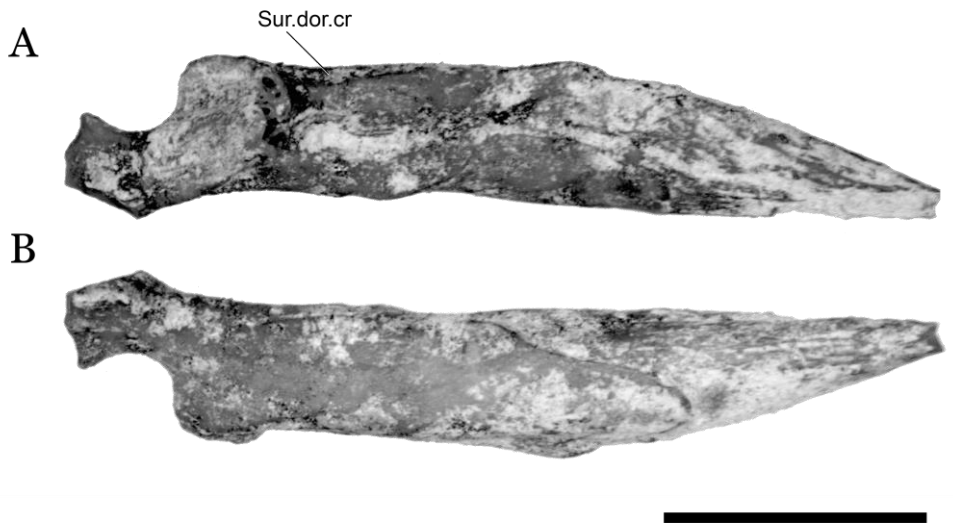
(Source: Aranda, 2019)

Figure 8. *Tarentola* fossil left articular and surangular MNHNCu 73.5349-I, in dorsal (A), ventral (B), and lateral (C) views. Scale bar = 5 mm.



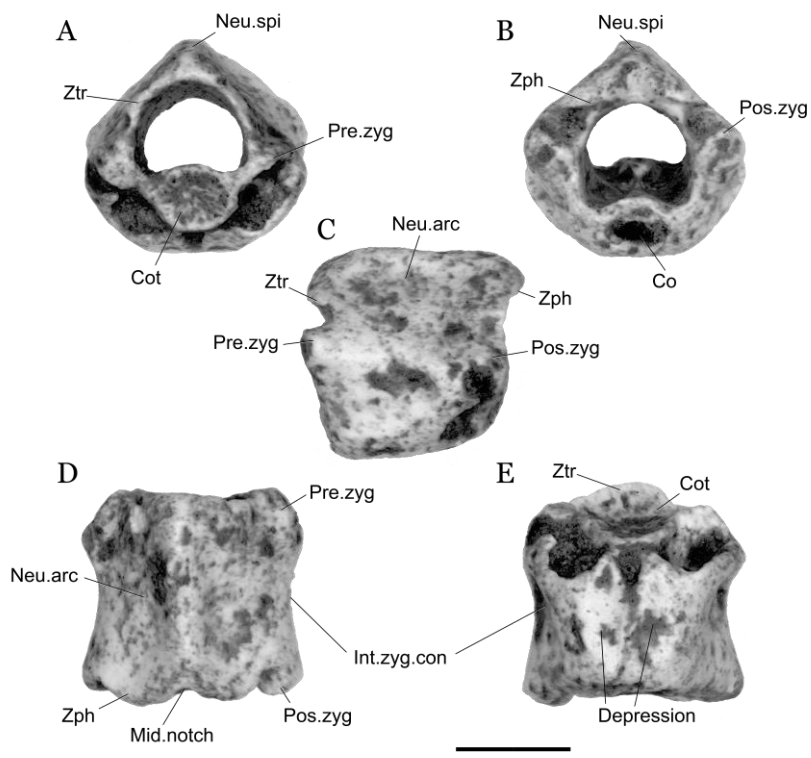
(Source: Aranda, 2019)

Figure 9. *Tarentola* fossil right articular and surangular MNHNCu 73.5349-II, in dorsal (A), and ventral (B) views. Scale bar = 5 mm.



(Source: Aranda, 2019)

Figure 10. *Gekkota insertae sedis*, fossil mid-body vertebra MNHNCu 73.5334, in anterior (A), posterior (B), lateral (C), dorsal (D), and ventral (E) views. Scale bar = 2 mm.



(Source: Aranda, 2019)

3.3 Family Teiidae Gray, 1827

Pholidoscelis auberi (Cocteau, 1838)

3.3.1 Frontal

Eight fossil frontals of CLV 3-I belong to Teiinae subfamily (Figure 11), all from the same locality. They present a cup-general shape, about 1.5 longer than wide. Lateral edges are concave, contributing dorsally to the orbit. Posterior base is about 1.6 times wider than anterior edge, and 2.3 times wider than the interorbital minimal width. Dorsal surface is rough, with small, blunt projections. A sulcus pattern is observed in the posterior half of the bone, describing a T-shaped anterior, linked by the posterior stem to the central peak of a W-shaped posterior. This pattern is an impression of the frontal scale boundary with frontoparietals, and of these with the interparietal (Harvey, Ugueto, & Gutberlet, 2012).

Anterior region present three triangular processes, one central about 1.4 times longer than both lateral or nasal processes. Mid-process in most exemplars is narrower than laterals, being 1.4 longer than the base width. Only one frontal presents a wider than long process. Posterior region presents two large postero-lateral processes, and another small, round mid-posterior process. Mid-posterior process inserts into the antero-central notch of the parietal.

Laterally, frontals develop cranial descending crests, in the first half of the bone. They are taller anteriorly than posteriorly. Almost the entire lateral surface of this crest is marked by a V-shaped facet, where articulates the prefrontal. Another V-shaped facet appears in the lateral side of the posterolateral process, where articulates the dorso-anterior end of the postfrontal. Ventrally, frontal present an open olfactory canal, delimited by both cranial crests. The roof of olfactory canal is domed, slightly divided into two lateral halves. Posterior half of frontal present a central, small keel. Both sides of the keel, surfaces appear slightly more elevated.

3.3.2 Parietal

Four parietals of CLV 3-II correspond to Teiinae morphology (Figure 12). From dorsal view, main body has an isosceles trapezoid-shaped, with the longest edge anteriorly, about 1.6 times wider than the posterior edge, and 1.5 longer than total length.

Anterior edge presents an antero-medial notch, where insert the postero-medial process of the frontal, and lateral round process on the corners. In lateral view, this lateral process forms the superior edge of a V-shaped deep facet where articulate postfrontal bones. Dorso-lateral edges are almost straight.

Dorsal surface is rough, with small, blunt projections. Two well-defined sulcus can be distinguished on surface, starting on both sides of the central notch of the anterior edge, almost to the posterior edge, where they meet in a round union, forming a U-shaped pattern. A pattern describing the mid-posterior edges of the interparietal scale (Harvey et al., 2012). Dorso-posterior edge has a slight, round W-shape, with a tiny central process. From postero-lateral corners emerge divergent supratemporal process, about the same length of the bone body. The opening average was 70°.

In lateral view, parietal present a descendent cranial crests from the antero-lateral process, until the posterior point of the supratemporal process. They have their most ventral point in the anterior half, the descendant process (Montero, Abdala, Moro, & Gallardo, 2004). Dorsal surface emerge over the descendant wall like a shelf, creating a cavity between both surfaces. In posterior view, descendant wall of the supratemporal process presents a central, V-shaped notch, that marks the parietal fossa. Two short, blunt processes appear each side of the notch, ventrally oriented. Ventrally, parietal roof is domed, together with descendant walls form the dorsal region of the braincase. The notches in the anterior and posterior edges are also noted from this view.

3.3.3 Maxilla

Fragmented maxillae of CLV 3-III represent this taxon (Figure 13), most pieces lack dorsal end of the facial process. Other pieces are fragments of the dental series. Dental series is located on a groove with labial and lingual wall, the second lower than the first. This structure gives the teeth a subpleurodont state (Presch, 1974). Posterior teeth are more robust than the anterior, with an intermediate pattern in the middle of dental series. Teeth are cylindrical in the base, they have two cusps in the crown, arranged on the antero-posterior axis. Anterior cusp is tiny and lower than posterior, which is higher and with a larger diameter. Some exemplars (CLV 3-II) present a third cusp in posterior teeth,

posteriorly to the main cusp and smaller than anterior cusp. Main cusp curve posterolingually, a character more pronounced in anterior teeth than in posterior.

Labial surface is smooth, with one row of foramina over the dental series, in addition to others scattered on the surface. Anteriorly, maxilla presents a nasal shelf, with a triangular antero-medial premaxillary process. Dorsal surface of this process is concave. A facial process rises dorsally, and slightly curve inwards. The base of this process is about half of the total length of the bone. Both the anterior and posterior margins curve into the bone, the anterior is more sloped. Posterior margin preserves the lacrimal and jugal articulation faces, nasal and prefrontal faces are broken off. From labial view, descending edge connects with raised dorsal edge of the posterior process of maxilla. Posterior process of the maxilla is about one-third of the total length of the bone, also it curves slightly towards the lateral.

Lingually, maxilla presents a palatal shelf over the dental series, throughout the longitudinal extension of the bone. A shallow groove occupies the shelf extension corresponding to the facial process. Facial process is between two large foramina, in frontal face appear the superior alveolar foramen, and in the posterior end, from the shelf, opens the posterior alveolar foramen. Behind the superior alveolar foramen, and over the palatal shelf appear a T-shaped base, lingually projected, where articulates the posterior region of the septomaxilla, and the antero-lateral edge of the vomer. Stem of the base is posteriorly sloped, and from the border of the posterior ramus appear a prominent semilunar crest, convex ridge that continues backward in the wall of the nasal capsule.

3.3.4 Dentary, Splenial, and Coronoid

Fossil dentaries belong to CLV 3-IV (Figure 14). Anterior end is acute and straight. Dentaries increase their size gradually backward, however, posterior third has a non-gradual increase, making an abrupt change in its width, besides curving labially. Dorsal edge of the dentary is slightly undulate, with two slight crests and troughs. Ventral edge of the dentary curve upward.

Labial surface is smooth, it presents a row of mental foramina along the dental series. Postero-dorsal surface is marked by a V-shaped scar where articulates the labial ramus of the coronoid. Posterior edge is concave in the ventral half, where articulate the angular and surangular bones.

Teeth have the same morphology of the maxilla, with a more frequency of tricuspid teeth and basal cement. Size and robustness of teeth gradually increase backward. Posterior teeth become from twice as many as four times as high as anterior teeth. Difference between posterior and middle teeth is smaller, from the same size up to 1.4 times higher. Labial wall is present and occupies from one third to half of the teeth.

Lingually, subdental border is high in the middle, about one third the total transversal section height. Posteriorly, it gradually becomes thinner. Meckel's canal is open, although not in all their extension. At the end of the dentary first half, dorsal and ventral edges of subdental border join but do not fused, and then open again gradually increasing their opening backward. Anterior opening of Meckel's canal is relatively shorter, about one-fifth to one-fourth of the total length. Posteriorly, Meckel's canal opens more than two-thirds the total height of the bone.

Three dentaries of the sample preserve the two anterior thirds of the splenial. This bone is inserted in the mid-posterior part of the lingual subdental region, where the meckel's canal open. It is a flat bone with a fine, triangular anterior process, that reach the anterior joining of the dorsal and ventral subdental edges. Mid-dorsally, splenial presents a large, oval inferior alveolar foramen. Antero-ventrally to this foramen, appears a small anterior mylohyoid foramen, circular in one, oval in another. A third exemplar presents two anterior mylohyoid foramina, instead of one as it could occur in Teiidae (Evans, 2008).

One exemplar preserve most part of coronoid articulated to postero-dorsal end of the dentary. Coronoid presents a blunt dorsal process, triangular-shaped. From this process descend two crests, one medial, and another lateral. Medial crests is almost perpendicular to the dentary antero-posterior axis. Lateral crests descend from the posterior edge of dorsal process, in an obtuse angle with antero-posterior axis, until the labial process of the coronoid. Antero-laterally, coronoid presents an elongated process that advances on dentary labial surface until the fourth tooth from back to front. Antero-medially, coronoid present a short process with a small central foramen, that does not pass the last tooth. This process has a straight anteroventral edge that articulates with splenial, and antero-dorsal edge articulates with the subdental border of the dentary. Coronoid posterior region is broken off.

3.3.5 Angular, Surangular and Articular

Pieces of CLV 2 correspond to posterior mandible bones (articular, angular, and surangular articulation) of Teiidae (Figure 15). Both have the anterior end, coronoid and dentary articulation fragmented and eroded, nevertheless they conserve the V-shaped scar anteriorly opened in the angular where the lower ramus of the dentary articulates. They present a deep mandibular fossa, medially oriented. The mandibular walls lost their anterior articular and surangular edges, however, it is possible to see that the articular edge is reduced until almost getting lost below the crest.

The angular presents a prominent lateral crest, with ornamentations in their ventral face, indicating a coossification with the skin. The crest continues from the angular to the articular until reaching the mandibular condyle. The angular articulates posteriorly with the articular. The articular has two well-defined processes, the angular and the retroarticular process. The former one is semioval, relatively wide at the base, and ventro-medial directed. Their posterior edge is almost perpendicular with the main axis of the piece; the anterior edge begins to come out, diagonally, in the middle of the mandibular fossa, until reach the lateral point of the process. The angular process present a well-defined medial ridge in dorsal view, that marks the posterior limit of the mandibular fossa and goes from the articular condyle until the end of the angular process.

The retroarticular process is U-shaped, relatively short and narrow, with parallel well-developed medial and tympanic crests. A shallow cavity is created between both crests. Anterior wall of the cavity is pierced by the chorda tympanica nerve foramen, just below the mandibular condyle. Retroarticular process connects with the angular process by a bony flange (Presch, 1970). The edge of the articular condyle form a convex oval, dorsally oriented.

3.3.6 Pelvic girdle

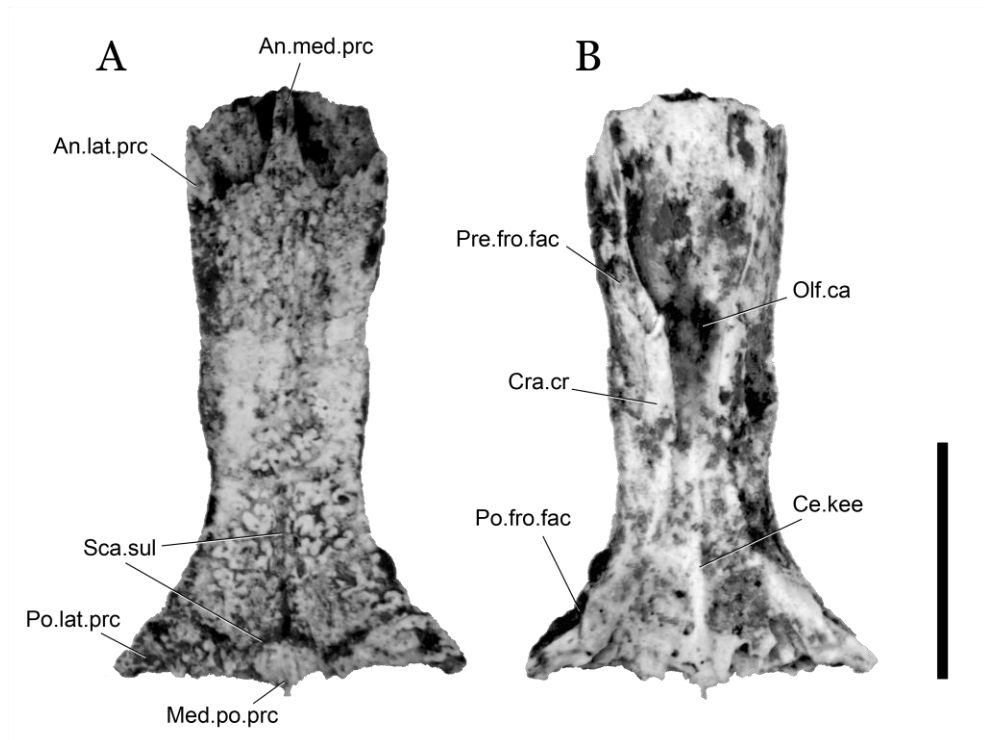
Pelves of MNHNCu 73.5312 belong to *Pholidoscelis* (Figure 16). Ischium, ilium, and pubis are firmly ankylosed forming the acetabulum. Acetabulum occupy all the central lateral face of the bone.

Ilium is almost twice the acetabulum diameter, about 2.2 times longer. It has a triangular shape with the base at the acetabulum articulation. It presents an elongated posterior

process that articulate with the backbone. This process turn on his own axis of about 30°, from vertical in the base, and oblique in the posterior end. Dorsally at the base, it presents a digitiform spine, with round tip, antero-laterally oriented. Ischium start from the ventral region of the acetabulu, almost as wide as its diameter. Ventral edge expands antero-posteriorly ventrally, with a long pointed anterior process.

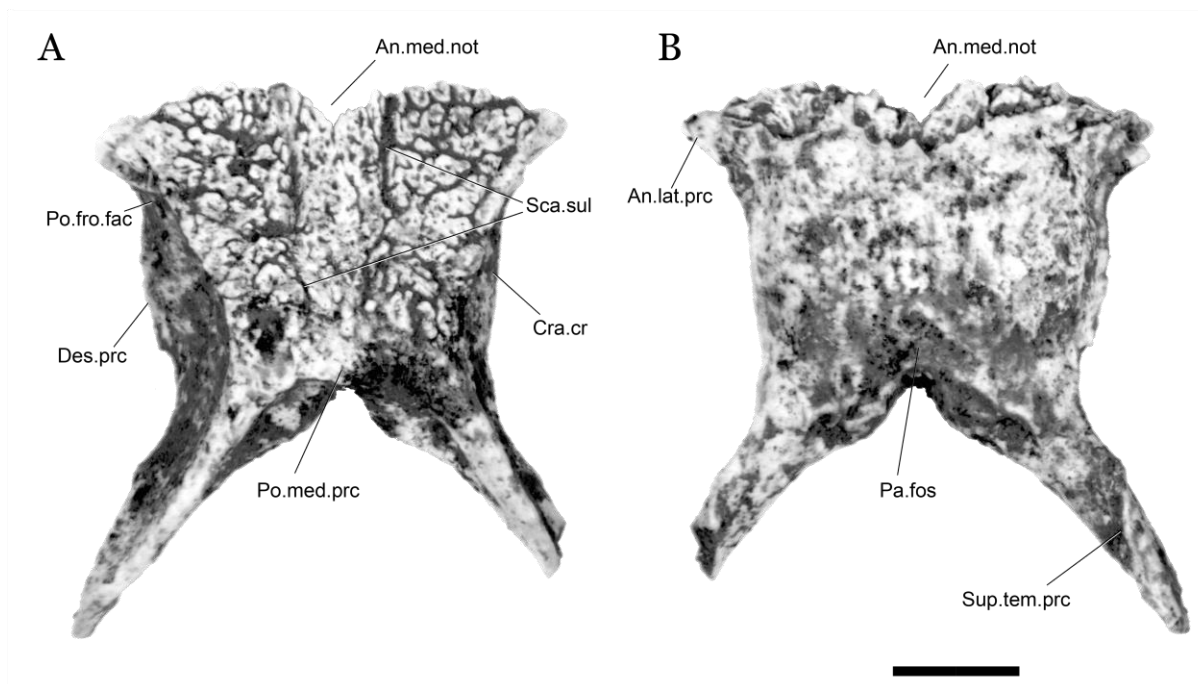
Pubis is convex outward, with the medial edge longer than the lateral edge. Lateral edge develops a round tubercle on their anterior end, ventrally oriented. A thin horizontal plate connects both edges. Dorsal surface is convex too, upward, leaving a medial line slightly higher than lateral and medial sides. Obturator foramen appear near acetabulum in the dorsal surface, postero-medially oriented. Anterior end of lateral edge posses a small pubic tubercle ventro-posteriorly oriented and curved inward.

Figure 11. *Pholidoscelis auberi* fossil frontal CLV 3-I in dorsal (A), and ventral (B) views. Scale bar = 5 mm.



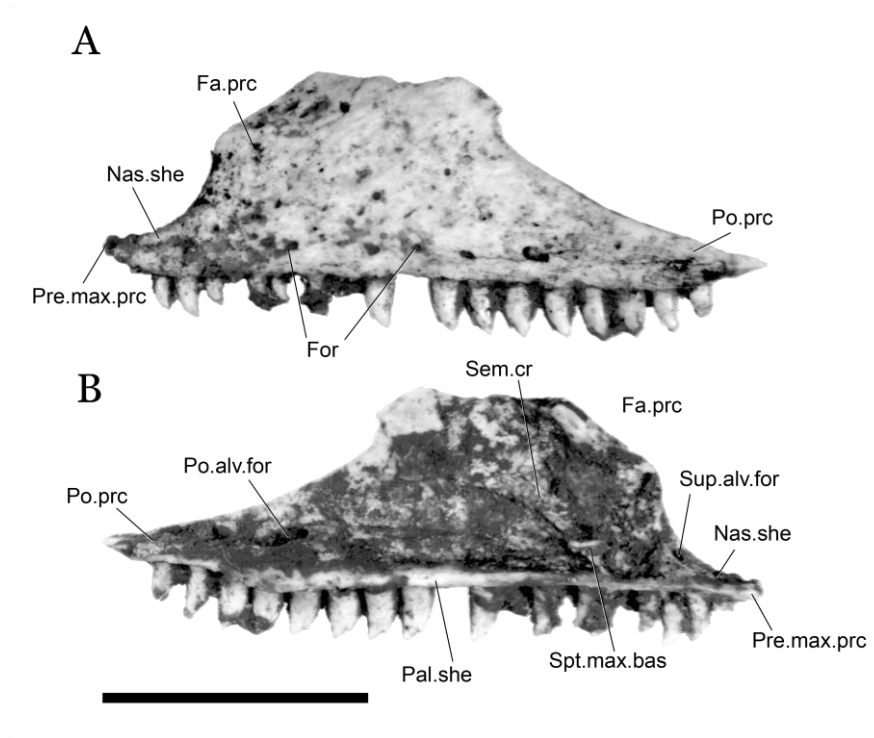
(Source: Aranda, 2019)

Figure 12. *Pholidoscelis auberi* fossil parietal CLV 3-II in dorsal (A), and ventral (B) views. Scale bar = 5 mm.



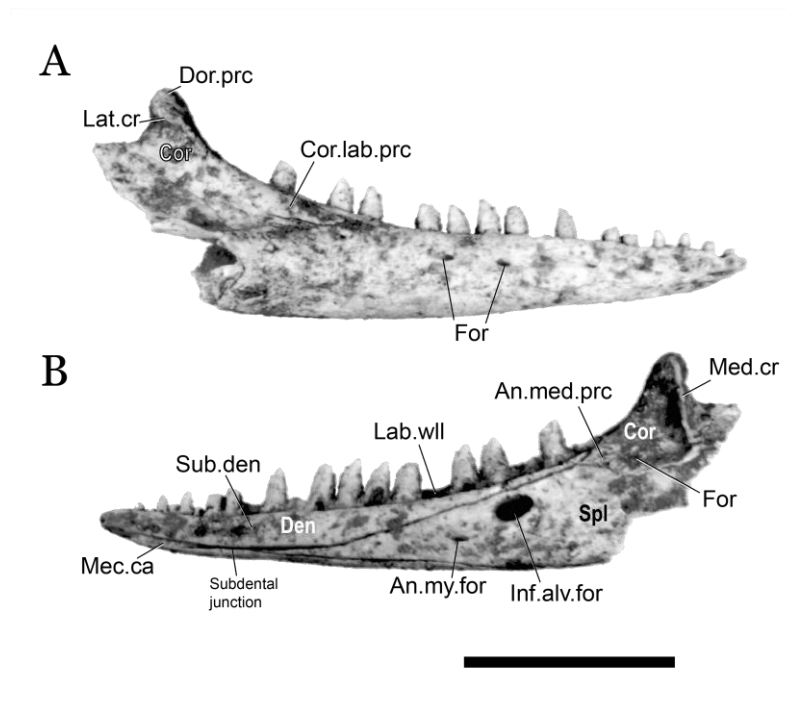
(Source: Aranda, 2019)

Figure 13. *Pholidoscelis auberi* fossil left maxilla CLV 3-III in labial (A), and lingual (B) views. Scale bar = 5 mm.



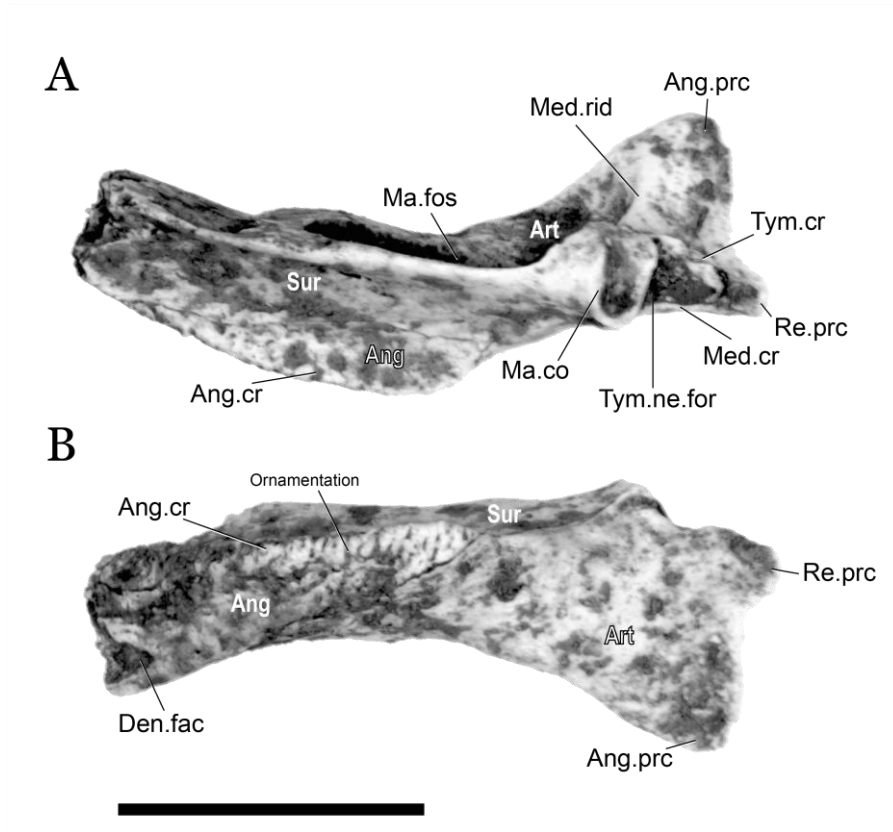
(Source: Aranda, 2019)

Figure 14. *Pholidoscelis auberi* fossil left anterior mandible CLV 3-IV: dentary, splenial and coronoid; in labial (A), and lingual (B) views. Scale bar = 5 mm.



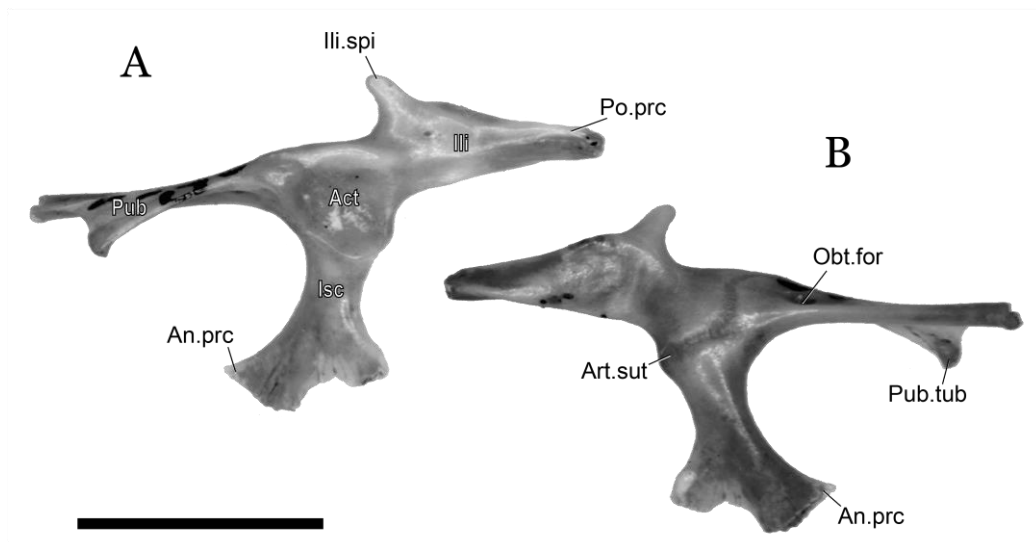
(Source: Aranda, 2019)

Figure 15. *Pholidoscelis auberi* left posterior mandible, articulation of articular, angular, and surangular bones CLV 2 in dorsal (A), and ventro-medially (B) views. Scale bar = 5 mm.



(Source: Aranda, 2019)

Figure 16. *Pholidoscelis auberi* right pelvis MNHNCu 73.5312 in lateral (A), and medial (B) views. Scale bar = 5 mm.



(Source: Aranda, 2019)

3.4 Family Leiocephalidae Frost, Etheridge, Janies and Titus, 2001

Genus Leiocephalus Gray 1827

3.4.1 Frontal

Fossil frontals from CLV 1-I, II, -III, -IV, CLV 6-I, II, -III, and -IV belong to Leiocephalus genus. They a general cup shape, elongated with a great widened posterior end, a narrow and short diaphysis, and a moderately widened anterior end (Figure 17). The posterior end is twice as wide as anterior end, and triples the diaphysis minimal width. All fossils have dermic coosification, which gives a rugose aspect to dorsal surface, without define sulcus of cephalic scales insertion. Frontals slightly curved downward, they present a convex aspect in lateral view, narrowest region being the one at highest point.

Rugose surface of anterior area presents three processes, two laterals nasal process, and a medial one, all with a triangular shape. Nasal processes are longer than medial one. In CLV 6 nasal process are more like fine crests over a shelf. Medial process is simple cusp, except for the tricuspid teeth in CLV 6-I (Figure 18C). Just below the rugose surface of the anterior area, occurs a smooth shelf that describes the forms of the lateral processes. In CLV 1-IV and CLV 6-I it is possible to see the medial process in ventral view (Figure 18). Rest of pieces the shelf hides the medial process. The shelf also expands laterally passing the nasals process.

Lateral margins are concave outwards. Its proximity in the middle of the bone makes the narrowest part of the piece. Posterior margin is straight, with a small notch in the middle, that corresponds to pineal foramen. In lateral view frontals present sharp cranial crests on both sides, that go from behind the anterior tip to the posterior end. Crests decrease their height backward until joint with the dorsal at the posterior end. They presents an anterior triangular facet where inserts the prefrontal, and a posterior, smaller, where inserts the postfrontal, both with the tips inwards. Anterior shelf occurs as a crest in the middle longitudinal line of the facets.

Between cranial crests open the olfactory canal, it becomes narrower in the diaphysis, and widened in anterior and posterior ends, more in the latter than in the first. Also in the diaphysis, the canal becomes less deep, after deepess part it continues with a central ridge dividing it in two halves. Only CLV 6-I do not present the central ridge. This ridge could be more or less wide.

3.4.2 Parietal

There are three single parietals belonging to genus *Leiocephalus*, CLV 1-V,-VI, and CLV 4-I (Figure 19). All conserve the central body of the bone, CLV 1-V and-VI lost the posterior endpoints, and CLV 4-I lost the left supratemporal ramus.

Parietals describe a low convex arc in anterior view. Anterior edge is straight, marked by process on the corners, laterally oriented. Postfrontal articulation facet appear on the lateral face of this process. In lateral view, fossils present smooth descendant cranial crests, slightly sloped from horizontal axis. Dorsally they have an isosceles trapezoid shape, with the larger bas anteriorly.

Supratemporal process on posterior corners are long and divergent. Dorsal surface is moderately rugose. It presents two curve sharp crests that start in anterolateral ends and tend to converge backward, describing a U-shaped ornamentation with a short horizontal baseline. From each corner of the dorsal crest baseline, emerge curve and sharp crests, that runs over the supratemporal process. Dorsal baseline and supratemporal process crests are relatively high and externally projected, between them it forms the parietal fossa.

3.4.3 Maxilla

Maxillae of *Leiocephalus* are composed by CLV 1-VII, CLV 6-V (Figure 20), and CZACC 4-I samples. They have no ornamentation on their labial surface. All have an ascending triangular facial process, where articulates nasal and prefrontal bones dorsally, and the lacrimal and jugal posteriorly. Frontal edge of the facial process is vertical in CLV 1-VII, and backward sloped in CLV 6-V and CZACC 4-I. Dorsal vertex of the facial process is located in the first third of the antero-posterior axis. A low keel rise from the antero-lateral part of the maxilla, until the prefrontal fact of the facial process. This keel divided the frontal from the lateral planes in the facial process. Facial process of CLV 6-V distingues by the presence of two dorsal lobes in the nasal and prefrontal facets, besides that the prefrontal facet form a nearly straight angle with the lacrimal-jugal facet. There are 5 to 7 labial foramina forming one supradental row, also there are few other foramina scattered in the labial surface. The jugal facet is long, reaching more than half of the facial process length.

First teeth are simple, bluntly conical and curve inward and slightly backward. Cuspitation is less prominent anterior teeth and becomes more conspicuous later. Posterior teeth are tall,

slender, straight-sided diaphysis, linguo-labially compressed to form a moderately sharp cutting edge, strongly tricuspid with a antero-posterior flared crown and curved inward. Anterior and posterior cusps of each tooth are smaller than the median cusp and separated from it by a groove that fades out at the base of the crown. Tricuspid teeth become closely crowded posteriorly, where the anterior cusp of each tooth is overlapped labially by the posterior cusp of the preceding tooth (Etheridge, 1965).

Anterior premaxillary process is bifurcated in two other small processes, a labial, on which there is a relatively big foramen, and a lingual, smaller. The dorsal surface of the premaxillary process is concave and forms part of the nasal cavity floor. On posterior process appears a relatively deep canal, where the jugal sutures to the maxilla. Superior alveolar foramen, located on the frontal wall of the facial process, is quite big. Posterior alveolar foramen opens on the palatal shelf, in the beginning of the last third of the bone. Palatal shelf extends lingually from anterior end to. It is convex upward, having their upper point about the middle. Dorsally, it has a triangular shape with a round lingual vertex. Posteriorly, maxilla develops a pointed posterior process, about one-fifth of the total length.

3.4.4 Dentary

About 60 dentaries revised correspond to *Leiocephalus*, belonging to different samples and morphologies, CLV 1-VIII,-IX,-X, CLV 5-I,-II, CZACC 4-II, 5, 6, 8, and MNHNCu 73.5041. In general they are big representatives of the genus (see Etheridge, 1965). Dorsal and ventral margins of dentaries are almost straight, except for the symphysis region that curved lingually, and dorsally, however, the dorsal inclination is little pronounced in CLV 1-X, due to the roundness of the anterior end (Figure 23). One of the diagnostic characters of *Leiocephalus* is the presence of vertical rows of small foramina in the narrow spaces between the teeth in lingual view (Etheridge, 1965). This character is present in all sample except in CLV 1-X.

Labial face of the dentary is smooth and convex (Figure 21). It presents among three and seven mental foramina. A large, shallow, and triangular depression in the postero-dorsal part of the labial face extends forwards, marking the former position of the labial process of the coronoid. Its penetration level varies from of the 20th to the 25th tooth, even into the same morphology.

Subdental border appears in lingual face, as a narrow shelf below the base of the tooth row. Teeth are like those of the maxilla, about half of them are protected labially by the labial wall. Meckel's canal is closed, leaving an elongated foramen in the region of the mandibular symphysis. Posteriorly, the subdental border bear a V-shaped notch where articulates the splenial, that extends anteriorly to the same level of the labial coronoid mark. The anterior inferior alveolar foramen occurs near this articulation. In CLV 1-VIII, CLV 5-I, and CZACC 4-II, dentary forms the alveolar foramen anterior border. Consequently, the dentary border adopts the oval shape of the foramen. In CLV 1-IX, and CZACC 5 is not observed the alveolar foramen border.

In some cases coronoid and splenial are present. Coronoid have four process, one dorsal, two medial, and one lateral. Dorsal process is relatively widened, elongated, laterally compressed, slightly curved backward, and with round tip. Dorsal line is oblique with respect to the longitudinal line of the dentary, so walls rotate in his vertical axis. Labially it presents an almost vertical fusiform groove. Lateral process is directed anteriorly, relatively large, triangular-shaped, with round anterior tip. Medial anterior process is positioned just behind the teeth series. Its ventral edge is concave, except that of CLV 1-IX (Figure 22), that present a central, triangular projection. None of fossils preserves posterior medial process. Just below the anterior medial process appear the anterior portion of the splenial, like a small finger. It presents two foramina. Most anterior and bigger foramen is the anterior inferior alveolar foramen, and the posterior and smaller is the anterior mylohyoid foramen.

3.4.5 Angular-Surangular-Articular complex

Exemplars CLV 1 (XI, XII, XIII), CLV 5 (III, IV, V, VI), and MNHNCu 73.5379 belong to *Leiocephalus*. All preserve articular and surangular bones, but just CLV 1 and CLV 5 preserve the angular bone (Figure 24), they even preserve the posterior end of the splenial and the postero-inferior ramus of the dentary. All pieces are broken off at the anterior ends of the articular and surangular, some also at the retroarticular process.

Angular is a small ventro-medial bone. External surface is oval-shaped, with two anterior processes, one medial, slender, and pointed, and another lateral, short, and round. Medial process is almost three times longer than the lateral. Posterior border of the oval is trilobulated, with irregular lobes. Angular articulates with the surangular laterally, with the

articular postero-medially, with the splenial antero-medially, and with the dentary anteriorly. CLV 1-XIII presents the posterior mylohyoid foramen in the edge of the base of the dorsal anterior process. Angular of CLV 1-XI do not present mylohyoid foramen. Although the size of the processes may vary, the posterior mylohyoid foramen is inside with the basis of the medial process.

Surangular is a fusiform bone that forms the lateral wall of the mandibular fossa. Laterally external surface is deeply forked anteriorly, developing a dorsal (longest) and a ventral (shortest) process. In the case of CLV 1 ventral process anterior tip is located behind the anterior surangular foramen. In CLV 5 and MNHNCu 73.5379 fossils, ventral process anterior tip is located before the anterior surangular foramen. The anterior surangular foramen occur in the ventral edge of the antero-dorsal process. Posteriorly it forms a cavity with raised walls, which articulates with the lateral side of the mandibular condyle. Laterally to this cavity occur the posterior surangular foramen. From the latero-ventral process to this last foramen, a low keel is present. Antero-dorsal surface, in front of the mandibular fossa, is flat and wide.

Mandibular fossa have a fusiform shape. Surangular wall is taller than articular one, what makes it opens dorso-medially. Articular is a dagger-shaped element with a posterior condylar part and a thin anterior process (Oelrich, 1956). Anterior process is flat dorsally and articulates with the flat process of the surangular. This flat zone is where articulates the posterior part of the coronoid. Posteriorly appears the mandibular condyle, hearth-shaped, with the lateral lobe slightly longer than the medial. Each lobe, sagittally divided by a low mid crest. Anterior round tip of the condyle projects antero-dorsally.

The angular process of the articular occur medially to the mandibular condyle, slightly curved forward. It appears relatively short, a little more than half wide of the mandibular condyle. In CLV 1 fossils, the angular process has a pointed tip (Figure 25), opening of 20.36° . In CLV 5 fossils angular process have a round tip, with an opening angle of between 13.07° (CLV 5-III) and 16.5° (CLV 5-IV).

Posterior to the mandibular condyle, occur the retroarticular process. It possesses two longitudinal crests that go from both corners of the condyle to the posterior transversal

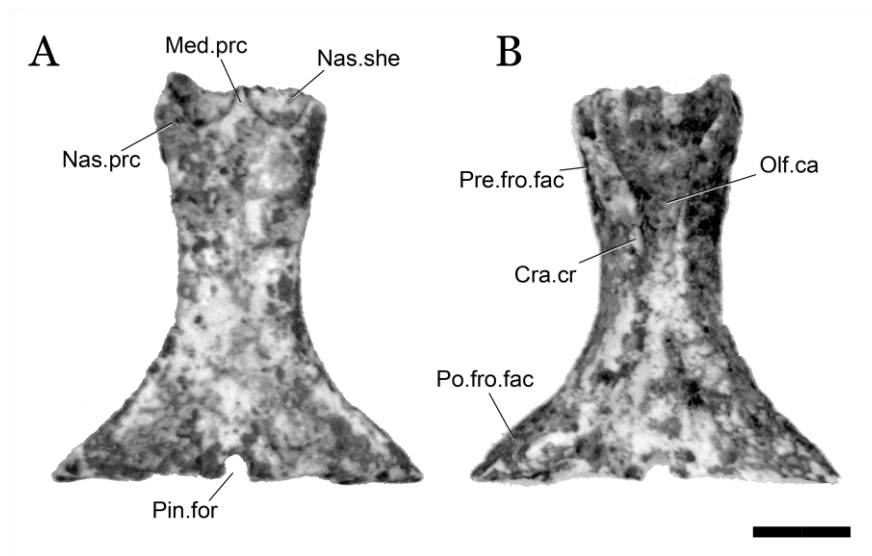
edge; tympanic crest (lateral), and medial crest. These crests seem parallel and define an almost rectangular fossa in the middle. In the antero-medial corner of the retroarticular fossa, occurs the chorda tympanica nerve foramen. From the postero-medial corner of the retroarticular process to the medial tip of the angular process appears a shelf. This shelf is slightly concave medially in all exemplars.

3.4.6 Pelvic girdle

Eleven pelves from CLV 4-II batch correspond to *Leiocephalus* (Figure 26). They have different preservation states. Ilium is present in the majority, sometimes incomplete, most ischia and pubes are fragmented or absent. Ischium, ilium, and pubis are firmly ankylosed, but not in all exemplars. In the meet point of three bones occur the acetabulum.

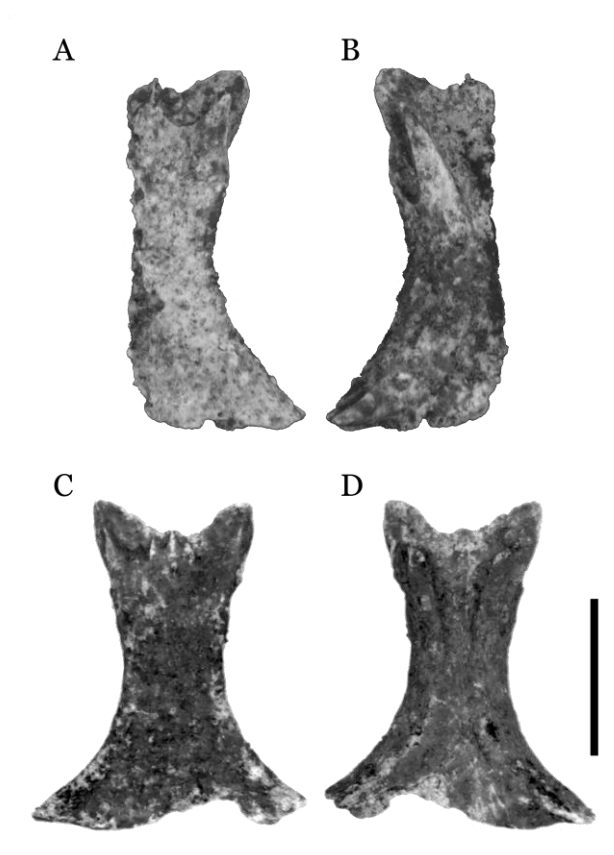
Ilium is more than twice longer than acetabulum diameter. It is a slender and latero-medially compress bone, with an evident widening in their anterior half. Medially at the wider section, it has a vertical impression like a scar, joining the dorsal and ventral edges. Dorsally at the base, it presents a triangular-shaped Ilium spine, with round dorsal tip, antero-laterally oriented. Laterally, from the posterior descendent edge of the spine, emerge a low horizontal crest that does not reach the midline of the ilium. Pubis is convex outward, with the medial edge longer than the lateral edge. A thin horizontal plate connects both edges. Medio-posteriorly in dorsal surface, appear the obturator foramen.

Figure 17. *Leiocephalus macropus* fossil frontal CLV 1-I in dorsal (A), and ventral (B) views. Scale bar = 2 mm.



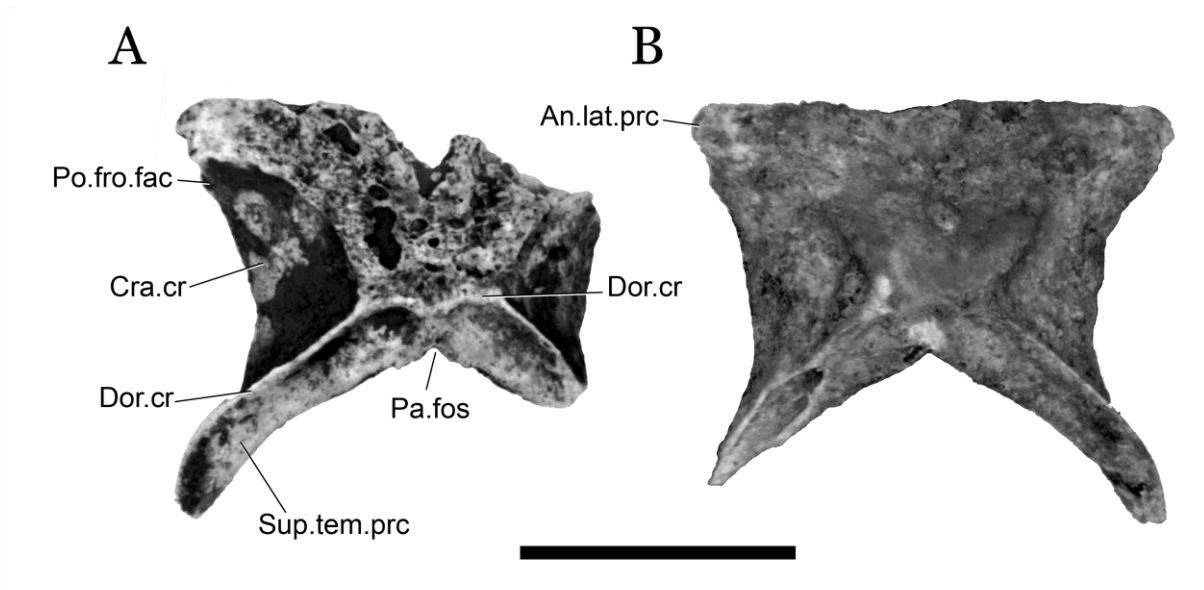
(Source: Aranda, 2019)

Figure 18. *Leiocephalus* fossil frontals of *L. carinatus* CLV 1-IV (A, B), and *Leiocephalus* sp. CLV 6-I (C, D) in dorsal (left), and ventral (right) views. Scale bar = 4 mm.



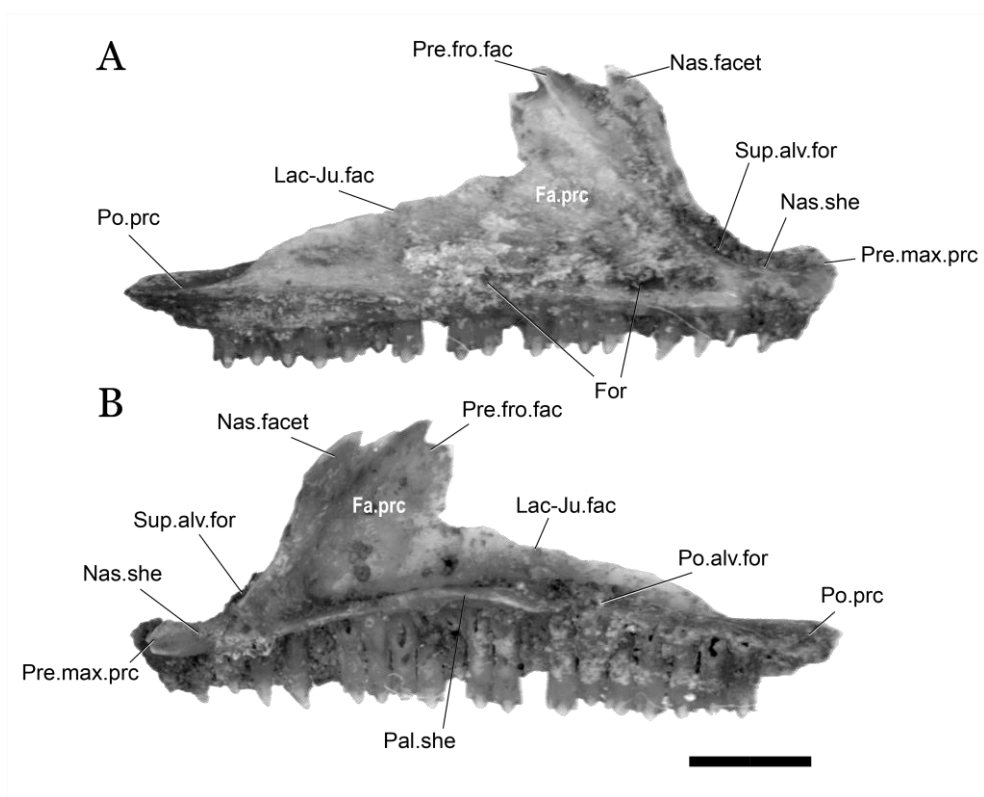
(Source: Aranda, 2019)

Figure 19. *Leiocephalus cubensis* fossil parietals CLV 1 -V (A) and CLV 4-I (B) in dorsal view. Scale bar = 5 mm.



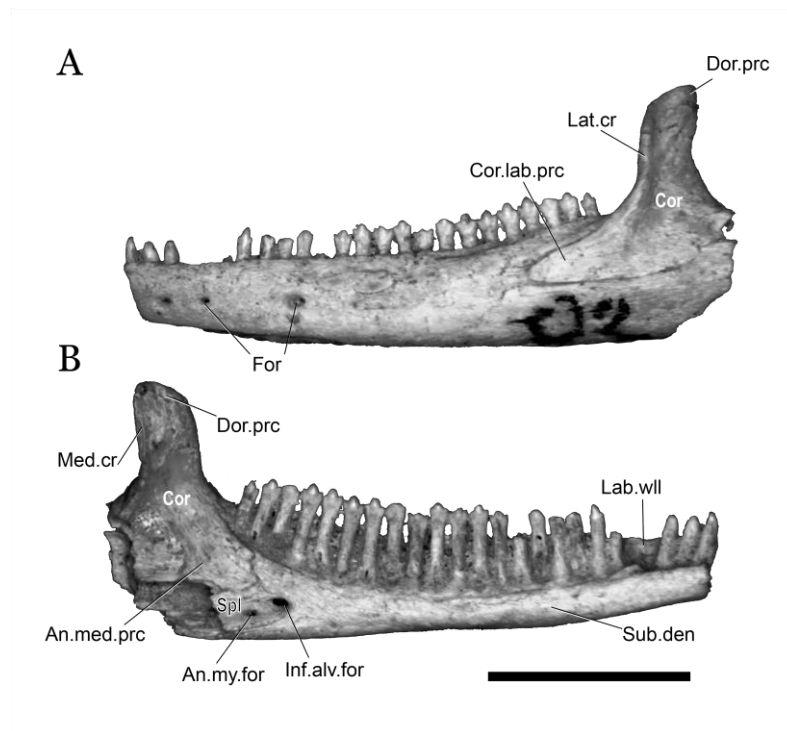
(Source: Aranda, 2019)

Figure 20. *Leiocephalus* sp. fossil right maxilla CLV 6-V in labial (A), and lingual (B) views. Scale bar = 2 mm.



(Source: Aranda, 2019)

Figure 21. *Leiocephalus* fossil left dentary CZACC 5 in labial (A), and lingual (B) views. Scale bar = 5 mm.



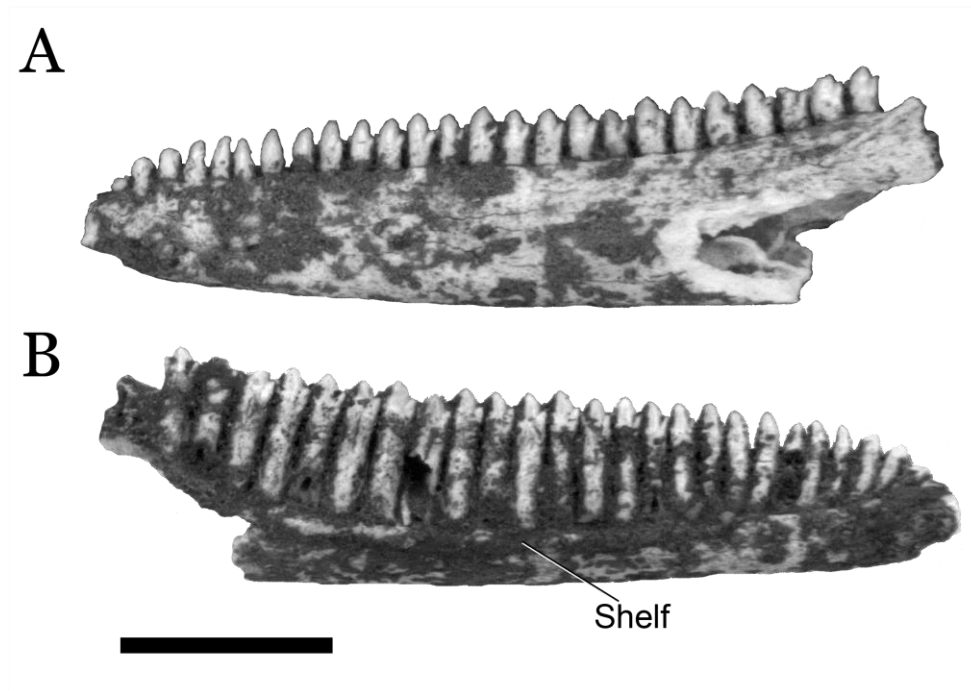
(Source: Aranda, 2019)

Figure 22. *Leiocephalus* fossil right dentary CLV 1-IX in labial (A), and lingual (B) views. Scale bar = 5 mm.



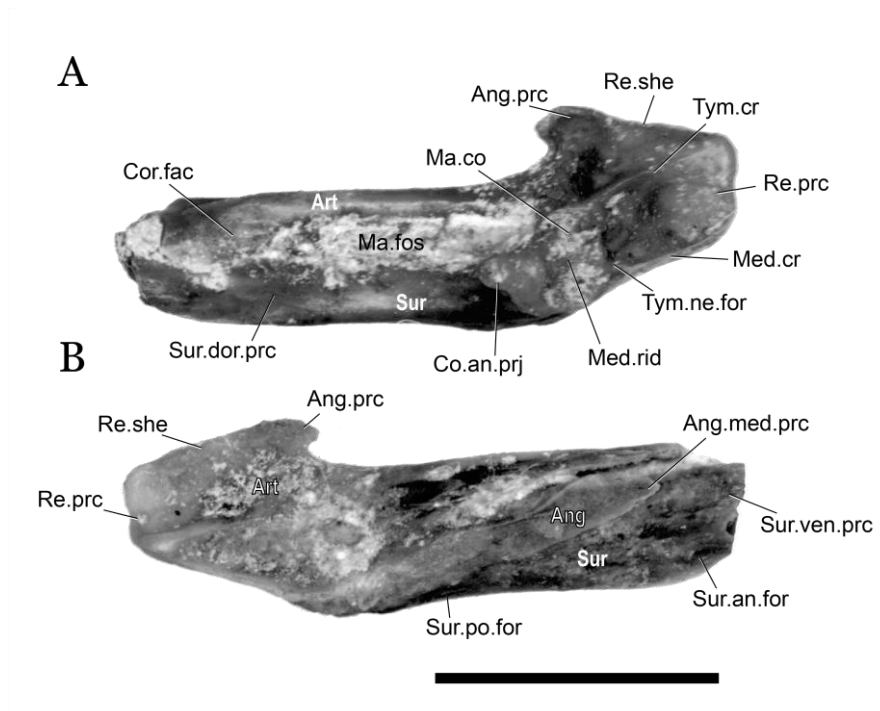
(Source: Aranda, 2019)

Figure 23. Fossil left dentary CLV 1-X in labial (A), and lingual (B) views. Scale bar = 5 mm.



(Source: Aranda, 2019)

Figure 24. *Leiocephalus* sp. fossil left posterior mandible (articular, angular and surangular) CLV 5-V in dorsal (A), and ventral (B) views. Scale bar = 5 mm.



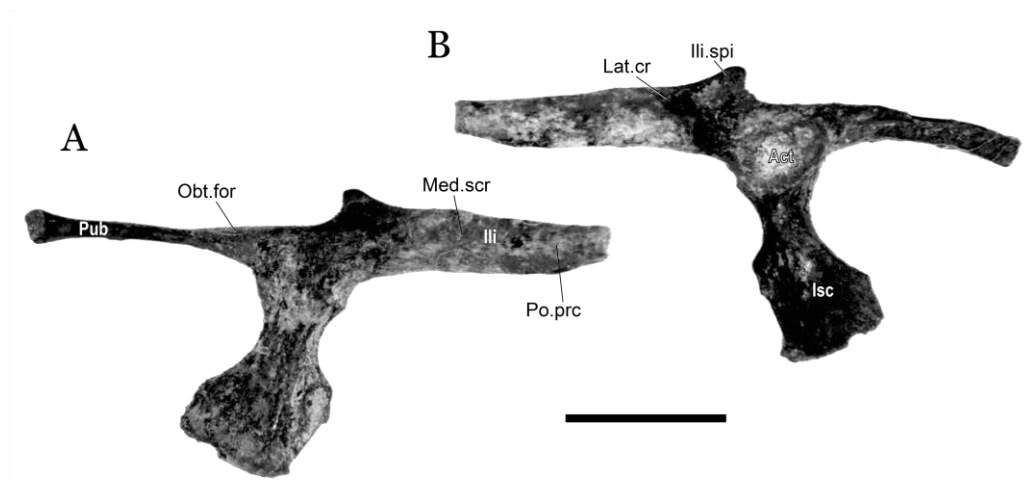
(Source: Aranda, 2019)

Figure 25. *Leiocephalus* cf. *carinatus* fossil right posterior mandibles (articular, angular and surangular) CLV 1-XI and -XII in dorsal views. Scale bar = 5 mm.



(Source: Aranda, 2019)

Figure 26. *Leiocephalus* sp. fossil left pelvis CLV 4 in medial (A), and lateral (B) views. Scale bar = 5 mm.



(Source: Aranda, 2019)

3.5 Family Boidae Gray 1825

Genus Chilabothrus Duméril and Bibron, 1844

3.5.1 Parietal

The piece MNHNCu 73.5311, is a robust, triangular parietal (Figure 27). The lateral sides of the parietal body form a well-defined globular area in the first half, that becomes thinner backward. It presents two robust supraorbital projections in the antero-lateral ends, perpendicular to the midline, with a wingspan more than two times the width of the globular area of the parietal. The lateral ends of these projections are eroded. A relative high sagittal crest occurs all over the dorsal midline of the parietal. The crest start above the level of the parietal roof. The crest turns taller in the posterior part of the parietal, as normally occurs in Boidae.

The dorsal suture with the frontals is W-shaped, with a little-pointed process in the middle, and two lateral round process each side, all three at the same horizontal plane. The lateral processes are more open than the globular area. The lateral process rises above the upper arc in frontal view of the parietal, they present frontal cavities for the articulation with the frontal. Laterally, parietal present descending process in the globular area, that descend of about one-third of total length. Anteriorly, this process surrounded a U-shaped opening, where pass the olfactory lobes of the brain.

Supratemporal process is well-develop, just behind the globular area. It is horizontal and flat, at the same level of the ventral surface of the postorbital projections. Posterior margin of the parietal form an elongate, slender and pointed processes.

3.5.2 Maxilla

Three specimens correspond to incomplete maxillae of *Chilabothrus*, MNHNCu 73.5029-I (Figure 28), 73.5322 (Figure 29), and CLV 9-I (Figure 30). In general aspect, maxilla is a slender long bone, concave towards the interior. The bone is laterally compressed in the first half, and dorso-ventrally flattened and swallow in the posterior half (suborbital and postorbital region). Tooth, when present, are conical and curved posteriorly. Dentition is heterodont (Kluge, 1991), they gradually pass from larger anterior tooth to shortest posterior. The total tooth count for 73.5029-I, the almost complete fossil, is 18th. Teeth

count of 12th until the ends of palatine process seems to be a stable character within the genus.

Maxillae are higher in anterior half, before the palatine process, and flattened in posterior half. Frontal edge of maxilla is backward oriented in 73.5029-I. Other two exemplars have them almost vertical, more verticalized in 73.5322. There are from three to four labial foramina, all directed anteriorly. Also, one or two foramina are present in a shallow groove on the antero-dorsal facet of the maxilla. The internal border of the groove match with a crest, more evident in larger exemplars (73.5322 and CLV 9-I).

All present two dorsal articular facets for the prefrontal. One anterior, over the body, just before the palatine process, and another posterior, over the same palatine process. Both appear as plane surfaces. The palatine process is prominent, relatively wide and long, postero-medially oriented. It presents two dorsal foramina, each accompanied by a shallow fossa on their fronts. Larger foramen is in the anterior edge, postero-medially oriented, and the smaller in the posterior edge of the process, posteriorly oriented. Anterior edge of the process rises diagonally to the principal axis of the maxilla. Lateral edge of the processes is curved. Posterior edge presents a notch like a hook.

Postorbital region of the maxilla (more complete in 73.5029-I) is shallow, tapering gradually to a point. At the beginning of this region appears a round, relatively medium size ectopterygoid process, medial side. Also, a medium size process appears on the lateral, slightly raised. Both processes mark the anterior edge of the ectopterygoid facet.

3.5.3 Pterygoid

Three specimens correspond to elongated, S-shaped pterygoids, MNHNCu 73.5335, 73.5380 (just a portion of the palatine ramus), and CLV 9-II (Figure 31). All present two rami, an anterior palatine ramus, medially curved, and the posterior quadrate ramus, longer and laterally curved. In *Eunectes* the palatine ramus is straight.

Palatal ramus is dentigerous, CLV 9-II counts 15 alveoli, 73.5380 counts 13, and 73.5335 has nine until the broken part. Most alveoli lack teeth, only the 73.5380 has some complete teeth, all relatively small. Teeth are conic, of smooth enamel surface, aligned in a single row, and with tooth tips recurved postero-medially. The dental series run through the middle of

the bone, describing the same curve of the palatine ramus, and ending in the middle of the transverse surface.

The palatine ramus is dorso-ventrally compressed. Anterior end is pointed, triangular-shaped in dorsal and ventral view. It presents one medial vertical palatine process, and two horizontal palatine facets both sides of this lamina. The palatine process has round edges that extend dorsal and anteriorly. Anterior edge sloped backward. In its postero-medially side open a foramen that connects to an internal canal.

Pterygoids expand transversally in the medial portion. Dorsally they present a deep depression. Laterally presents a well-developed, circular cavity that articulates with the ectopterygoid. Two foramina are present at the bottom of the cavity. In the ventral surface of the cavity, appear another, also present in recent individuals.

Two crests begin in middle region, one medially and another medio-ventrally, and continues backward until the articulation facet with the quadrate, leaving a medial deep groove, where attach the protractor pterygoid muscle (Gauthier et al., 2012). This groove starts opening medially, and gradually backward turns up, remain open until almost the posterior end. Posterior end is laterally compressed.

3.5.4 Quadrate

An almost complete quadrate (CLV 9-III) corresponds to the genus *Chilabothrus* (Figure 32). The quadrate is relatively broad dorsally, narrows centrally, and ends ventrally with a wide triangular-shaped base. Central column is straight, with about 60° of torsion between dorsal and ventral edges. Dorsally the bone is S-shaped, where the central and wider branch corresponds to the cephalic condyle. Cephalic and mandibular condyle articular surfaces are eroded, exposing the internal spongy tissue. Above the base present a constraint of the same width that the articular surface of the mandibular condyle.

The body present one lateral and pointed projection, small, but evident, located in the dorsal third of the bone. Medial edge presents a stylohyal process, oval facet, bigger than the anterior, located in the middle third of the bone. Articular surface of this process is eroded, just like the mandibular and cephalic condyles.

Quadrato antero-lateral surface is flat. Antero-medially, the quadrato present a deep V-shaped fossa, site of attachment for the abductor's muscle. The fossa opens from the constraint until the dorsal edge. This depth is reflected in the quadrato head making it wider laterally. Dorsal edge of the fossa ascends postero-medially oriented describing a curve, from the stylohyal process to the medial end of the cephalic condyle.

The base is triangular, preserves the mandibular condyle, but it lacks the pterygoid projection. Although eroded, the edges of the mandibular condyle are defined as a round M-shaped, shorter than the quadrato base length. The medial cusp of the "M" is higher than the lateral, and the middle notch is wide separate from the ventral margin. Posteriorly it defines a circumference arc that inflexes dorsally. Above the mandibular condyle, there is a semicircular fossa, on both the anterior and posterior faces. The anterior one presents a central foramen, also present in recent individuals.

3.5.5 Dentary

Four pieces correspond to almost complete dentaries of *Chilabothrus*, CLV 7-I, -II, CLV 9-IV (Figure 33), and MNHNCu 73.5029-II. The first two are considerably large, of 43.79 and 43.54 mm respectively. The anterior end is round, curved inward and slightly dorsally. The ventral axis of the bone is straight. Teeth are conic, of smooth enamel surface, and with tooth tips recurved postero-medially. Besides they are closely spaced, with Aletinophidian snakes implantation type (sensu Zaher & Rieppel, 1999). Alveoli and base of teeth are wider transversely than antero-posteriorly. Anterior teeth are wider and longer than the posterior ones. Size gradually decrease, having the first teeth more than twice as long as the last teeth.

The posterior region of the dentary is completely open, due to the U-shaped articulation with the compound bone. The anterior end of the articulation is located at the 10-11 alveoli of the dentary, what makes the dentary posterior region deeply forked, developing a dorsal and ventral acute process. The postero-dorsal process is long and dentigerous.

The subdental vertical border relatively high, approximately half the height in the middle section of the bone. Meckel's canal is completely open along its medial side, except under the first tooth range. It starts with a foramen, that open posteriorly, only CLV 7-I does not present a foramen, probably closed during life. Ventral margin stays straight from the

anterior to the posterior end. The dorsal margin is curved, begins to rise continuously about half the dentary.

The lateral output of the alveolar trigeminal nerve forms a single, big, oval mental foramen, with a shallow groove in his front. This foramen opens at the end of the first third of the bone, near the fifth tooth level, in antero-laterally direction.

All dentaries present a narrow shelf in the postero-medially region, above the Meckel's canal. This structure starts almost at the same level as the anterior margin of the compound bone suture by the lateral face. Dorsal surface of the shelf is almost horizontal, starts acute and become gradually wider backward, ending with a little notch at his posterior end. In medial view, this shelf has a V-shape groove where articulates the postero-dorsal border of the splenial.

3.5.6 Compound Bone

Four exemplars, 73.5328, CLV 8-I (Figure 35), -II (Figure 36), CLV 9-V (Figure 34), correspond to complete compound bones, a fusion of surangular, prearticular, and articular bones. All are complete, except for 73.5328 that anterior process of the surangular was fragmented.

In lateral view, the compound bone is a relatively high and robust bone. Surangular wall presents a fusiform lateral depression after the anterior process. Ventral edge of this depression rises in a long and curve shelf that could (CLV 8-I, and-II) or could not (73.5328, CLV 9-V) connects with the lateral prominence of the articular by a ridge. When present, this ridge connection occurs below the articular condyle. Anteriorly, this shelf is more laterally projected in CLV 8-II, moderately projected in 73.5328, and is reduced in CLV 8-I and CLV 9-V. Posteriorly, the shelf is more laterally projected in CLV 8-I and moderately projected in the other sample.

A long, round anterior surangular process occupies the first third of the bone, which enters between the two posterior prongs of the deeply bifurcated dentary. This process present dorsal and ventral canals (dorsal longer and deeper than ventral), where lies the postero-dorsal and postero-ventral processes of the dentary respectively. At the posterior end of the dorsal canal occur the anterior surangular foramen, situated at the base of the surangular crest, antero-laterally directed.

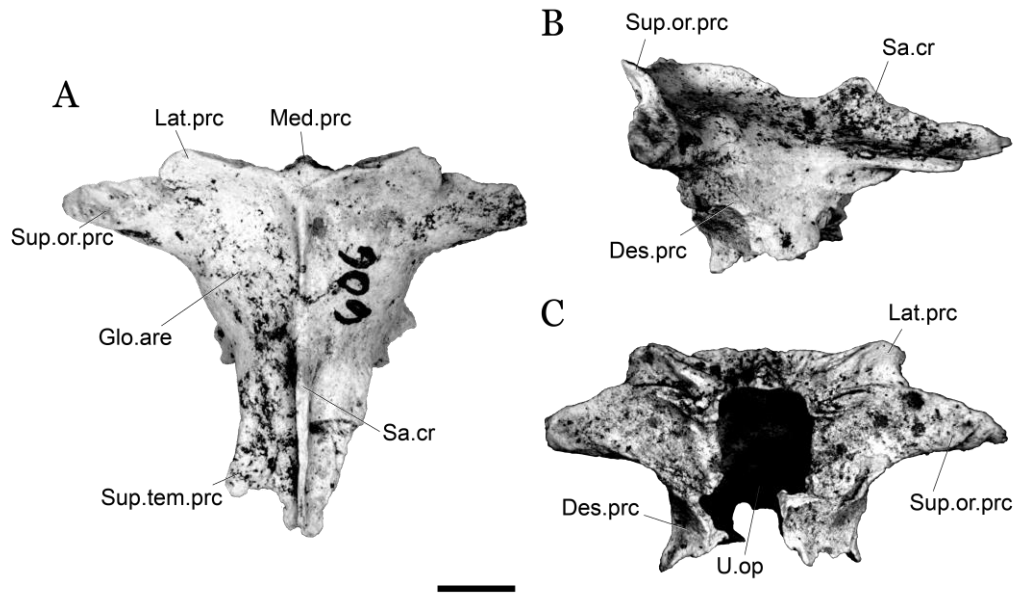
From the postero-medial half of the anterior surangular, process emerges a robust prominence in an acute angle with respect to the long axis of the compound bone. Dorsally, the prominence presents a groove where runs the coronoid and medially presents a V-shaped groove where articulates the angular. Near the posterior tip of the groove appear the second mylohyoid foramen, anterior to the apex of the surangular crest. It also presents two anterior prongs, one dorsal, and another ventral, both approximately the same size.

Both the prearticular and the surangular develop asymmetrical vertical crests. The crest margins reach their higher point in the anterior half of the bone and become lower in the posterior half until meeting the articular condyle. Surangular anterior part is like a peak, while the prearticular, is like a round hill. Also, the anterior part of the surangular is former and higher than that of the prearticular, and posterior margin of the prearticular is taller than that of the surangular. In antero-medial surface of the surangular crest, occurs a narrow triangular surface where articulates the coronoid. Only in CLV 8-I, anterior margin of prearticular crest is like a peak, both crests elevations approximate to the same high. The surangular posterior margin of the crest is slightly concave, unlike prearticular margin that is almost straight.

The surangular and prearticular crests form the walls of the deep mandibular fossa, which begins at the posterior margin of the coronoid and finish just anterior to the quadrate articulation. Mandibular fossa opens dorsally; its depth gradually decreases backward, until it is almost disappeared at posterior end. In CLV 8-I and 73.5328 lateral margins of the mandibular fossa diverge anteriorly, which gives the impression of a wider opening, in the rest of dentaries lateral margins tend to be parallel.

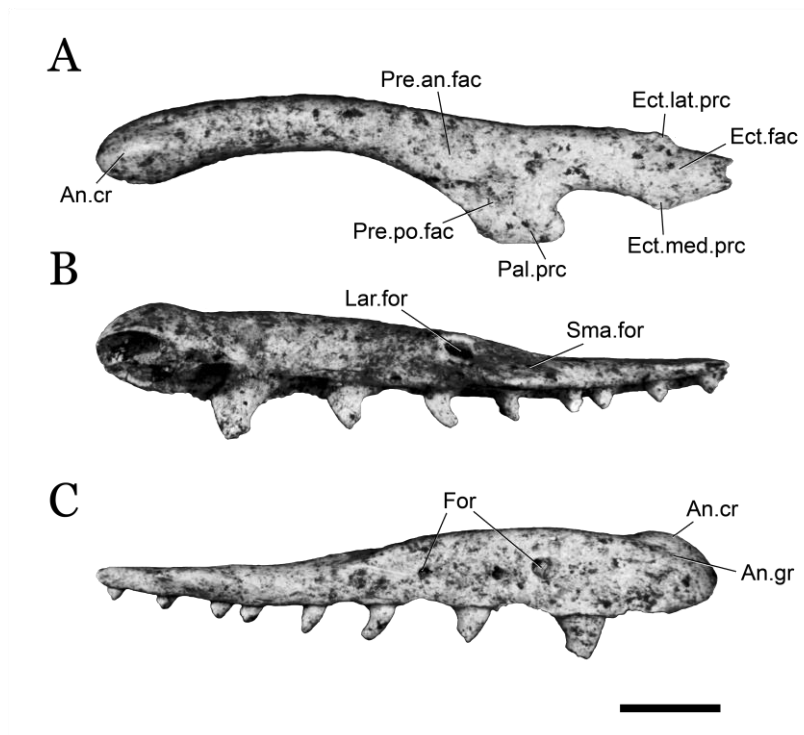
The articular condyle is relatively short, located posterior to both crests, and ventro-medially directed. It presents a medial ridge and two concave surfaces at both sides of this ridge that bend laterally. Anterior and posterior transversal rims of the articulation surface are raised and sharpened. The anterior is longer and higher than the posterior. Laterally, it presents a short, round prominence. Posterior to the articular condyle, it retains a round, short (shorter and narrower than condyle), and ventro-medially inflected retroarticular process. It posses a blunt spine below the condyle and a small foramen for the chorda tympani nerve at the anterior end of the medial surface.

Figure 27. *Chilabothrus angulifer* fossil parietal MNHNCu 73.5311 in dorsal (A), lateral (B), and anterior (C) views. Scale bar = 5 mm.



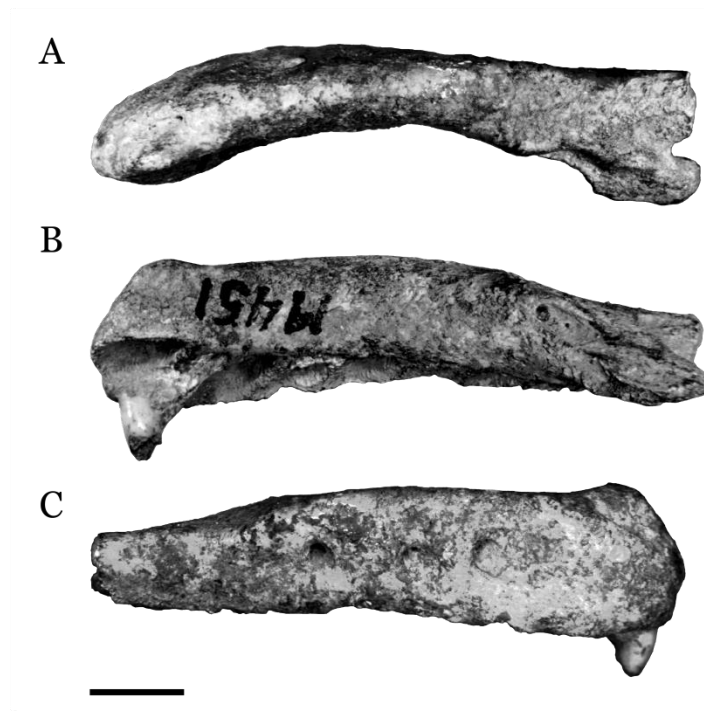
(Source: Aranda, 2019)

Figure 28. *Chilabothrus angulifer* fossil right maxilla MNHNCu 73.5029 in dorsal (A), lingual (B), and labial (C) views. Scale bar = 5 mm.



(Source: Aranda, 2019)

Figure 29. *Chilabothrus* sp. fossil right maxilla MNHNCu 73.5322 in dorsal (A), lingual (B), and labial (C) views. Scale bar = 5 mm.



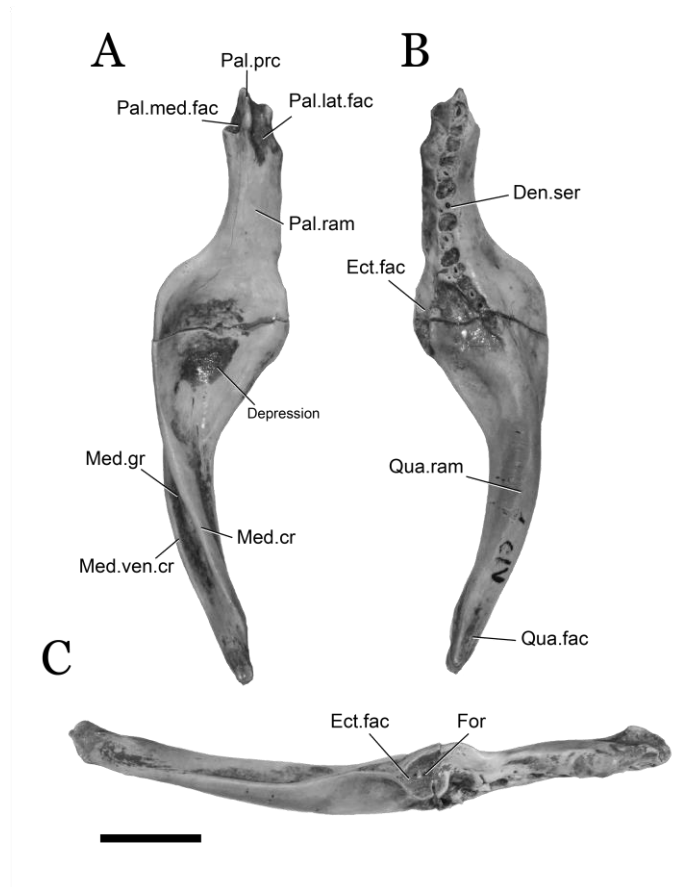
(Source: Aranda, 2019)

Figure 30. *Chilabothrus* sp. fossil left maxilla CLV 9-I in dorsal (A), lingual (B), and labial (C) views. Scale bar = 5 mm.



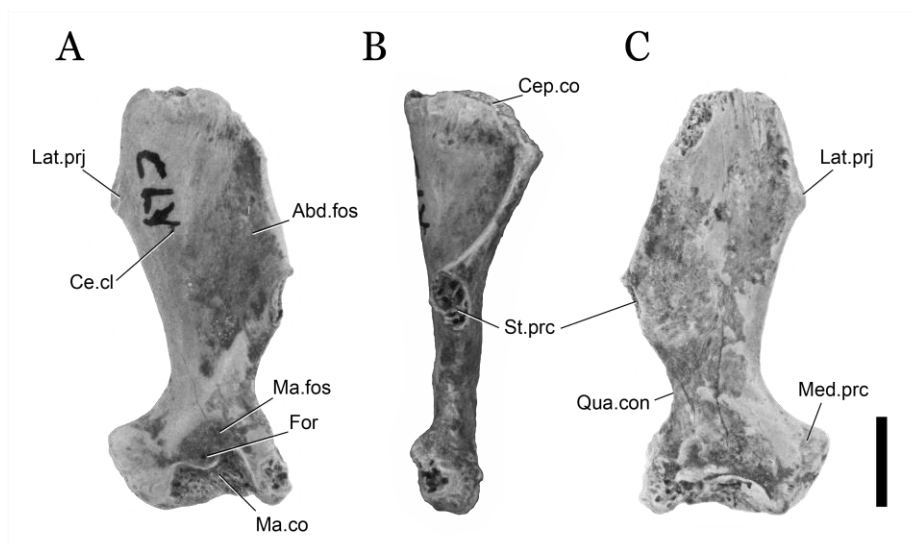
(Source: Aranda, 2019)

Figure 31. *Chilabothrus* cf. *angulifer* fossil right pterygoid CLV 9-II in dorsal (A), ventral (B), and lateral (C) views. Scale bar = 10 mm.



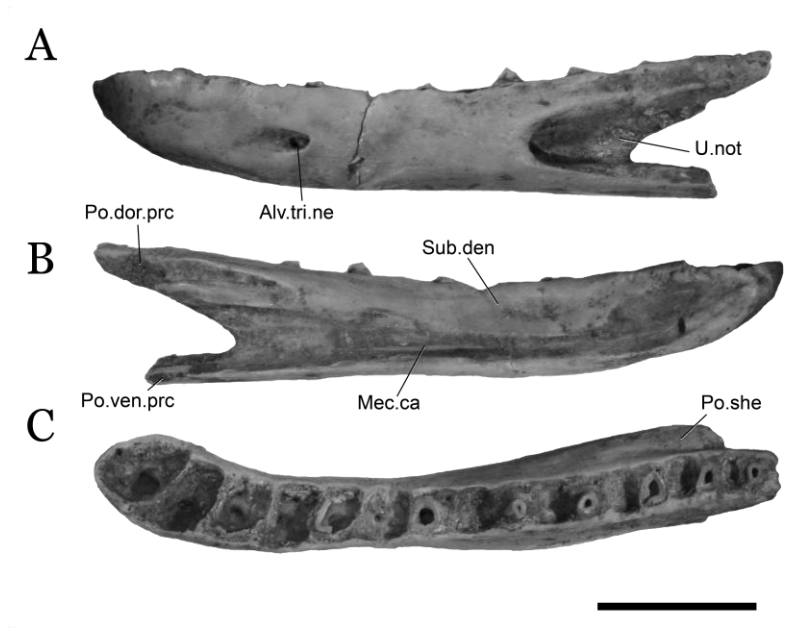
(Source: Aranda, 2019)

Figure 32. *Chilabothrus* sp. fossil right quadrate CLV 9-III in anterior (A), medial (B), and posterior (C) views. Scale bar = 3 mm.



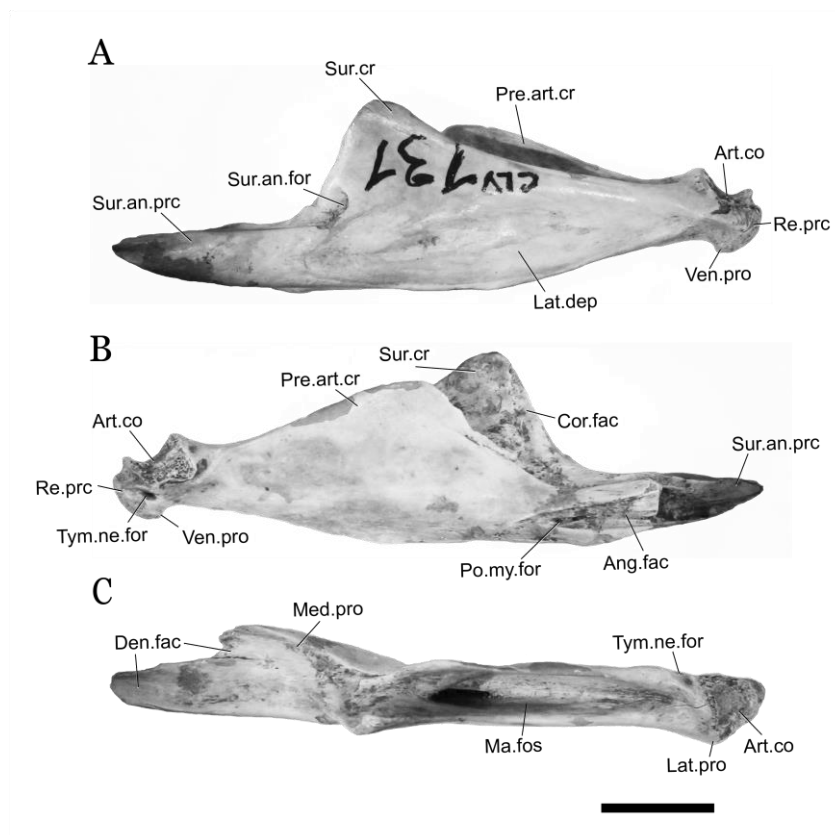
(Source: Aranda, 2019)

Figure 33. *Chilabothrus* sp. fossil left dentary CLV 9-IV in labial (A), lingual (B), and ventral (C) views. Scale bar =10 mm.



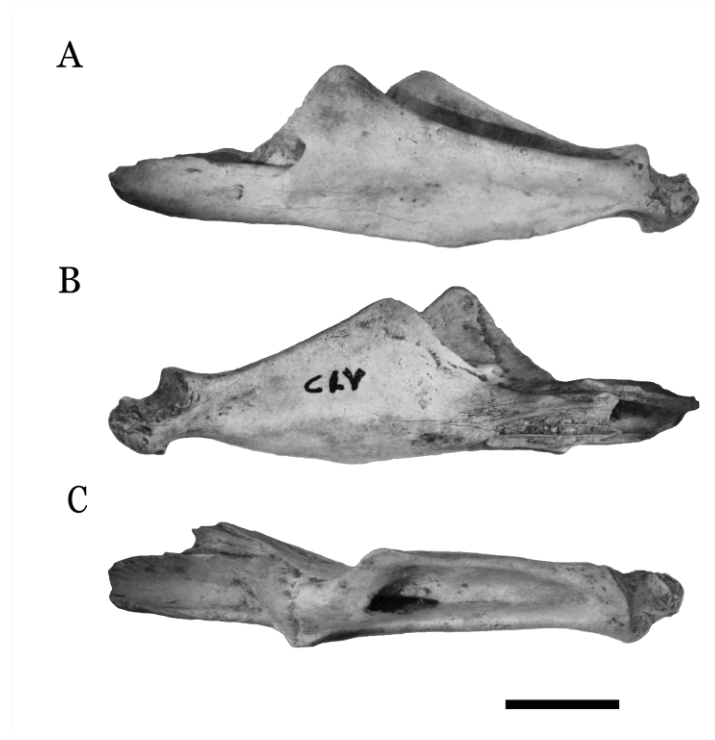
(Source: Aranda, 2019)

Figure 34. *Chilabothrus* fossil left compound bone CLV 9-V in lateral (A), medial (B), and dorsal (C) views. Scale bar = 10 mm.



(Source: Aranda, 2019)

Figure 35. *Chilabothrus* sp. fossil left compound bone CLV 8-I in lateral (A), medial (B), and dorsal (C) views. Scale bar = 10 mm.



(Source: Aranda, 2019)

Figure 36. *Chilabothrus angulifer* fossil right compound bone CLV 8-II in lateral (A), medial (B), and dorsal (C) views. Scale bar = 10 mm.



(Source: Aranda, 2019)

3.6 Family Colubridae Opel, 1811

Cubophis cf. cantherigerus (Bibron, 1840)

3.6.1 Compound Bone

The specimen MNHNCu 73.5376 correspond to a complete and well preserved compound bone of *Cubophis* (Figure 37). The bone is thin, elongated, and concave in general aspect, with pointed anterior and posterior ends. It presents a deep mandibular fossa, limited by a tall medial prearticular crest, and by a small labially surangular crest. Anterior surangular foramen is located far anteriorly of the mandibular fossa, in the posterior half of the surangular anterior process. Posteriorly, it finished with a relatively long, pointed and ventromedially directed retroarticular process. The foramen of the tympanic cord open medially, between the articular condyle and the retroarticular process. In dorsal view, the articular condyle is concave by their four sides.

A sharp ventral edge of the body is present in lateral view. Medially, a small crest occurs in the surangular wall of the mandibular fossa. This crest starts at the anterior edge of the articular condyle, and run two thirds forward of the mandibular fossa. Dorsal to this shelf, appears a shallow fossa.

A long anterior surangular process occupies the anterior half of the bone, which enters between the two posterior prongs of the dentary. Dorsally, the anterior end of the process is pointed, triangular-shaped. Over the triangle appear an also triangular groove, where articulates the dorsal posterior process of the dentary. In the medial base of the triangle emerged a small, and round prominence. Antero-ventrally appears a shortest, triangular groove, where articulates the postero-ventral process of the dentary.

From the middle to the antero-medial face a longitudinal V-shaped facet medially opens anteriorly in the anterior surangular process. In this facet articulates the angular bone. Anterior to this V-facet, it also opens the Meckel's canal. In the anterior end of the dorsal edge emerged the anteriorly mentioned small, transverse projection. Two longitudinal parallel ridges occur in the middle of the facet, one above the other, and between them appears a small groove. Anteriorly the ridges present another V-shaped opening, which forms part of the largest anterior opening of the Meckel's canal.

Both the prearticular and the surangular develop convex crests in the posterior half of the bone. Prearticular crest is almost twice higher than reduced surangular crest, what makes the mandibular fossa faces laterally. From dorsal view, both crests describe an oval limit of the mandibular fossa. Anterior end is pointed, and the posterior is round, like an elongate water drop. Anteriorly, it lacks an eminence for the support of the coronoid.

The articular condyle, wider than long, is located posterior to the mandibular fossa. It is dorsally oriented, with a convex surface that bends laterally. Anterior and posterior edges are raised and sharpened, both of the same height. Posterior to the glenoid fossa, occur an elongated, pointed retroarticular process (longer than articular condyle), that slightly curve medially. A foramen for the chorda tympani nerve opens in the antero-medially surface of the retroarticular process.

3.6.2 Vertebra

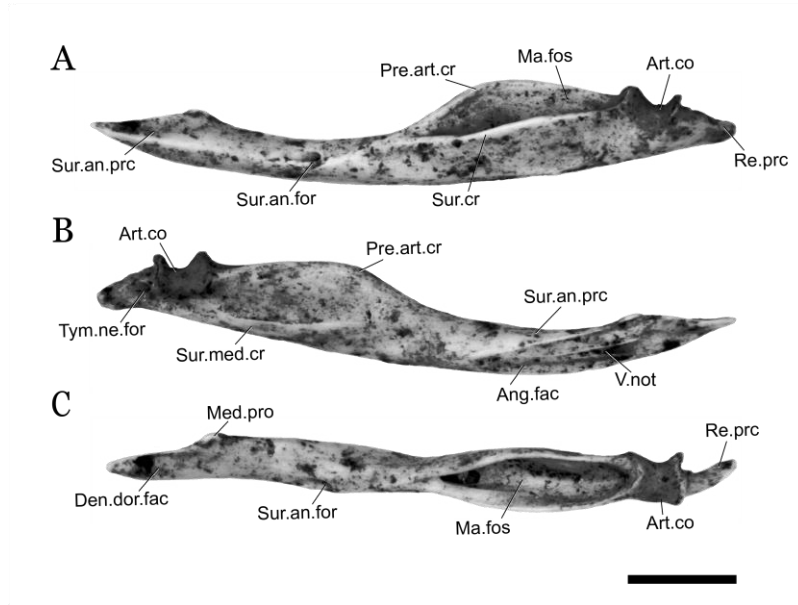
Two vertebrae belong to the genus *Cubophis*. One of the posterior half of the body (MNHN Cu 73.5382-I, Figure 38) and another one of the end of the body (-II). The first presents foramen paracotilar, subcentral, lateral and zygantral. The roof of the zygosphenes does not extend beyond the lateral extremities, it is convexly high, with the articular surfaces inclined towards the outside. Prezygoapophyses are almost horizontal, with articulate faces drop water shaped. The prezygapophysial process is visible dorsally and tilted latero-anteriorly. The cotyle is circular, deep, has two small ventral projections at the base. Parapophyses process is well developed, visible in dorsal view. Diapophyses is ventrally overturned and is smaller than parapophysis.

Neural arch is depressed dorsoventrally. It has a long neural spine (about 80% of the total length of the body), moderately high (about a third the total height of the vertebra), with the anterior lamina anteriorly sloped and slightly higher than the posterior one sloping caudally. The intezygapophysial lamina is well developed, projected laterally, and concave in dorsal view. In the posterior region the neural arch is well developed, keeled. The articular facets of the zygantra are longer than wide. The neural canal is slightly trilobed, with no foramen at the base. Condyle is rounded, slightly depressed in the dorsal region, and sloped antero-posteriorly.

Ventral groove is underdeveloped, different from its hemal keel that is well developed. The latter is thinner than wider all over the body except at the posterior end, where it widens into a small round process. Ventral margin of the body in lateral view is sloped ventrally in the posterior area.

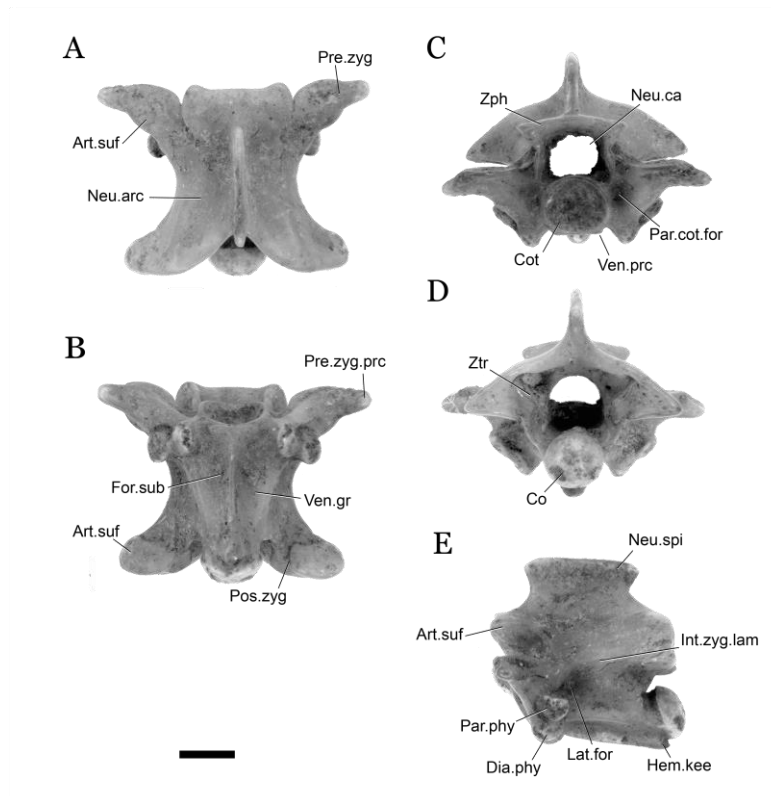
The second vertebra, of the end of the body, presents the neural spine broken. It is very similar to the previous vertebra, except for some differences. It presents two foramina at the base of the neural canal, absent in previous vertebra. Cotyle and condyle are dorso-ventrally flattened. The articular surface of the pre-and postzygapophyses has a more straight external edge. Neural arch is not so depressed in posterior view. Paracotilar and lateral foramen are more wide, subcentral remains the same. Ventral groove is deeper in the anterior region of the body. Ventral margin of the body is straight, with the hemal keel more projected ventrally in the posterior half. Condyle is more sloped ventrally, slightly more distant from the body in relation to the anterior vertebra. However, these differences may reflect the size and position of the vertebra.

Figure 37. *Cubophis* fossil left compound bone MNHNCu 73.5376 in lateral (A), medial (B), and dorsal (C) views. Scale bar = 5 mm.



(Source: Aranda, 2019)

Figure 38. *Cubophis* fossil mid-body vertebra MNHNCu 73.5382 in dorsal (A), ventral (B), anterior (C), posterior (D), and lateral (E) views. Scale bar = 2 mm.



(Source: Aranda, 2019)

4 Discussion

4.1 Comparison and Comments

4.1.1 cf. *Amphisbaena* Linnaeus 1758

The presence of a poorly developed neural spine and a V-shaped ridge in the posterior medial margin is typical of amphisbaenian vertebrae (Blain, Canudo, Cuenca-Bescós, & López-Martínez, 2010; Bolet et al., 2014). Besides, a smooth posterior margin differentiates Amphisbaenidae from Rhineuridae and Trogonophiidae, who are have a denticulate vertebral posterior margin (Čerňanský, Augé, & Rage, 2015). However, this characteristic is variably present inside Amphisbaenidae, for example, the posterior margin of *Amphisbaena alba* vertebrae is smooth, whereas it is indented in the African *Monopeltis* (Kearney, 2003).

Inside Amphisbaenidae, sampled vertebra differentiate from *Leposternon* mainly in the divergence of pre- and postzygapophyses (see Camolez & Zaher, 2010), and in the neural spine, present in *Leposternon*, and absent in sampled vertebra.

Three species of *Amphisbaena* exist in Cuba, *A. barbouri*, *A. carlgansi*, and *A. cubana*. The combination of morphological characters described above allows to identify a member of the Amphisbaenidae, but due to the fact that isolated amphisbaenian vertebrae are generally not diagnostic, a precise taxonomic allocation is not possible (Bolet et al., 2014; Mandriola, Delfino, Bailon, & Pitruzzella, 2011; Rage, Pickford, & Senut, 2013; Scanferla, Montero, & Agnolín, 2006).

According to the current distribution of the species, *A. carlgansi* is restringed to the East region of the island (Thomas & Hedges, 1998), outside of the geographic range of the deposit location. Because of that, it is suggested that fossil identity should be between *A. barbouri* and *A. cubana*.

4.1.2 *Tarentola* (Gray, 1831)

There are two autochthonous families of Gekkota in Cuba, Phyllodactylidae and Sphaerodactylidae (Gamble, Bauer, Greenbaum, & Jackman, 2008), and one introduced, Gekkonidae (Gamble et al., 2011). Phyllodactylidae have *Tarentola americana* (Gray, 1831)

and *T. crombiei* species (Díaz & Hedges, 2008), Sphaerodactylidae has one introduced genera and two autochthonous, *Sphaerodactylus* (Wagler, 1830) and *Aristelliger* (Cope, 1862). By the big size and robust aspect of fossils, similar species could be *Tarentola americana* and *Aristelliger*.

Most parietal fossils resembles that of the recent *Tarentola americana*, only MNHNCu 73.5343-I presented differences. A frequent character of Gekkota are the parietal paired (Evans, 2008; Gauthier et al., 2012). Recent *Tarentola americana* shows this character. Two fossil exemplars (73.5343-I) present a fusion of parietal halves, without midline mark. In *Gonatodes*, and *Aristelliger* the parietals are fused, but the middle line of the fusion is still seen (Griffing, Daza, DeBoer, & Bauer, 2018; Stephenson, 1960). According to Etheridge (1965), parietal merging occur in individuals above 110 mm of SVL. Recent Cuban *Tarentola* rarely over passes 110 mm, the longest record is 114.5 mm (Díaz & Hedges, 2008). Among Caribbean specimens, only a great fossil exemplar of *Aristelliger lar* [*A. titan*] (longer than 150 mm) shows merging of parietals (Hecht, 1951).

Parietal of *Tarentola americana* present a medial constriction on lateral edge as observed in fossils. This constriction is absent in *T. mauritanica*, *T. annularis*, *Thecadactylus rapicuda*, and in *Aristelliger*. Even further comparison is needed, this parietal constriction could be a diagnostic character of *T. americana* among Caribbean geckos. A postero-medial process is present in observed in comparative materials of *Tarentola*, and *Thecadactylus*, but absent in *Aristelliger* (Griffing et al., 2018; Hecht, 1951).

Fossil occipital bones and pterygoids have no differences with observed specimens of *Tarentola*. Except for the fusion of occipital bones in fossils, which appear separated in recent *Tarentola*. In the case of occipitals, *Tarentola* differ from *Thecadactylus* in having lower supraoccipital crests, higher and wider *processus ascendens*, narrower and longer paraoccipital process, and longer sphenoccipital tubercles. Also, *Thecadactylus* alar process of prootics are rounded, while in *Tarentola* are pointed, and they present a pointed process in the anterior end of the medial prootic groove, absent in *Tarentola*.

Dentary of *Tarentola* and *Aristelliger* are similar. Teeth are moderately slender, pointed, and curved lingually, and different from *Thecadactylus* which are longer, less sharply pointed and

little curved lingually (Etheridge, 1964). As in *Aristelliger*, *Tarentola* present a deep scar for the coronoid insertion, which extends forward to the level of the penultimate dental socket (Hecht, 1951). One of main differences that Hecht (1951) enounced between Caribbean *Tarentola* and *Aristelliger* dentary was the number of posterior process, two in the first and three in the second, although, it was observed three posterior process in *Tarentola* instead of two, as *Aristelliger*. Besides, Vila et al. (2018) confirm the presence of three process in European *Tarentola*. In present work others differences were found, the postero-ventral process of dentary is relatively longer in *Tarentola* than in *Aristelliger*. Also, the medial notch in the posterior subdental surface for the angular insertion is V-shaped in *Aristelliger*, different of the U-shaped in *Tarentola* and fossils.

In the articular surangular complex, only the exemplar 73.5349-III do not present an antero-dorsal surangular foramen, and the latero-dorsal area of it is more rounded than the rest of exemplars, with a slightly indication of a ventral keel. Perhaps, this exemplar belonged to a young individual, since within the sample it is the smallest. However, comparative material of adult *Tarentola* have the same condition, except for the absence of the antero-dorsal foramen. In articular wall of fossils who preserve it, appear a groove in dorsal view, accompanied by a small crest on the medial edge, structure absent in comparative materials. Surangular of MNHNCu 73.5349-II, present a flat surface near the articular condyle, another difference with recent *Tarentola*.

The amphicoelous condition of the vertebrae is one of the diagnostic characters among gekkotans (Vasilyan, Zazhigin, & Böhme, 2017). Among Cuban representatives only *Spaherodactylus* has procoelus vertebrae (Noble, 1921), the rest have the amphicoelous condition. Another charater is the presence of zygantra and zygosphene in the fossil as in recent *Tarentola* and *Aristelliger*. Main difference appear in the neural spine, posteriorly raised in all mid-body vertebrae of recent species, sloped backward, and low of the fossil.

We recognize the presence of *Tarentola americana*, besides another species of *Tarentola* not described for Cuba, evidence by parietals of MNHNCu 73.5343-I (Figure 3), and articular-surangular complex of MNHNCu 73.5349-II (Figure 9).

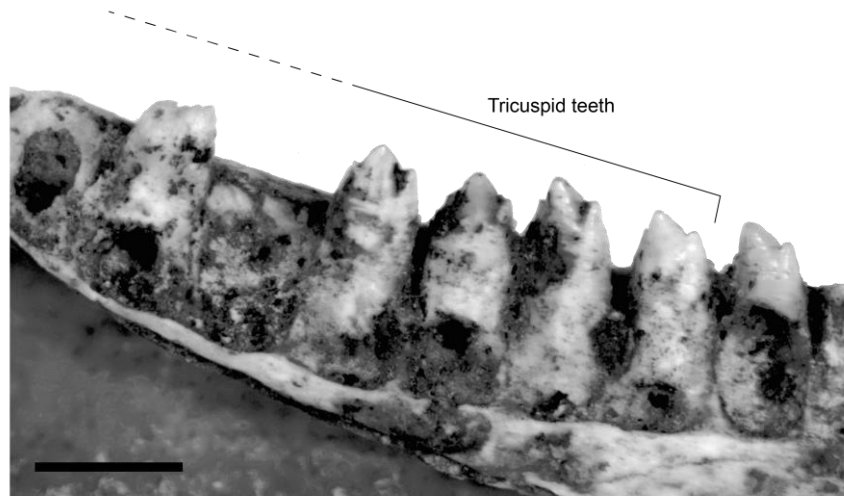
4.1.3 *Pholidoscelis auberi* Gray, 1827

Only one species of Teiidae is known for Cuban archipelago, *Pholidoscelis auberi* (Torres et al., 2017). Although a morphologic revision of Caribbean Teiidae is needed (Harvey et al., 2012), no osteologic differences were found were found between fossils and recent Cuban teid. *Pholidoscelis* genus was revalidated recently, separating the Caribbean and continental *Ameiva*, in a molecular revision of the superfamily (Goicoechea et al., 2016), but still undifferentiated morphologically.

In frontals, one of exemplars presents a central process wider than longer, character observed in a young recent material of *Pholidoscelis auberi* (MNHNCu 63.105), indicating that this character could vary according to with ontogeny state. Among fossil parietals, analyzed specimens have an opening of the supratemporal processes of 75°, higher than the 70° observed in the fossils, nevertheless, the parietal is one of the most variable bones of the skull of lizards (Etheridge, 1959; Torres-Carvajal, 2003). Further studies are needed to determine if the difference of 5° is really a diagnostic character.

Amount of tricuspid teeth vary interspecifically in *Pholidoscelis* (Etheridge, 1965), *P. chrysolaeama*, from Hispaniola, posses no more than 4 tricuspid teeth on the rear of the maxilla and no more than 5 tricuspid teeth on the rear of the dentary. *Pholidoscelis taeniurus* and *P. lineolatus* posses, also from Hispaniola, posses 6-11 tricuspid teeth on the rear of the maxilla and from 7-13 on the rear of the dentary. *Pholidoscelis auberi* is closer to the last condition. Young individual present 7 tricuspid teeth in maxilla, and 8 in dentary, while adult and fossils who preserve it (Figure 39), present 3 in maxilla and 5 in the dentary. However, a little care should be taken, because tricuspid teeth could become bicuspid and then blunt from young individuals to ancients, as was observed in fossils of *P. griswoldi* in Antigua (Pregill et al., 1988). A blunt condition was observed in some fossils, most present bicuspid teeth, and others tricuspid.

Figure 39. Zoom in posterior section of dental series of *Pholidoscelis auberi* (CLV 3-IV) in lingual view. Scale bar = 1 mm.



(Source: Aranda, 2019)

Approximation of dorsal and ventral subdental borders, seeing in fossils and recent *P. auberi*, almost closing the Meckel's canal is more similar to *Cnemidophorus* than to *Ameiva* (Camolez & Zaher, 2010). The opening of the canal before the approach of the borders is shorter in fossils than in recent specimens. In the formers, this opening occupies about one-fifth to one-fourth of the total length, while in recent occupies one-third or more of the total length. The condition of two anterior mylohyoid foramina observed in one of exemplars was not seeing in recent individuals, however, is a observed structure in the family (Evans, 2008).

Angular crest is distinct in the Teiinae subfamily (*Ameiva*, *Cnemidophorus*, *Dicrodon*, *Kentropyx*, and *Teius*) (Camolez & Zaher, 2010; Presch, 1970), however, it is present in a fossil specimen of *Tupinambis*, subfamily Tubinambinae (Hsiou, 2007). A recent young individual does not present angular crest, so this character may be associated with ontogeny.

4.1.4 *Leiocephalus* Gray 1827

Leiocephalidae is a monotypic family of the Great Antilles and Bahamas with 31 species. Six species are known only by Quaternary fossil remains, and other three are recent extinctions. Although his radiation was not explosive like that of *Anolis*, neither was it insignificant for a

terrestrial squamate (Pregill, 1992). Six species exist in Cuba, *Leiocephalus carinatus*, *L. cubensis*, *L. macropus*, *L. onaneyi*, *L. raviceps*, and *L. stictigaster* (Torres et al., 2017). *Leiocephalus carinatus* is the largest living of the family, reaching until 130 mm of SVL (Pregill, 1992). By a period, *Leiocephalus* were inside Tropicoduridae family due to an enlarged sternal fontanelle, and presence of femoral pores (Etheridge & de Queiroz, 1988), posteriorly was elevated as a family by total evidence (Frost, Etheridge, Janies, & Titus, 2001).

Sharply cranial crests, as those presented in fossils, define *Leiocephalus* frontals from another Caribbean iguanid (Etheridge, 1966b). Fossils frontals show informative structures for the identification of Cuban *Leiocephalus*. Different to what describe Pregill (1992) it was found exposed nasal process in *Leiocephalus cubensis*, this species together with *L. macropus* and *L. carinatus* have wide nasals process. Other species have nasal process reduce, as a thin line. CLV 1-I, and -IV (Figure 17, Figure 18A) show a wide condition, however, they differ from *L. cubensis* in the projection of the medial process. *Leiocephalus cubensis* presents a narrow medial process almost a line, its lateral edges do not meet with medial edges of nasal process, while fossils medial process are wider, with lateral edges meet with medial edges of the nasal process. Medial process of CLV 1-I is pointed, together with a smoothing of the dorsal surface makes it closer to *L. macropus*, while CLV 1-IV is blunt, with a rugose dorsal surface, making it closer to *L. carinatus*.

CLV 6-I and -II presents tricuspid medial processes, a condition not observed in any of the Cuban species. Three processes are pointed like a fork, with the central slightly longer than laterals. Central process has concave lateral edges. Laterals have convex edges laterally and concave medially. In CLV 6-I are well developed (Figure 18), while in CLV 6-II lateral processes are poorly develop.

There are two basic forms in the parietal of *Leiocephalus*, V-shaped and U-shaped (Pregill, 1992). Both shapes differ by the presence or absence of a transversal ridge at the posterior edge of the parietals, which makes the parietal roof a trapezoidal or a triangular shape. Pregill described U-shaped for all Cuban species (except for *L. onaneyi*, from which he did not obtain specimens, nor the present study). This statement was verified for *L. cubensis*, *L.*

macropus, *L. raviceps*, and *L. stictigaster*, but not for *L. carinatus*, this species had a V-shaped. Fossils present U-shaped parietals roof.

Raised parietal crests are also present in sample fossils. Among recent species with U-shaped parietals species, only *L. cubensis* and *L. macropus* showed this characteristic, and together with the best definition of the interparietal sulcus scales on the dorsal rugosities in *L. cubensis*, it is suggested that they belong to this species (in *L. macropus* the lines do not take the interparietal scale shape).

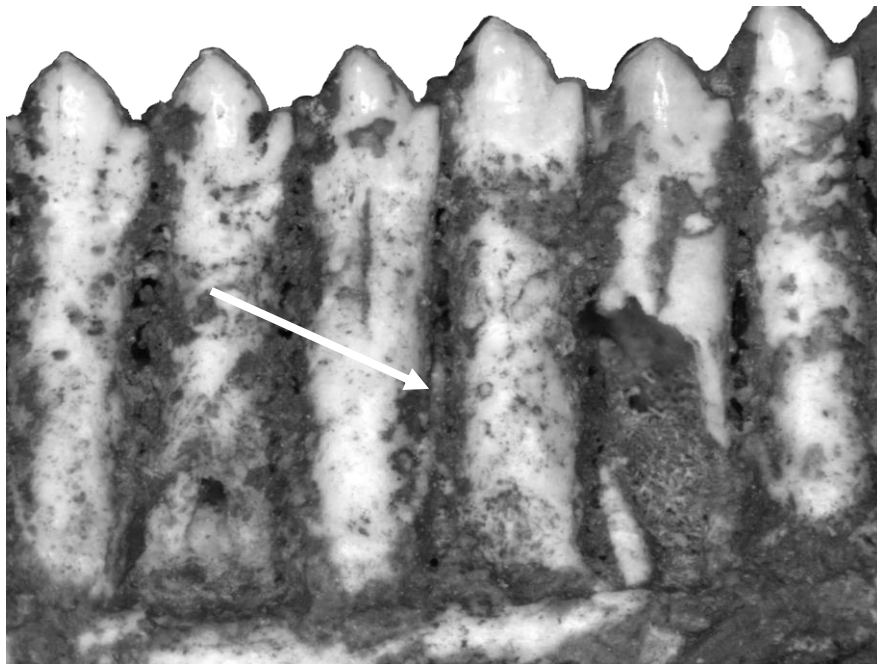
Fossil maxillas of CZACC 4-I differ from that of CLV 6-V and CZACC 11 in the facial process. The first has a vertical ascending frontal edge, as observed in current Cuban species. The last two have a frontal edge sloped backward, none of the known Cuban species present this character. CLV 6-V, the most complete maxilar (Figure 20), presents other distinctive characters in the facial process. Apex is divided into two lobes, one on the nasal facet, and another on the prefrontal facet; the prefrontal facet edge makes a nearly straight angle with the lacrimal-jugal facets edge (recent specimens have an openly obtuse angle), and keel dividing frontal and lateral planes is more pronounced than in Cuban species. Because of that, it is suggested that CLV 6-V belongs to a *Leiocephalus* species not recorded for Cuba. The keel is also pronounced in CZACC 11, but fragmentation of dorsal edges hamper the observation of other characters.

Dentary is quite conserved in the current Cuban species of *Leiocephalus*. Only some differences could be found. The anterior border of the inferior alveolar foramen in *Leiocephalus carinatus*, *L. stictigaster*, and *L. raviceps* is formed by the dentary, as occurs in exemplars CLV 1-I, CLV 5-I, and CZACC 4. Consequently, the dentary border adopts the oval shape of the foramen. In *L. cubensis*, and *L. macropus* alveolar foramen is all enclosed in the splenial, as observed in CLV 1-II, and CZACC 5.

One of the diagnostic characters of *Leiocephalus* is the presence of vertical rows of small foramina in the narrow spaces between the teeth in lingual view (Etheridge, 1965). This character is present in all sample except in CLV 1-X (Figure 40). Also, CLV 1-X present a prominent shelf in the dorsal edge of the subdental border, that extends more than half of the dentary (Figure 23), absent in recent Cuban species. Space between teeth is reduced,

what gives the impression of teeth overlapping. Mandibular symphysis is round, and with robust aspect in labial view. CLV 1-X should be a new species record for Cuba, most probably a new genus record. It is 20.31 mm long exceeds 18.1 mm of *L. cuneus*, the largest fossil of *Leiocephalus* found to date (Etheridge, 1964, 1965). Although statistical analyzes are needed, it is very likely that it will exceed the size of *L. carinatus*, the largest species of the genus.

Figure 40. Zoom in exemplar CLV 1-X. . Arrows show the absence of foramina in a narrow space between teeth without crusting . Scale bar = 0.5 mm



(Source: Aranda, 2019)

Leiocephalus cubensis and *L. raviceps* have angulars with medial and lateral process pointed, different from described fossils where only medial process is pointed and lateral is round; also, lateral process is almost two-thirds of the medial process, different from fossil where medial process triples the lateral. Posterior mylohyoid foramen location may vary according to the extent of the angular medial process, as seen in fossils and recent, it can be enclosed in the process, or in their ventral edge, in the boundary with dentary.

In the case of CLV 1 anterior tip of surangular ventral process is located behind the anterior surangular foramen, just like in *L. carinatus*, *L. stictigaster*, and *L. macropus*. Ventral process of CLV 5 and MNHNCu 73.5379 have their anterior tip located before the anterior surangular

foramen, just like in *L. cubensis*. Surangular of *L. raviceps* possess the dorsal process too short and does not present anterior surangular foramen in the external surface. Among Cuban recent species configuration of the angular and retroarticular processes of the articular varies considerably, a feature shared with the rest of Caribbean *Leiocephalus* (Etheridge, 1964). However, some patterns could be identified. In CLV 1 fossils, the angular process has a pointed tip as in similar to *L. carinatus*. In CLV 5 and MNHNCu 73.5379 fossils, angular process has a round tip, similar to *L. cubensis*, *L. raviceps*, *L. macropus*.

Fossils of CLV 1 are more related to *L. carinatus*. CLV 5 and MNHNCu 73.5379 are more like *L. cubensis*, but they differ from this in the retroarticular process form, *L. cubensis* that present a circular posterior end. In this structure, they are more related to *L. raviceps* and *L. stictigaster*.

4.1.5 *Chilabothrus* Duméril and Bibron, 1844

Chilabothrus genus is a distinctive taxon from the Antilles and the Bahamas. It has 13 valid species, of which only one, *Chilabothrus angulifer*, occurs in Cuba. Formerly the species belonged to the genus *Epicrates* (Duméril & Bibron., 1844), due to its very similar morphology to continental species, and recently it was raised at the level of genus, based on molecular data (Reynolds et al., 2013). Adult *Chilabothrus exsul*, *C. fordii*, *C. gracilis* and *C. monensis* are considerably smaller than all other species in *Chilabothrus*. *Chilabothrus chrysogaster* is of intermediate size, and *C. angulifer* is the largest of the genus (Kluge, 1989).

In the parietal of MNHNCu 73.5311 (Figure 27), sagittal crest occurs all over the dorsal midline of the parietal, indicator of an adult individual (Smith & Scanferla, 2016). Character see in *Chilabothrus angulifer*, but also in *C. subflavus* (Kluge, 1989, Figure 8A), and *C. inornatus*, in others *Chilabothrus* the crest begins a little before the transition from globular area to thinner area. In *C. subflavus* and *C. inornatus* frontal lateral process is located in an anterior horizontal plane before the medial process, while in *C. angulifer*, both processes are in the same plane. Also, the crest starts almost at the same level high of the parietal roof in *C. subflavus* and *C. inornatus*, while in *C. angulifer* start above the level of the parietal roof, a condition observed in MNHNCu 73.5311. In the fossil, crest is considerably high, more than in comparative material of *C. angulifer*, but this could be due to ontogeny. Further studies

are needed to verify this hypothesis, until now, it is suggested that MNHNCu 73.5311 belongs to *C. angulifer*.

In MNHNCu 73.5322 and CLV 9-I, frontal edge of the maxilla is almost vertical, differing from recent *Chilabothrus* known species, where frontal edge slope backward, as in the another exemplar, MNHNCu 73.5029. First, two fossils are considerably large, considering that *C. angulifer* is the largest species, this character could lead to an unknown species. However, observed specimens do not reach this size, and further comparison with large recent species is needed.

Fossils maxilla have an ectopterygoid process of relatively medium size, different from *Eunectes* and *Corallus* where these processes are too small (Camolez & Zaher, 2010). Kluge (1989), considered this (character no. 50) as large in *Chilabothrus angulifer*, *C. inornatus*, *C. striatus*, and *C. subflavus*, and smaller in the rest of species. No differences were found between fossils and *C. angulifer* with respect to this character, neither with *C. inornatus*, *C. striatus* nor *C. subflavus*, except for the variability in the presence/absence of the lateral process.

Fossil pterygoids most probably belongs to *C. angulifer*. Palatine and quadrate ramus curve medial and laterally respectively, as do in recent *C. angulifer*, but also in *C. exsul*, *C. inornatus*, *C. striatus*, and *C. subflavus*. In *C. chrysolaeus*, *C. gracilis*, *C. fordii*, *C. monensis* and *C. strigilatus* palatine ramus is straight.

Quadrate CLV 9-III presents a pointed projection on their lateral edge, above the level of the stylohyal process, none of known *Chilabothrus* present it. *C. angulifer* presents a lateral edge that curve in the same area, but not projects laterally. Additional differences of CLV 9- III with *C. angulifer* are the depth and opening angle of the abductor fossa, greater in the fossil, and smaller in recent *C. angulifer*. Antero-lateral surface of the fossil is flat, different to *C. angulifer* where is slightly concave. In the fossil, dorsal edge of abductor fossa ascends postero-medially oriented describing a curve, from the stylohyal process to the medial end of the cephalic condyle, in *C. angulifer* the edge ascends straight.

It differs from *C. exsul*, *C. fordii*, *C. gracilis*, *C. inornatus*, *C. monensis*, *C. striatus*, *C. strigilatus*, and *C. subflavus*, in the same features as *C. angulifer*. In *C. gracilis* abductor fossa do not

reach the shaft of the body, and stylohyal process is not well defined due to their continuation with the dorso-medial edge. In CLV 9-III ventral vertex of the V-shaped abductor fossa lies on the body shaft, and stylohyal process is well defined in an oval facet. In *C. exsul*, *C. chrysogaster*, *C. fordii*, *C. gracilis*, and *C. monenis*, stylohyal process lies on the ventral third of the body, just above the shaft, while in CLV 9- III presents their stylohyal process in the middle third of the body. Central column of *C. subflavus* and *C. chrysogaster* is concave laterally, while CLV 9- III is straight. No comparative material of the species *C. argentum*, *C. granti*, or *C. schwartzi* was found. However, it is known that they are much smaller species than *C. angulifer* (Reynolds, Collar, et al., 2016; Reynolds, Puente-Rolón, Burgess, & Baker, 2018; Reynolds, Puente-Rolón, Geneva, Aviles-Rodriguez, & Herrmann, 2016).

CLV 8-II compound bone, is pretty much like that of *C. angulifer*, however CLV 8-I and CLV 9-V show differences from the *C. angulifer* pattern. In fossils, prearticular crest rise like a peak as do surangular crest, having an obtuse angle of less than 110° between most adjust tangential lines of anterior and posterior margins of the crest. Measurements in *C. angulifer* always were above 120°. Also, CLV 8-I and CLV 9-V tend to be more robust, ventral edge of compound bone is markedly convex, while in *C. angulifer* it is straight, sometimes slightly curved. Others species of *Chilabothrus* do not resemble this fossil, most similar species are *C. striatus* and *C. subflavus*, but they still have the same differences that *C. angulifer*.

4.1.6 *Cubophis* cf. *cantherigerus* (Bibron, 1840)

Colubridae presents five genera in Cuba, *Cubophis*, *Caraiba*, *Nerodia*, *Tretanorhinus*, and *Arrhyton*. All with only one species except for *Arrhyton* that have 8 species (Torres et al., 2017). *Cubophis cantherigerus* is the largest in the island, reaching up to 1333 mm of snout-vent length distance (Domínguez & Moreno, 2006), and also the only Cuban racer that colonized other Caribbean islands.

A compound bone is referred to this species. In Cuba, *Cubophis* differ from *Caraiba* in having a taller prearticular crest, being almost twice that surangular in the former, and slightly surpassing the surangular crest in latter. Compound bone of *Arrhyton* makes a concave inflection in the ventral edge at the level of the mandibular fossa, which gives an S-shape to

the bone in lateral view. This inflection is absent in *Cubophis*, instead, it's gradually decreases until it ends in the retroarticular process. *Cubophis* also differ from *Caraiba* and *Arrhyton*, by the presence of a prominent crest on the medial face of the surangular wall. This crest is absent or little develop in the latest genera.

No material of *Tretanorhinus variabilis* or *Nerodia clarkii* was available, but the compound bone is inseparable from *Cubophis cantherigerus*, that is why it is suggested as most probably identification.

4.2 Cuban Fossil record

The Squamata fossil record in the Antilles and Bahamas has about 38 localities and 79 taxa identified (Appendix A), and goes from de Eocene to Late Holocene. From the lower Eocene is the tooth of an unidentified iguanid from Jamaica (Pregill, 1999), although paleogeographically it belongs to Central America (Iturralde-Vinent, 2005), not to the Antilles. From the Miocene are *Anolis* (Queiroz et al., 1998; Rieppel, 1980), and *Sphaerodactylus* (Böhme, 1984; Daza & Bauer, 2012; Daza, Bauer, Wagner, & Böhme, 2013), embedded in Dominican amber, besides a vertebra of Boidae and of Iguanidae from a lignitic clayey sand in Puerto Rico (MacPhee & Wyss, 1990).

The most abundant record is from Quaternary, with numerous localities of Squamata fossils on Anguilla, Antigua and Barbuda, Barbados, Cuba, Dominican Republic, Guadeloupe, Haiti, Jamaica, Puerto Rico, Saint Martin, and The Bahamas. There are known *Alsophis*, *Amphisbaena*, *Anolis*, *Antillotyphlops*, *Aristelliger*, *Boa*, *Borikenophis*, *Capitellum*, *Celestus*, *Chilabothrus*, *Clelia*, *Cubophis*, *Cyclura*, *Diploglossus*, *Erythrolampus*, *Iguana*, *Leiocephalus*, *Mabuya*, *Magliophis*, *Nerodia*, *Pantherophis*, *Pholidoscelis*, *Sphaerodactylus*, *Tarentola*, *Thecadactylus*, and *Typhlops* (Appendix A).

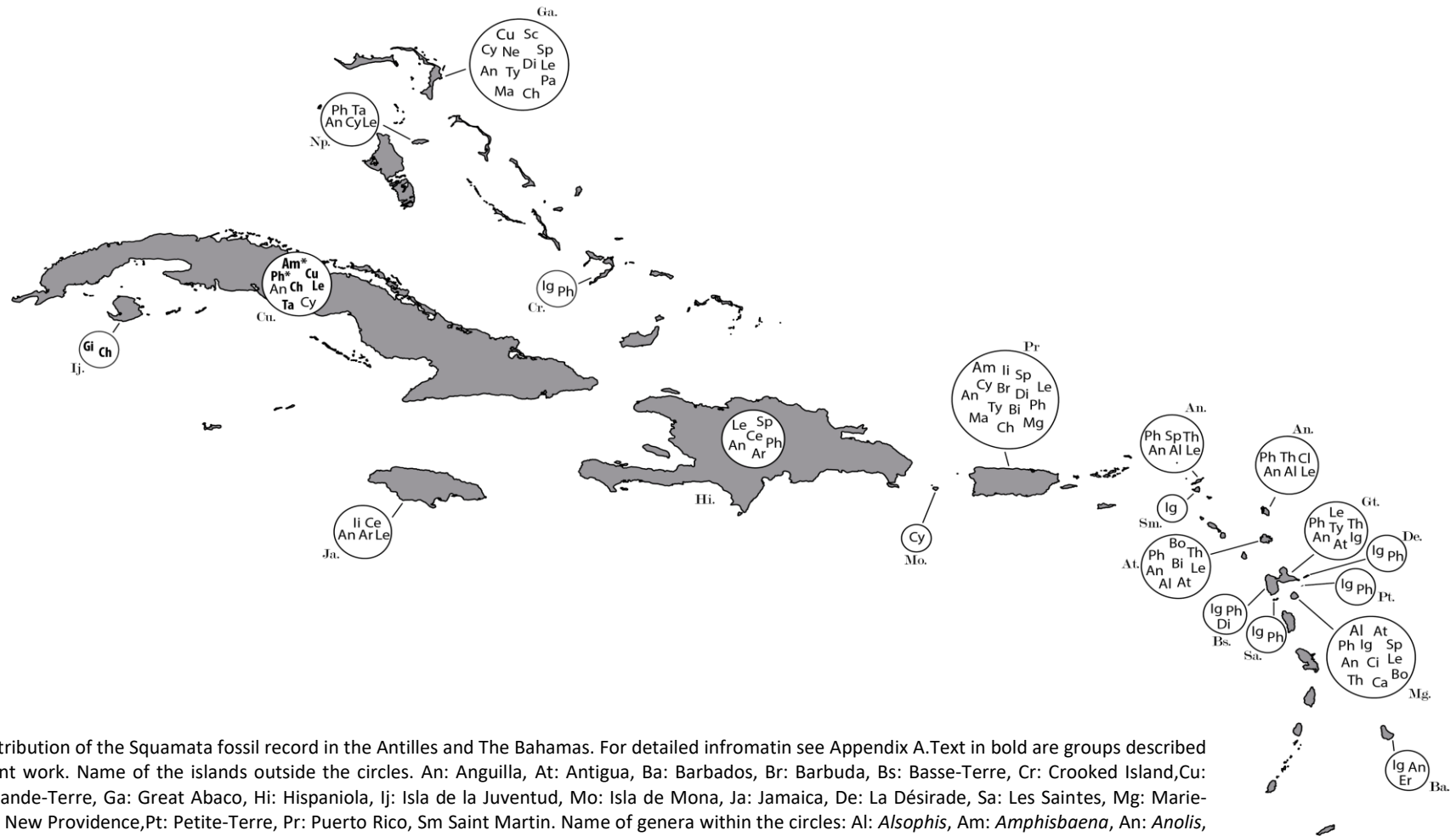


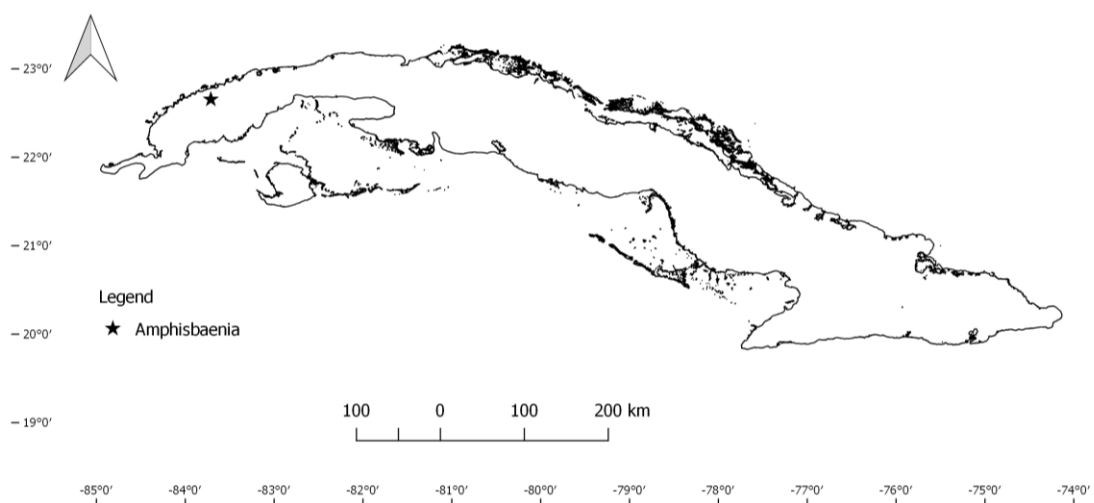
Figure 1. Distribution of the Squamata fossil record in the Antilles and The Bahamas. For detailed information see Appendix A. Text in bold are groups described in the present work. Name of the islands outside the circles. An: Anguilla, At: Antigua, Ba: Barbados, Br: Barbuda, Bs: Basse-Terre, Cr: Crooked Island, Cu: Cuba, Gt: Grande-Terre, Ga: Great Abaco, Hi: Hispaniola, Ij: Isla de la Juventud, Mo: Isla de Mona, Ja: Jamaica, De: La Désirade, Sa: Les Saintes, Mg: Marie-Galante, Np: New Providence, Pt: Petite-Terre, Pr: Puerto Rico, Sm: Saint Martin. Name of genera within the circles: Al: *Alsophis*, Am: *Amphisbaena*, An: *Anolis*, At: *Antillotyphlops*, Ar: *Aristelliger*, Bo: *Boa*, Bi: Boidae indet., Br: *Borikenophis*, Ca: *Capitellum*, Ce: *Celestus*, Ch: *Chilabothrus*, Cl: *Clelia*, Ci: Colubridae indet., Cu: *Cubophis*, Cy: *Cyclura*, Di: *Diploglossus*, Er: *Erythrolamprus*, Ge: Gekkonidae, Gi: Gekkota indet., Ig: *Iguana*, Ii: Iguanidae indet., Le: *Leiocephalus*, Ma: *Mabuya*, Mg: *Magliophis*, Ne: *Nerodia*, Pa: *Pantherophis*, Ph: *Pholidoscelis*, Si: *Scolecophidia* indet., Sp: *Sphaerodactylus*, Ta: *Tarentola*, Th: *Thecadactylus*, Ty: *Typhlops*. * New genus record for Cuba.

(Source: Aranda, 2019)

Cuban fossil records belong to Quaternary, mainly associated with cave deposits, and they represent 20% of the Antillean and Bahamas fossil records. There is a greater concentration of localities in the western of the country than in the central or eastern part. Something similar to what happens with fossil birds (Suárez, 2004) and fossil of mammals (Silva et al., 2007), which may be due to a greater collection effort in this region. To date, 11 species have been recorded, *Anolis lucius*, *A. equestris*, *A. porcatus*, *A. luteogularis*, *A. chamaleonides*, *Tarentola americana*, *Leiocephalus cubensis*, *L. carinatus*, *Cyclura nubila*, *Chilabothrus angulifer*, and *Cubophis cantherigerus* (Appendix A), representing 7.3% of the current Cuban fauna of Squamata (Mancina & Cruz, 2017).

By the first time in Cuba are describe fossil of *Amphisbaena* and *Pholidoscelis auberi*. One jaw and two vertebrae of *Amphisbaena* were found outside of Cuba, in a Pleistocene deposit in Puerto Rico (Pregill, 1981). As in the present study, no diagnostic characters were found that could lead to a more specific identification, and biogeographical criteria were used. *Amphisbaena* is widely distributed throughout the archipelago (Rodríguez-Schettino et al., 2013), the fossil record in the western region (Map 1) of the country enters in its current distribution.

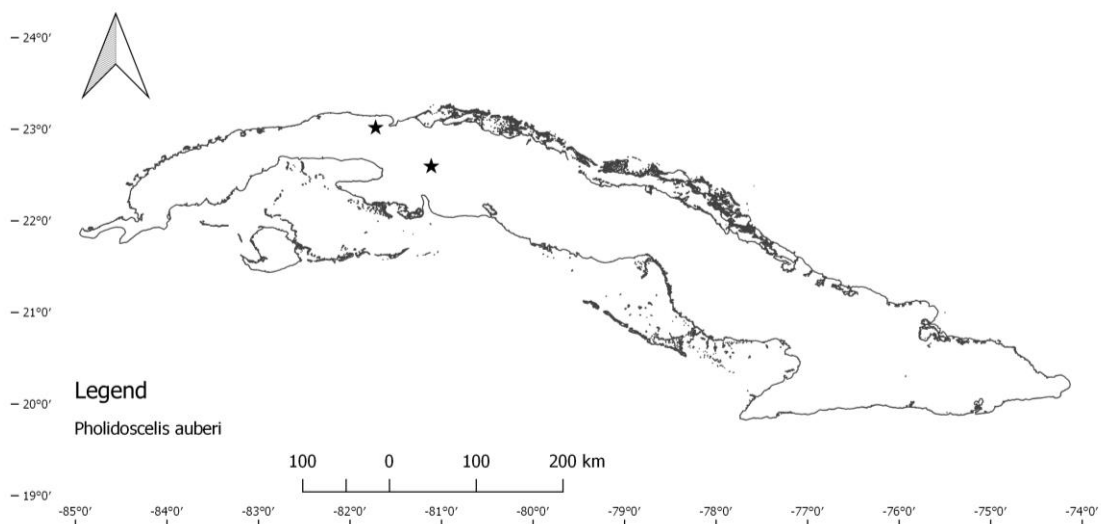
Map 1. Distribution of *Amphisbaena* fossil in Cuba.



(Source: Aranda, 2019)

Pholidoscelis have a good representation in the fossil record of Antilles. It was found in New Providence (Etheridge, 1966b), Puerto Rico (Pregill, 1981), Guadeloupe (Bochaton et al., 2017; Pregill et al., 1994), Antigua (Pregill et al., 1988; Steadman, Pregill, & Olson, 1984), and Barbuda (Etheridge, 1964). Even the first fossil species of the genus was recently described, *Pholidoscelis turukaeraensis* (Bochaton et al., 2017). Except for *P. turukaeraensis* all fossil records are representative of currents faunas in their respective islands, as occur with *Pholidoscelis auberi* in present work. *Pholidoscelis auberi* is widespread in Cuba, with many geographic variations in their size and coloration patterns (Schwartz & McCoy, 1970). Fossil locality records (Map 2) are enclosed in its current distribution.

Map 2. Distribution of fossil *Pholidoscelis auberi* in Cuba.

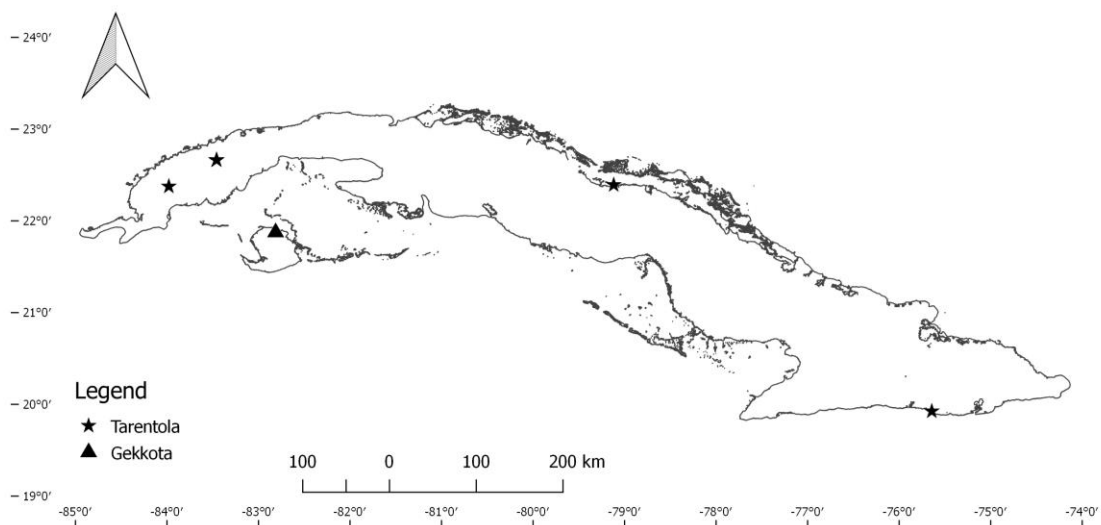


(Source: Aranda, 2019)

Ancestor of *Tarentola americana* probably arrived in South America from North Africa by multiple trans-Atlantic dispersion during Middle Neogene (Gamble et al., 2011). Fossils found are insufficient to verify these events. First mentions for Cuba was made by Hecht (1951) about some Pleistocene Cuban exemplars carried by Ernest Williams and Karl Koopman to the USA. Hecht (1951) tentatively attributes to *Tarentola americana*, but does not mention locations or provide greater descriptions of the material. Two fossil records of *Tarentola* are previously known, one in Camagüey, center of the island (Koopman & Ruibal,

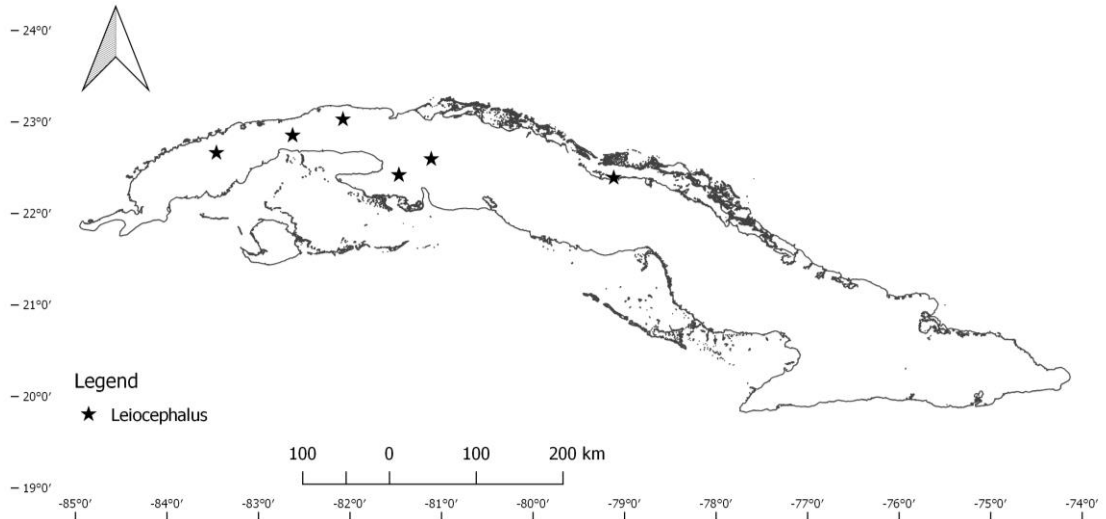
1955), and another in Mayabeque, east of Havana (Jiménez et al., 2005). The records presented in this work expand the distribution of the fossils to the entire island, from the eastern region to the western (Map 3). Nowadays *Tarentola americana* is also found throughout the entire Cuban territory (Rodríguez-Schettino et al., 2013), so it seems that since the Quaternary it was a widely distributed genus. Out of Cuba *Tarentola* is only known for New Providence (Etheridge, 1966b), area where it currently occurs.

Map 3. Distribution of fossil sample of *Gekkota* in Cuba.



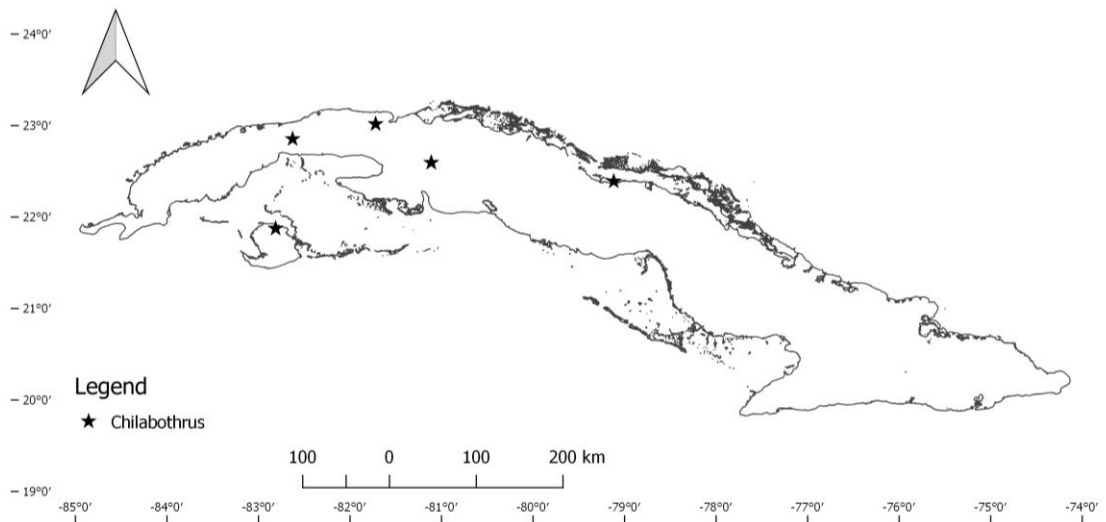
(Source: Aranda, 2019)

Among the fossils of the Antilles and The Bahamas, *Leiocephalus* and *Pholidoscelis* are the most dispersed genera with more number of records, after *Anolis* (Appendix A). *Leiocephalus* being that with more extinct species identified (Pregill, 1992). In Cuba, it has only two previously known records, one in Mayabeque (Jiménez et al., 2005) and another in Camagüey. The localities registered in this work increase the records in the central-western area of the country, with five new locations (Map 4). Of the six current species in Cuba, three were recorded in the present work, *L. carinatus*, *L. cubensis*, and *L. macropus*. The first two were already known among the Cuban fossil remains (Appendix A), *L. macropus* is a new record.

Map 4. Fossil sample distribution of *Leiocephalus*, Cuba.

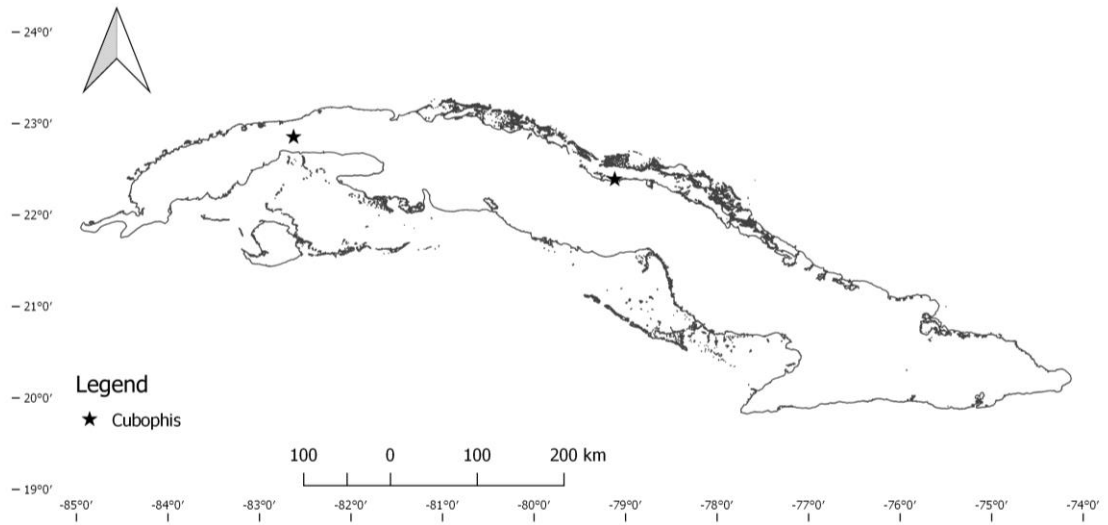
(Source: Aranda, 2019)

Fossil remains of *Chilabothrus* are found in The Bahamas and Puerto Rico (Mead & Steadman, 2017; Pregill, 1981; Steadman et al., 2007, 2014). Thanks to one of the fossils of Puerto Rico (MacPhee & Wyss, 1990), certainly the family was already present in the Antilles since the Miocene, possibly the ancestor of the current lineage. In Cuba, *Chilabothrus* is known only by vertebrae and dentaries. Although fossils discovered by speleologists from many localities are known, only 11 localities have been formally published (Arredondo & Villavicencio, 2004; Jiménez et al., 2005; Koopman & Ruibal, 1955; Varona & Arredondo, 1979). Our study provides four more locations (Map 5), one in Isla de la Juventud, the second largest island of the Cuban archipelago, and which is of special interest in zoogeographical analysis (Fernández-Milera & Correoso, 2003).

Map 5. Fossil sample distribution of *Chilabothrus*, Cuba.

(Source: Aranda, 2019)

Cubophis have fossil representation in the Bahamas (Mead & Steadman, 2017; Steadman et al., 2014) and Cuba (Jiménez et al., 2005), enclosed in its current distribution range that also includes the Swan Islands (Hedges, Couloux, & Vidal, 2009). With *Cubophis* the same happens as with *Chilabothrus* in Cuba, where many locations with fossils have been discovered, but formal reports are scarce. In this case, a single previous record of La Habana (Jiménez et al., 2005) is known. The records of this work extend its fossil distribution to the center of the country (Map 6).

Map 6. Fossil sample distribution of *Cubophis*, Cuba.

(Source: Aranda, 2019)

5 Conclusions

Based on the osteological descriptions and the geographical location of the records, we reached the following conclusions.

- Detailed descriptions of frontal, parietal, occipital, maxillae, dentaries, articulate-surangular complexes, vertebrae, and pelvis of Cuban Squamata fossils are provided, using characters described in the scientific literature.
- Six genera and seven species were identified.
- The genera *Amphisbaena* and *Pholidoscelis* are reported by the first time in the fossil record of Cuba. *Amphisbaena* based on a vertebra of the middle of the body, and *Pholidoscelis* from frontals, parietals, maxillae, dentaries, articular-surangular complexes, and pelvis.
- The presence in the fossil record of *Tarentola americana*, *Leiocephalus cubensis*, *L. carinatus*, *Chilabothrus angulifer*, and *Cubophis cantherigerus* is confirmed, with descriptions of new fossilized bones.
- New records of species not present in Cuba are described. It is necessary to compare with other Antillean and continental species for the taxonomic identification.
 - From the genus *Leiocephalus*, two frontals, and a dentary that does not coincide with the living species of the genus are described.
 - From the genus *Tarentola*, two parietals and two articular-surangular complexes are described with forms different from those currently present in Cuba.
 - From the genus *Chilabothrus*, a quadrate and two compound bones are described, distinct even of known Antillean species.
- The number of reported localities with Squamata fossil remains was increased from 10 known to 19.
- The Squamata fossil record was extended to practically the whole country, by including one locality in Santiago de Cuba and another in Isla de la Juventud.
- The localities of fossil remains coincide with the current distribution of living species.

References

- Ali, J. R. (2012). Colonizing the Caribbean: Is the GAARlandia land-bridge hypothesis gaining a foothold? *Journal of Biogeography*, 39(3), 431–433. <https://doi.org/10.1111/j.1365-2699.2011.02674.x>
- Alonso, R., Crawford, A. J., & Bermingham, E. (2012). Molecular phylogeny of an endemic radiation of Cuban toads (Bufonidae: *Peltophryne*) based on mitochondrial and nuclear genes. *Journal of Biogeography*, 39(3), 434–451. <https://doi.org/10.1111/j.1365-2699.2011.02594.x>
- Aranda, E. (2018). *Systematics of Quaternary Squamata from Cuba*. Zoology Museum, São Paulo University.
- Arredondo, C. A. (1997). Composición de la fauna de vertebrados terrestres extintos del Cuaternario de Cuba. *Revista Electrónica Órbita Científica*, 2(8), 1–14.
- Arredondo, C. A., & Villavicencio, R. (2004). Tafonomía del depósito arqueológico solapa del Megalocnus en el NE de Villa Clara, Cuba. *Revista de Biología*, 18(2), 160–170.
- Benites, J. P. de A. (2015). *Estudio comparativo de restos fósseis e recentes de Amphisbaenia. Abordagens filogenéticas, Paleoecológicas, Paleobiogeográficas*. Master dissertation. Paulista State University.
- Blain, H. A., Canudo, J. I., Cuenca-Bescós, G., & López-Martínez, N. (2010). Amphibians and squamate reptiles from the latest Maastrichtian (Upper Cretaceous) of Blasi 2 (Huesca, Spain). *Cretaceous Research*, 31(4), 433–446. <https://doi.org/10.1016/j.cretres.2010.06.001>
- Bochaton, C., Boistel, R., Grouard, S., Ineich, I., Tresset, A., & Bailon, S. (2017). Evolution, diversity and interactions with past human populations of recently extinct Pholidoscelis lizards (Squamata: Teiidae) from the Guadeloupe Islands (French West-Indies). *Historical Biology*, (DOI: 10.1080/08912963.2017.1343824).

- Bochaton, C., Grouard, S., Cornette, R., Ineich, I., Lenoble, A., Tresset, A., & Bailon, S. (2015). Fossil and subfossil herpetofauna from Cadet 2 Cave (Marie-Galante, Guadeloupe Islands, F. W. I.): Evolution of an insular herpetofauna since the Late Pleistocene. *Comptes Rendus - Palevol*, *14*(2), 101–110. <https://doi.org/10.1016/j.crpv.2014.10.005>
- Böhme, W. (1984). Erstfund eines fossilen Kugelfinger-gecko (Sauria: Gekkonidae: Sphaerodactylinae) aus Dominikanischen Bernstein der Oligozän von Hispaniola, Antillen. *Salamandra*, *20*, 212–220.
- Bolet, A., Delfino, M., Fortuny, J., Almécija, S., Robles, J. M., & Alba, D. M. (2014). An amphisbaenian skull from the European Miocene and the evolution of Mediterranean worm lizards. *PLoS ONE*, *9*(6).
- Brattstrom, B. H. (1958). More fossil reptiles from Cuba. *Herpetologica*, *13*, 278.
- Buskirk, R. E. (1985). Zoogeographic Patterns and Tectonic History of Jamaica and the Northern Caribbean. *Journal of Biogeography*, *12*(5), 445–461. <https://doi.org/10.2307/2844953>
- Camolez, T., & Zaher, H. (2010). Levantamento, identificação e descrição da fauna de Squamata do Quaternário Brasileiro (Lepidosauria). *Arquivos de Zoologia*, *41*, 1–96.
- Čerňanský, A., Augé, M. Louis, & Rage, J. (2015). A complete mandible of a new amphisbaenian reptile (Squamata, Amphisbaenia) from the late middle eocene (Bartonian, Mp 16) of France. *Journal of Vertebrate Paleontology*, *35*(1), e902379. <https://doi.org/10.1080/02724634.2014.902379>
- Čerňanský, A., & Smith, K. T. (2018). Eolacertidae: a new extinct clade of lizards from the Palaeogene; with comments on the origin of the dominant European reptile group—Lacertidae. *Historical Biology*, *30*(7), 994–1014. <https://doi.org/10.1080/08912963.2017.1327530>
- Conrad, J. L. (2008). Phylogeny and systematics of squamata (reptilia) based on morphology. *Bulletin American Museum of Natural History*, *310*(310), 182. <https://doi.org/10.1206/310.1>

- Consuegra, R. R. (2014). Columna ilustrada del registro macrofósil de Cuba. *Anuario de La Sociedad Cubana de Geología*, 2, 13–18.
- Cope, E. D. (1862). On the genera Panolopus, Centropyx, Aristelliger and Sphaerodactylus. *Proceedings of the Academy of Natural Sciences of Philadelphia*, 13, 494–500.
- Daza, J. D., Abdala, V., Thomas, R., & Bauer, A. M. (2008). Skull Anatomy of the Miniaturized Gecko *Sphaerodactylus roosevelti* (Squamata: Gekkota). *Journal of Morphology*, 269, 1340–1364. <https://doi.org/10.1002/jmor.10664>
- Daza, J. D., & Bauer, A. M. (2012). A new amber-embedded sphaerodactyl gecko from hispaniola, with comments on morphological synapomorphies of the Sphaerodactylidae. *Breviora*, 529, 1–28.
- Daza, J. D., Bauer, A. M., Wagner, P., & Böhme, W. (2013). A reconsideration of *Sphaerodactylus dommeli* Böhme, 1984 (Squamata: Gekkota: Sphaerodactylidae), a Miocene lizard in amber. *Journal of Zoological Systematics and Evolutionary Research*, 51(1), 55–63. <https://doi.org/10.1111/jzs.12001>
- Díaz-Franco, S. (2004). Análisis de la extinción de algunos mamíferos cubanos, sobre la base de evidencias paleontológicas y arqueológicas. *Revisa Biología*, 18(2), 147–154.
- Díaz, L. M., & Hedges, S. B. (2008). A new gecko of the genus *Tarentola* (Squamata: Gekkonidae) from Eastern Cuba. *Zootaxa*, 1743, 43–52.
- Domínguez, M., & Moreno, L. (2006). *Alsophis cantherigerus*. Size record. *Herpetological Review*, 37(3), 349.
- Duméril, A. M. C., & Bibron., G. (1844). *Erpetologie Générale ou Histoire Naturelle Complete des Reptiles* (Vol. 16). Paris: Encyclopédique Roret.
- Estes, R., Queiroz, K., & Gauthier, J. A. (1988). Phylogenetic relationships within Squamata. In R. Estes & G. Pregill (Eds.), *Phylogenetic relationships of the lizard families* (pp. 119–281). Stanford: Stanford University Press.
- Etheridge, R. (1959). *The relationships of the Anoles (Reptilia: Sauria: Iguanidae) an interpretation based on skeletal morphology*. University of Michigan.

- Etheridge, R. (1964). Late Pleistocene lizards from Barbuda, British West Indies. *Bulletin of the Florida State Museum*, 9(2), 43–75.
- Etheridge, R. (1965). Fossil lizards from the Dominican Republic. *Quarterly Journal of The Florida Academy of Sciences*, 27–28, 83–105.
- Etheridge, R. (1966a). An extinct lizard of the genus *Leiocephalus* from Jamaica. *Quarterly Journal of the Florida Academy of Sciences*, 29, 47–59.
- Etheridge, R. (1966b). Pleistocene lizards from New Providence. *Quarterly Journal of The Florida Academy of Sciences*, 28, 349–358.
- Etheridge, R., & de Queiroz, K. (1988). A phylogeny of Iguanidae. In R. Estes & G. Pregill (Eds.), *Phylogenetic relationships of the lizard families. Essays commemorating Charles L. Camp* (pp. 283–367). Stanford, C.A: Stanford Univ. Press.
- Evans, S. E. (2008). The Skull of Lizards and Tuatara. In C. Gans, A. S. Gaunt, & K. Adler (Eds.), *Biology of the Reptilia* (Vol. 20, pp. 1–347). Ithaca: Society for the Study of Amphibians and Reptiles.
- Fernández-Milera, J., & Correoso, M. (2003). Los moluscos terrestres y fluviales de la Isla de la juventud. *Cocuyo*, 13, 15–18.
- Frazetta, T. H. (1959). Studies on the morphology and function of the skull in the Boidae (Serpentes). Part I. Cranial differences between *Python sebae* and *Epicrates cenchrus*. *Bulletin of the Museum of Comparative Zoology*, 119(8), 453–472.
- Frost, D. R., Etheridge, R. E., Janies, D., & Titus, T. A. (2001). Total evidence, sequence alignment, evolution of Polychrotid lizards, and a reclassification of the Iguania (Squamata: Iguania). *American Museum Novitates*, 3343(3343), 38pp. [https://doi.org/10.1206/0003-0082\(2001\)343<0001:TESAEO>2.0.CO;2](https://doi.org/10.1206/0003-0082(2001)343<0001:TESAEO>2.0.CO;2)
- Gamble, T., Bauer, A. M., Colli, G. R., Greenbaum, E., Jackman, T. R., Vitt, L. J., & Simons, A. M. (2011). Coming to America: multiple origins of New World geckos. *Journal of Evolutionary Biology*, 24, 231–244. <https://doi.org/10.1111/j.1420-9101.2010.02184.x>

- Gamble, T., Bauer, A. M., Greenbaum, E., & Jackman, T. R. (2008). Out of the blue: A novel, trans-atlantic clade of geckos (Gekkota, Squamata). *Zoologica Scripta*, 37(4), 355–366. <https://doi.org/10.1111/j.1463-6409.2008.00330.x>
- Gauthier, J. A., Kearney, M., Maisano, J. A., Rieppel, O., & Behlke, A. D. B. (2012). Assembling the Squamate Tree of Life: Perspectives from the Phenotype and the Fossil Record. *Bulletin of the Peabody Museum of Natural History*, 53(1), 3–308.
- Goicoechea, N., Frost, D. R., De la Riva, I., Pellegrino, K. C. M., Sites, J., Rodrigues, M. T., & Padial, J. M. (2016). Molecular systematics of teioid lizards (Teioidea/Gymnophthalmoidea: Squamata) based on the analysis of 48 loci under tree-alignment and similarity-alignment. *Cladistics*, 32(6), 624–671. <https://doi.org/10.1111/cla.12150>
- Gray, E. J. (1831). A synopsis of the species of Class Reptilia. In G. Cuvier (Ed.), *The animal kingdom arranged in conformity with its organisation* (p. 591). London: Whittaker.
- Griffing, A. H., Daza, J. D., DeBoer, J. C., & Bauer, A. M. (2018). Developmental Osteology of the Parafrontal Bones of the Sphaerodactylidae. *Anatomical Record*, 301(4), 581–606. <https://doi.org/10.1002/ar.23749>
- Harvey, M. B., Ugueto, G. N., & Gutberlet, R. L. (2012). Review of Teiid Morphology with a Revised Taxonomy and Phylogeny of the Teiidae (Lepidosauria: Squamata). *Zootaxa*, 3459, 1–156.
- Hecht, M. K. (1951). Fossil lizards of the West Indian genus *Aristelliger* (Gekkonidae). *American Museum Novitates*, 1538, 1–33.
- Hedges, S. B. (1989). Evolution and biogeography of West Indian frogs of the genus *Eleutherodactylus*: slow evolving loci and the major groups. In C. A. Woods (Ed.), *Biogeography of the West Indies: past, present, and future* (pp. 305–370). Gainesville, Florida: Sand Hill Crane Press.
- Hedges, S. B. (1996). Historical biogeography of West Indian vertebrates. *Annu. Rev. Ecol. Syst.*, 27, 163–196.

- Hedges, S. B. (2001). Biogeography of the West Indies: An Overview. In C. A. Woods & F. E. Sergile (Eds.), *Biogeography of the West Indies: Patterns and Perspectives* (pp. 15–33). Boca Raton: CRC Press.
- Hedges, S. B. (2006). Paleogeography of the Antilles and origin of West Indian Terrestrial Vertebrates. *Annals of the Missouri Botanical Garden*, *93*, 231–244.
- Hedges, S. B., Couloux, A., & Vidal, N. (2009). Molecular phylogeny, classification, and biogeography of West Indian racer snakes of the Tribe Alsophiini (Squamata, Dipsadidae, Xenodontinae). *Zootaxa*, *2067*, 1–28.
- Hsiou, A. S. (2007). A new teiidae species (squamata, scincomorpha) from the late pleistocene of rio grande do sul state, brazil. *Revista Brasileira de Paleontologia*, *10*(3), 181–194.
- Ikeda, T. (2007). A Comparative Morphological Study of the Vertebrae of Snakes Occurring in Japan and Adjacent Regions A Comparative Morphological Study of the Vertebrae of Snakes Occurring in Japan and Adjacent Regions. *Current Herpetology*, *26*(1), 13–34. [https://doi.org/10.3105/1345-5834\(2007\)26](https://doi.org/10.3105/1345-5834(2007)26)
- Instituto Cubano de Cartografía y Catastro. (1957). Cartografía Topográfica de Cuba 1:50 000. Aero Service Corporation.
- Iturralde-Vinent, M. A. (2005). La paleogeografía del Caribe y sus implicaciones para la biogeografía histórica. *Revista Del Jardín Botánico Nacional*, *26*, 49–78.
- Iturralde-Vinent, M. A. (2006). Meso-Cenozoic Caribbean Paleogeography: Implications for the Historical Biogeography of the Region. *International Geology Review*, *48*, 791–827.
- Jiménez, O., Condis, M. M., & García, E. (2005). Vertebrados post-glaciales en un residuario fósil de *Tyto alba scopoli* (Aves: Tytonidae), en el occidente de Cuba. *Revista Mexicana de Mastozoología*, *9*, 85–112.
- Jiménez, O., & Valdés, P. (1995). Los vertebrados fósiles de la Cueva del Indio, San José la Lajas, Habana, Cuba. *Congreso Internacional 55 Aniversario de La Sociedad Espeleológica de Cuba*. La Habana.

- Kearney, M. (2003). Systematics of the Amphisbaenia (Lepidosauria: Squamata) Based on Morphological Evidence from Recent and Fossil Forms. *Herpetological Monographs*, 17(2003), 1–74.
- Kluge, A. (1989). A Concern for Evidence and a Phylogenetic Hypothesis of Relationships Among *Epicrates* (Boidae, Serpentes). *Systematic Zoology*, 38(1), 7–25.
- Kluge, A. (1991). Boine Snake Phylogeny and Research Cycles. *Miscellaneous Publications - Museum of Zoology, University of Michigan*, 178, 1–58.
- Koopman, K. F., & Ruibal, R. (1955). Cave Fossil vertebrates from Camagüey, Cuba. *Breviora, Museum of Comparative Zoology*, 46, 1–8.
- Losos, J. B., & Ricklefs, R. E. (2010). *The theory of island biogeography revisited*. Oxford: Princeton University Press.
- MacPhee, R. D. E., & Wyss, A. R. (1990). Oligo-Miocene Vertebrates from Puerto Rico, with a Catalog of Localities. *American Museum Novitates*, 2965, 1–45.
- Mancina, C. A., & Cruz, D. D. (2017). *Diversidad biológica de Cuba: métodos de inventario, monitoreo y colecciones biológicas*. (C. A. Mancina & D. D. C. Flores, Eds.). La Habana: AMA.
- Mandriola, L. F., Delfino, M., Bailon, S., & Pitruzzella, G. (2011). The Late Pliocene amphibians and reptiles from “Capo Mannu D1 Local Fauna” (Mandriola, Sardinia, Italy). *Geodiversitas*, 33(2), 357–382. <https://doi.org/10.5252/g2011n2a10.ABSTRACT>
- Mead, J. I., & Steadman, D. W. (2017). Late Pleistocene snakes (Squamata: Serpentes) from Abaco, The Bahamas. *Geobios*, 50(3), 431–440. <https://doi.org/10.1016/j.geobios.2017.09.001>
- Montero, R., Abdala, V., Moro, S., & Gallardo, G. (2004). Atlas de *Tupinambis rufescens* (Squamata: Teiidae). Anatomía externa, osteología y bibliografía. *Cuadernos de Herpetología*, 18(1), 17–32.
- National Office of Statistic and Information. (2017). *Anuario Estadístico de Cuba 2016. Capítulo 1: Territorio*. Habana.

- Noble, G. K. (1921). The bony structure and phyletic relations of the *Sphaerodactylus* and allied lacertilian genera, with the description of a new genus. *American Museum Novitates*, 4, 1–16.
- Oelrich, T. M. (1956). The Anatomy of the Head of *Ctenosaura pectinata* (Iguanidae). *Miscellaneous Publication Museum of Zoology, University of Michigan*, 94, 1–122.
- Orihuela, J. (2012). Late Holocene Fauna from a Cave Deposit in Western Cuba: post-Columbian occurrence of the Vampire Bat *Desmodus rotundus* (Phyllostomidae: Desmodontinae). *Caribbean Journal of Science*, 46(2–3), 297–312. <https://doi.org/10.18475/cjos.v46i2.a17>
- Pregill, G. K. (1981). Late Pleistocene Herpetofaunas from Puerto Rico. *Miscellaneous Publication, University of Kansas, Museum of Natural History.*, 71, 1–72.
- Pregill, G. K. (1992). Systematics of the West Indian lizard genus *Leiocephalus* (Squamata: Iguania: Tropiduridae). *The University of Kansas Museum of Natural History, Miscellaneous Publications*, (84), 1–69.
- Pregill, G. K. (1999). Eocene lizard from Jamaica. *Herpetologica*, 55(2), 157–161.
- Pregill, G. K., & Olson, S. L. (1981). Zoogeography of West Indian vertebrates in relation to Pleistocene climatic cycles. *Ann. Ret. Ecol. Syst.*, 12, 75–98.
- Pregill, G. K., Steadman, D., Olson, S., & Grady, F. (1988). Late Holocene Fossil Vertebrates from Burma Quarry, Antigua, Lesser Antilles. *Smithsonian Contributions to Zoology*, 463, 1–27. <https://doi.org/10.5479/si.00810282.463>
- Pregill, G. K., Steadman, D. W., & Watters, D. R. (1994). Late quaternary vertebrate faunas of the Lesser Antilles: historical components of Caribbean biogeography. *Bulletin of Carnegie Museum of Natural History*, 30, 1–51.
- Presch, W. F. (1970). *The evolution of Macroteiid lizards: an osteological interpretation*. University of Southern California.
- Presch, W. F. (1974). A Survey of the Dentition of the Macroteiid Lizards (Teiidae: Lacertilia). *Herpetologica*, 30(4), 344–349. <https://doi.org/jstor.org/stable/3891430>

- Queiroz, K. D. E., Chu, L., & Losos, J. B. (1998). A Second *Anolis* Lizard in Dominican Amber and the Systematics and Ecological Morphology of Dominican Amber Anoles. *American Museum Novitates*, 3249, 1–23.
- Rage, J. C., Pickford, M., & Senut, B. (2013). Amphibians and squamates from the middle Eocene of Namibia, with comments on pre-Miocene anurans from Africa. *Annales de Paleontologie*, 99(3), 217–242. <https://doi.org/10.1016/j.annpal.2013.04.001>
- Reynolds, R. G., Collar, D. C., Pasachnik, S. A., Niemiller, M. L., Revell, L. J., & Puente-rol, A. R. (2016). Ecological specialization and morphological diversification in Greater Antillean boas. *Evolution*, 70(8), 1882–1895. <https://doi.org/10.1111/evo.12987>
- Reynolds, R. G., Niemiller, M. L., Hedges, S. B., Dornburg, A., Puente-rolón, A. R., & Revell, L. J. (2013). Molecular phylogeny and historical biogeography of West Indian boid snakes (Chilabothrus). *Molecular Phylogenetics and Evolution*, 68(3), 461–470. <https://doi.org/10.1016/j.ympev.2013.04.029>
- Reynolds, R. G., Puente-Rolón, A., Burgess, J., & Baker, B. (2018). Rediscovery and a Redescription of the Crooked-Acklins Boa, *Chilabothrus schwartzi* (Buden, 1975), Comb. Nov. *Breviora*, 558(1), 1–16.
- Reynolds, R. G., Puente-Rolón, A. R., Geneva, A. J., Aviles-Rodriguez, K. J., & Herrmann, N. C. (2016). Discovery of a remarkable new boa from the Conception Island Bank, Bahamas. *Breviora*, 549(1), 1–19. <https://doi.org/10.3099/brvo-549-00-1-19.1>
- Rieppel, O. (1980). Green anole in Dominican amber. *Nature*, 286, 486–487.
- Rodríguez-Schettino, L. (2003). *Anfibios y reptiles de Cuba*. (L. Rodríguez-Schettino & J. J. Larramendi, Eds.). La Habana: Instituto de Ecología y Sistemática.
- Rodríguez-Schettino, L., Mancina, C. A., González, V. R., Rodríguez-Schettino, L., Mancina, C. A., & Rivalta, V. (2013). Reptiles of Cuba: checklist and geographic distributions. *Smithsonian Herpetological Information Service*, 144, 1–96. <https://doi.org/10.5479/si.23317515.144.1>

- Rohlf, F. J. (2001). *tpsDig – thin plate spline digitizer, version 2.11*. New York: State University of New York at Stony Brook.
- Russell, A. P., & Bauer, A. M. (2008). The Appendicular Locomotor Apparatus of Sphenodon and Normal-limbed Squamates. In C. Gans, A. S. Gaunt, & K. Adler (Eds.), *Biology of the Reptilia 21* (pp. 1–465). Ithaca: Society for the Study of Amphibians and Reptiles.
- Salgado, E. S. J., Calvache, D. G., Macphee, R. D. E., & Gould, G. C. (1992). The Monkey caves of Cuba. *Cave Science*, *19*(1), 25–28.
- Savage, J. M. (1964). Studies on the Lizard Family Xantusiidae. V. The Cuban Night Lizard, *Cricosaura typica* Gundlach and Peters. *Copeia*, *1964*(3), 536–542. <https://doi.org/10.2307/1441520>
- Scanferla, C. A., Montero, R., & Agnolín, F. L. (2006). The First Fossil Record of *Amphisbaena Heterozonata* from the late Pleistocene of Buenos Aires province, Argentina. *South American Journal of Herpetology*, *1*(2), 138–142.
- Scanferla, C. A., Smith, K. T., & Schaal, S. F. K. (2016). Revision of the cranial anatomy and phylogenetic relationships of the Eocene minute boas *Messelophis variatus* and *Messelophis ermannorum* (Serpentes, Booidea). *Zoological Journal of the Linnean Society*, *176*(1), 182–206. <https://doi.org/10.1111/zoj.12300>
- Schwartz, A., & McCoy, C. J. (1970). A systematic review of *Ameiva auberi* Cocteau (Reptilia, Teiidae) in Cuba and the Bahamas. I. The Cuban subspecies. II: The Bahamian subspecies. III. Discussion. *Annals of the Carnegie Museum*, *41*(4), 45–168.
- Silva, G. T., Duque, W. S., & Díaz-Franco, S. (2007). *Compendio de los Mamíferos Terrestres Autóctonos de Cuba. Vivientes y Extinguidos*. La Habana: Boloña.
- Smith, K. T., & Scanferla, C. A. (2016). Fossil snake preserving three trophic levels and evidence for an ontogenetic dietary shift. *Palaeobiodiversity and Palaeoenvironments*, *96*(4), 589–599. <https://doi.org/10.1007/s12549-016-0244-1>

- Steadman, D. W., Albury, N. A., Kakuk, B., Mead, J. I., Soto-Centeno, J. A., Singleton, H. M., & Franklin, J. (2015). Vertebrate community on an ice-age Caribbean island. *Proceedings of the National Academy of Sciences*, *112*(44), E5963–E5971. <https://doi.org/10.1073/pnas.1516490112>
- Steadman, D. W., Albury, N. A., Maillis, P., Mead, J. I., Slapcinsky, J., Krysko, K. L., ... Franklin, J. (2014). Late-Holocene faunal and landscape change in the Bahamas. *The Holocene*, *24*(2), 220–230. <https://doi.org/10.1177/0959683613516819>
- Steadman, D. W., Franz, R., Morgan, G. S., Albury, N. A., Kakuk, B., Broad, K., ... Dilcher, D. L. (2007). Exceptionally well preserved late Quaternary plant and vertebrate fossils from a blue hole on Abaco, The Bahamas. *PNAS*, *104*(50), 19897–19902. <https://doi.org/10.1007/s11120-007-9246-1>
- Steadman, D. W., Pregill, G. K., & Olson, S. L. (1984). Fossil vertebrates from Antigua, Lesser Antilles: Evidence for late Holocene human-caused extinctions in the West Indies. *Proceedings of the National Academy of Science*, *48*, 4448–4451.
- Stephenson, N. G. (1960). The Comparative Osteology of Australian Geckos and Its Bearing on Their Morphological Status. *Journal of the Linnean Society of London, Zoology*, *44*(297), 278–299. <https://doi.org/10.1111/j.1096-3642.1960.tb01616.x>
- Stephenson, N. G., & Stephenson, E. M. (1956). The Osteology of the New Zealand Geckos and its Bearing on Their Morphological Status. *Transactions and Proceedings of the Royal Society of New Zealand*, *84*(2), 341–358.
- Suárez, W. (2004). Biogeografía de las aves fósiles de Cuba. In M. Iturralde-Vinent (Ed.), *CD. Origen y Evolución del Caribe y sus biotas Marinas y Terrestres* (pp. 1–17). La Habana: Centro Nacional de Información Geológica.
- Thomas, R., & Hedges, S. B. (1998). A New Amphisbaenian from Cuba. *Journal of Herpetology*, *32*(1), 92–96.
- Torres-Carvajal, O. (2003). Cranial osteology of the Andean lizard *Stenocercus guentheri* (Squamata: Tropicuridae) and its postembryonic development. *Journal of Morphology*, *255*(1), 94–113. <https://doi.org/10.1002/jmor.10051>

- Torres, J. L., Rodríguez-Cabrera, T. M., & Romero, R. M. (2017). Reptiles. In C. A. Mancina & D. D. Cruz (Eds.), *Diversidad biológica de Cuba: métodos de inventario, monitoreo y colecciones biológicas* (pp. 376–411). La Habana: Editorial AMA.
- Uetz, P., Freed, P., & Hošek, J. (2018). The Reptile Database. Retrieved December 2, 2018, from <http://www.reptile-database.org>
- Varona, L. S., & Arredondo, O. (1979). Nuevos táxones fósiles de Capromyidae (Rodentia: Caviomorpha). *Poeyana*, *195*, 1–51.
- Vasilyan, D., Zazhigin, V. S., & Böhme, M. (2017). Neogene amphibians and reptiles (Caudata, Anura, Gekkota, Lacertilia, and Testudines) from the south of Western Siberia, Russia, and Northeastern Kazakhstan. *PeerJ*, *5*, e3025. <https://doi.org/10.7717/peerj.3025>
- Villa, A., Daza, J. D., Bauer, A. M., & Delfino, M. (2018). Comparative cranial osteology of European gekkotans (Reptilia, Squamata). *Zoological Journal of the Linnean Society*, *XX*, 1–39. <https://doi.org/10.1093/zoolinnean/zlx104>
- Wagler, J. G. (1830). *Natürliches System der Amphibien, mit vorangehender Classification der Säugetiere und Vögel. Ein Beitrag zur vergleichenden Zoologie*. München: Stuttgart, and Tübingen.
- Zaher, H., & Rieppel, O. (1999). Tooth Implantation and Replacement in Squamates, with Special Reference to Mosasaur Lizards and Snakes. *American Museum Novitates*, *3271*, 1–19.
- Zaher, H., & Scanferla, C. A. (2012). The skull of the Upper Cretaceous snake *Dinilysia patagonica* Smith-Woodward, 1901, and its phylogenetic position revisited. *Zoological Journal of the Linnean Society*, *164*(1), 194–238. <https://doi.org/10.1111/j.1096-3642.2011.00755.x>
- Zangerl, R. (1945). Contributions to the Osteology of the Post-Cranial Skeleton of the Amphisbaenidae. *The American Midland Naturalist*, *33*(3), 764–780. <https://doi.org/10.2307/2421188>

Zheng, Y., & Wiens, J. J. (2016). Combining phylogenomic and supermatrix approaches, and a time-calibrated phylogeny for squamate reptiles (lizards and snakes) based on 52 genes and 4162 species. *Molecular Phylogenetics and Evolution*, *94*, Part B, 537–547. <https://doi.org/http://dx.doi.org/10.1016/j.ympev.2015.10.009>

Appendices

Appendix A. Squamata fossils known in the Antilles and The Bahamas.

The localities of Cuba are the ones reported before the present work.

Island	Age	Localidad	Taxon	Reference
Antigua	Late Holocene	Burma	<i>Alsophis antillensis</i>	Steadman et al. 1984
			<i>Alsophis cf. antillensis</i>	Pregill 1988
	<i>Anolis bimaculatus</i> <i>leachi</i>		Pregill 1988	
	<i>Antillotyphlops</i> <i>monastus</i>		Pregill 1988	
	Boidae		Pregill 1988, Steadman et al. 1984	
	<i>Leiocephalus cuneus</i>		Pregill 1988	
	<i>Pholidoscelis griswoldi</i>		Pregill 1988, Steadman et al. 1984	
	<i>Thecadactylus</i> <i>rapicauda</i>		Pregill 1988	
	Indian Creek		<i>Boa cf. constrictor</i>	Steadman et al. 1984
	Mill Reef		<i>Alsophis antillensis</i>	Steadman et al. 1984
		<i>Pholidoscelis griswoldi</i>	Steadman et al. 1984	
Barbuda	Pleistocene	Two Fot Bay	<i>Alsophis sp.</i>	Pregill et al. 1994
			<i>Anolis bimaculatus</i>	Etheridge 1964

			<i>Anolis wattsi</i>	Pregill et al. 1994
			<i>Clelia cf. clelia</i>	Pregill et al. 1994
			<i>Leiocephalus cuneus</i>	Etheridge, 1964
			<i>Pholidoscelis griswoldi</i>	Etheridge 1964
			<i>Thecadactylus rapicauda</i>	Etheridge 1964
<hr/>				
Barbados	Pleistocene		<i>Anolis extremus</i>	Pregill et al. 1994
			<i>Erythrolamprus perfuscus</i>	Pregill et al. 1994
			<i>Iguana iguana</i>	Pregill et al. 1994
<hr/>				
Cuba	Pleistocene	Caimito	<i>Chilabothrus angulifer</i>	Present work
			<i>Cubophis cantherigerus</i>	Present work
		Camaguey	<i>Anolis equestris</i>	Koopman and Ruibal 1955
			<i>Anolis lucius</i>	Koopman and Ruibal 1955
			<i>Chilabothrus angulifer</i>	Koopman and Ruibal 1955
			<i>Leiocephalus sp.</i>	Koopman and Ruibal 1955
			<i>Tarentola americana</i>	Koopman and Ruibal 1955
		Jagüey Grande	<i>Chilabothrus sp.</i>	Present work

	<i>Leiocephalus cubensis</i>	Present work
	<i>Leiocephalus macropus</i>	Present work
	<i>Pholidoscelis auberi</i>	Present work
La Habana	<i>Anolis chamaeleonides</i>	Jiménez and Valdés 1995
	<i>Anolis equestris</i>	Jiménez and Valdés 1995
	<i>Anolis lucius</i>	Koopman and Ruibal 1955
	<i>Anolis luteogularis</i>	Arredondo 1997
	<i>Anolis</i> sp.	Jiménez and Valdés 1995
	<i>Chilabothrus angulifer</i>	Varona and Arredondo 1979
	<i>Leiocephalus cubensis</i>	cf. Jiménez and Valdés 1995
La Palma	<i>Chilabothrus angulifer</i>	Varona and Arredondo 1979
	<i>Cyclura nubila</i>	Varona and Arredondo 1979
Las Villas	<i>Chilabothrus angulifer</i>	Arredondo and Villavicencio 2004
	<i>Cyclura nubila</i>	Arredondo and Villavicencio 2004

	Los Palacios	<i>Leiocephalus</i> sp.	Present work
		<i>Tarentola americana</i>	Present work
	Matanzas	<i>Chilabothrus</i> sp.	Iturralde-Vinent et al. 2000
	Pinar	cf. <i>Amphisbaena</i> sp.	Present work
		<i>Cyclura nubila</i>	Arredondo 1970
	Quivicán	<i>Anolis porcatus</i>	Jiménez et al. 2005
		<i>Anolis</i> sp.	Jiménez et al. 2005
		<i>Chilabothrus angulifer</i>	Jiménez et al. 2005
		<i>Cubophis cantherigerus</i>	Jiménez et al. 2005
		<i>Leiocephalus carinatus</i>	cf. Jiménez et al. 2005
		<i>Tarentola americana</i>	Jiménez et al. 2005
	Santiago de Cuba	<i>Tarentola americana</i>	Present work
	Viñales	<i>Chilabothrus</i> sp.	Jaimez et al. 1992
		<i>Cyclura nubila</i>	Jaimez et al. 1992
	Yaguajay	<i>Chilabothrus angulifer</i>	Present work
		<i>Cubophis</i> sp.	Present work
		<i>Leiocephalus</i> sp.	Present work
		<i>Tarentola americana</i>	Present work
Isla de la Juventud	Nueva Gerona	<i>Chilabothrus angulifer</i>	Present work

			Gekkota indet.	Present work
St. Martin	Pleistocene	Saint Martin	cf. <i>Iguana</i> sp.	Pregill et al. 1994
Basse- Terre	Holocene		<i>Diploglossus</i> <i>montisserrati</i>	Bochaton et al. 2015
			<i>Diploglossus</i> sp.	Bochaton et al. 2015
			<i>Iguana delicatissima</i>	Bochaton et al. 2017
			<i>Pholidoscelis</i> cf. <i>major</i>	Bochaton et al. 2017
Grande- Terre	Holocene		<i>Anolis marmoratus</i>	Pregill et al. 1994
			cf. <i>Antillotyphlops</i> <i>monastus</i>	Pregill et al. 1994
			<i>Iguana delicatissima</i>	Bochaton et al. 2017
			<i>Iguana</i> sp.	Pregill et al. 1994
			<i>Leiocephalus</i> cf. <i>cuneus</i>	Pregill et al. 1994
			<i>Pholidoscelis</i> <i>cineraceus</i>	cf. Pregill et al. 1994
			<i>Pholidoscelis</i> cf. <i>major</i>	Bochaton et al. 2017
			<i>Thecadactylus</i> <i>rapicauda</i>	Pregill et al. 1994
			<i>Typhlops dominicanus</i>	Pregill et al. 1994
La Désirade	Holocene		<i>Iguana delicatissima</i>	Bochaton et al. 2017
			<i>Pholidoscelis</i> cf. <i>major</i>	Bochaton et al. 2017

Les Saintes	Holocene		<i>Iguana delicatissima</i>	Bochaton et al. 2017
			<i>Pholidoscelis cf. major</i>	Bochaton et al. 2017
			<i>Pholidoscelis turukaeraensis</i>	Bochaton et al. 2017
Marie-galante	Holocene	Marie-galante	<i>Alsophis sp.</i>	Bailon et al. 2015, Bochaton et al. 2015
			<i>Anolis ferreus</i>	Bailon et al. 2015, Bochaton et al. 2015
			<i>Antillotyphlops sp.</i>	Bochaton et al. 2016
			<i>Boa blanchardensis</i>	Bochaton and Bailon 2018
			<i>Boa sp.</i>	Bailon et al. 2015, Bochaton et al. 2015
			cf. <i>Capitellum mariagalante</i>	Bochaton et al. 2015
			Colubridae	Bailon et al. 2015
			<i>Iguana delicatissima</i>	Bochaton et al. 2017
			<i>Leiocephalus cf. cuneus</i>	Bailon et al. 2015
			<i>Pholidoscelis turukaeraensis</i>	Bochaton et al. 2017
			<i>Sphaerodactylus fantasticus</i>	Bochaton et al. 2015
			<i>Thecadactylus rapicauda</i>	cf. Bailon et al. 2015

Petite- terre	Holocene	Petite-terre	<i>Iguana delicatissima</i>	Bochaton et al. 2017
			<i>Pholidoscelis cf. major</i>	Bochaton et al. 2017
Jamaica	Eocene	Guy's Hill	Iguanidae	Pregill 1999
	Pleistocene	Runaway Bay	<i>Anolis garmani</i>	Hecht 1951
			<i>Aristelliger praesignis</i>	Hecht 1951
			<i>Celestus hewardi</i>	Hecht 1951
		St. Ann Parish	<i>Aristelliger lar</i>	Hecht 1951
			<i>Leiocephalus jamaicensis</i>	Etheridge, 1966
Isla de Mona	Pleistocene	Isla de Mona	<i>Cyclura stejnegeri</i>	Frank and Benson 1998
Puerto Rico	Miocene	Cibao	Boidae	MacPhee and Wyss 1990
			Iguanidae	MacPhee and Wyss 1990
	Pleistocene	Blackbone I	<i>Amphisbaena sp.</i>	Pregill, 1981
			<i>Anolis cristatellus</i>	Pregill, 1981
			<i>Anolis cuvieri</i>	Pregill, 1981
			<i>Anolis evermanni</i>	Pregill, 1981
			<i>Anolis krugi</i>	Pregill, 1981
			<i>Anolis occultus</i>	Pregill, 1981
			<i>Borikenophis</i>	Pregill, 1981

			<i>portoricensis</i>	
			<i>Chilabothrus inornatus</i>	Pregill, 1981
			<i>Cyclura pinguis</i>	Pregill, 1981
			<i>Diploglossus pleei</i>	Pregill, 1981
			<i>Mabuya mabouya</i>	Pregill, 1981
			<i>Magliophis exiguum</i>	Pregill, 1981
			<i>Pholidoscelis exsul</i>	Pregill, 1981
			<i>Sphaerodactylus</i> sp.	Pregill, 1981
			<i>Typhlops</i> sp.	Pregill, 1981
		Guanicá	<i>Leiocephalus partitus</i>	Pregill, 1981
		Morovis	<i>Leiocephalus etheridgei</i>	Pregill, 1981
Anguilla	Pleistocene	Anguilla	<i>Alsophis rijgersmai</i>	Pregill et al. 1994
			<i>Anolis</i> sp.	Pregill et al. 1994
			<i>Leiocephalus</i> cf. <i>cuneus</i>	Pregill et al. 1994
			<i>Pholidoscelis plei</i>	Pregill et al. 1994
			<i>Sphaerodactylus</i> sp.	Pregill et al. 1994
			<i>Thecadactylus rapicauda</i>	Pregill et al. 1994
Hispaniola	Miocene	La Toca	<i>Anolis</i> cf. <i>chlorocyanus</i> species group	Queiroz et al. 1998
			<i>Anolis dominicanus</i>	Rieppel, 1980
			<i>Sphaerodactylus</i>	Daza and Bauer 2012

			<i>ciguapa</i>	
			<i>Sphaerodactylus dommeli</i>	Bohme 1984, Daza et al. 2013
Pleistocene	l'Artibonite		<i>Anolis ricordii</i>	Hecht 1951
			<i>Aristelliger lar</i>	Hecht 1951
			<i>Celestus sp.</i>	Hecht 1951
			<i>Leiocephalus anonymous</i>	Pregill, 1984
			<i>Pholidoscelis chrysolemus</i>	Hecht 1951
		Pedro Santana	<i>Leiocephalus apertosulcus</i>	Etheridge, 1965
			<i>Leiocephalus personatus</i>	Etheridge, 1965
		San Francisco	<i>Pholidoscelis chrysolemus</i>	Etheridge 1965
			<i>Pholidoscelis taeniurus</i>	Etheridge 1965
Crooked Island	Holocene		<i>Anolis brunneus</i>	Steadman et al. 2017
			<i>Anolis sagrei</i>	Steadman et al. 2017
			<i>Leiocephalus punctatus</i>	Steadman et al. 2017
Great Abaco	Late Holocene	Gilpin Point	<i>Anolis cf. distichus</i>	Steadman et al. 2014
			<i>Anolis cf. sagrei</i>	Steadman et al. 2014

		<i>Chilabothrus cf. exsul</i>	Steadman et al. 2014
		<i>Cubophis cf. vudii</i>	Steadman et al. 2014
		<i>Cyclura cf. carinata</i>	Steadman et al. 2014
		Gekkonidae	Steadman et al. 2014
		<i>Leiocephalus</i>	<i>cf.</i> Steadman et al. 2014
		<i>carinatus</i>	
Pleistocene	Abaco	<i>Mabuya cf mabouya</i>	Steadman et al. 2015
		<i>Sphaerodactylus</i>	<i>cf</i> Steadman et al. 2015
		<i>notatus</i>	
		<i>Anolis sagrei</i>	Steadman et al. 2007
		<i>Chilabothrus cf. exsul</i>	Mead and Steadman 2017
		<i>Chilabothrus striatus</i>	Steadman et al. 2007
		<i>Cubophis cf. vudii</i>	Mead and Steadman 2017
		<i>Cubophis sp.</i>	Steadman et al. 2007
		<i>Nerodia sp.</i>	Mead and Steadman 2017
		<i>Pantherophis sp.</i>	Mead and Steadman 2017
		Scolecophidia	Mead and Steadman 2017
		<i>Typhlops sp.</i>	Steadman et al. 2007

New Providence	Pleistocene	<i>Anolis carolinensis</i>	Etheridge 1966
		<i>Anolis distichus</i>	Etheridge 1966
		<i>Anolis sagrei</i>	Etheridge 1966
		<i>Cyclura</i> sp.	Etheridge 1966
		<i>Leiocephalus carinatus</i>	Etheridge 1966
		<i>Pholisdoscelis auberi</i>	Etheridge 1966
		<i>Tarentola americana</i>	Etheridge 1966

Appendix B. Localities of fossil sample, Cuba.

Genus	Specimen	Province	Municipality	Locality
<i>cf. Amphisbaena</i>	CZACC 1	Pinar del Río	Viñales	Geda Cave
<i>Tarentola</i>	CZACC 2	Santiago de Cuba	Santiago de Cuba	Daiquiri Cave
	CZACC 3	Pinar del Río	Minas Matahambre	Chefa Cave, Majaguas-Canteras system
	CZACC 7	Sancti Spíritus		
	MNHNCu 73.5342	Pinar del Río	Los Palacios	Abrón Cave
	MNHNCu 73.5343	Pinar del Río	Los Palacios	Abrón Cave
	MNHNCu 73.5345	Pinar del Río	Los Palacios	Abrón Cave
	MNHNCu 73.5347	Pinar del Río	Los Palacios	Abrón Cave
	MNHNCu 73.5349	Pinar del Río	Los Palacios	Abrón Cave
	MNHNCu 73.5350	Pinar del Río	Los Palacios	Abrón Cave
	MNHNCu 73.5351	Pinar del Río	Los Palacios	Abrón Cave
<i>Gekkota</i>	MNHNCu 73.5334	Isla de la Juventud	Nueva Gerona	Marble quarry, Sierra de Casas
	<i>Pholidoscelis</i>	CLV 2	Matanzas	Jagüey Grande
	CLV 3	Matanzas	Jagüey Grande	J4 quarry
	MNHNCu 73.5312	Matanzas	Matanzas	Nesophontes Cave, Palenque Hill
<i>Leiocephalus</i>	CLV 1	Matanzas	Jagüey Grande	J4 quarry
	CLV 4	Matanzas	Jagüey Grande	Afán Cave, Agramonte
	CLV 5	Matanzas	Jagüey Grande	Afán Cave, Agramonte
	CLV 6	Matanzas	Jagüey Grande	Afán Cave, Agramonte

	CZACC 4	Artemisa	Caimito	Paredones Cave
	CZACC 5	Mayabeque	San José de las Lajas	Indio Cave, Tapaste
	CZACC 6	Artemisa	Caimito	Paredones Cave
	CZACC 8	Mayabeque	San José de las Lajas	Indio Cave, Tapaste
	MNHNCu 73.5041	Sancti Spíritus	Yaguajay	Humboldt Cave, Punta Caguanes
	MNHNCu 73.5379	Pinar del Río	Los Palacios	Abrón Cave
<i>Chilabothrus</i>	CLV 7	Matanzas	Jagüey Grande	J4 quarry
	CLV 8	Matanzas	Jagüey Grande	J4 quarry
	CLV 9	Matanzas	Jagüey Grande	J4 quarry
	MNHNCu 73.5029	Artemisa	Caimito	Paredones Cave
	MNHNCu 73.5311	Matanzas	Matanzas	Nesophontes Cave, Palenque hill
	MNHNCu 73.5322	Matanzas	Matanzas	El Gato Cave, Gelpis plateau
	MNHNCu 73.5328	Isla de la Juventud	Nueva Gerona	Sierra de Casas marble quarry
	MNHNCu 73.5335	Isla de la Juventud	Nueva Gerona	Sierra de Casas marble quarry
	MNHNCu 73.5380	Sancti Spíritus	Yaguajay	Humboldt Cave, Punta Caguanes
<i>Cubophis</i>	MNHNCu 73.5376	Artemisa	Caimito	Paredones Cave
	MNHNCu 73.5382	Sancti Spíritus	Yaguajay	Humboldt Cave, Punta Caguanes